ME450 Design Review 4 Report

Mechanical Shock Testing Machine for Space Physics Research Laboratory

Team 21: Nathan Gustafson, Joseph Harrington, Ice Kulsetsophon, Kalen O'Connor

Table of Contents

Abstract **5**
1 Project Introduction and Background **5**
2 Design Context **6**
2.1 Public Health, Safety, and Welfare Implications 7
2.2 Global and Social Considerations 7
2.3 Environmental Considerations 8
2.4 Ethical Considerations 8
2.5 Inclusivity and Power Dynamics 8
3 User Requirements and Engineering Specifications **9**
3.1 Requirements Development Process 9
3.2 List of Requirements and Specifications 10
4 Concept Generation **13**
5 Concept Selection **14**
6 Selected Concept: Hammer striking ringing plate **16**
6.1 Alpha Design 17
6.2 Small-scale Prototype Shock Tester 17
7 Problem Analysis and Future Engineering Work **19**
7.1 The Ringing Plate 19
7.2 Information Gaps 20
7.3 Anticipated Challenges 20
8 Engineering Analysis **21**
8.1 Hammer Impact Force 21
8.2 ANSYS Explicit Dynamics Model 22
8.3 Smallwood Algorithm 25
8.4 Empirical Shock Response Spectra with Small Scale Prototype Shock Tester 29
8.5 Comparison of Analytical to Empirical Shock Response Spectra 33
8.6 Subframe Structural Analysis 34
8.7 Hammer Structural Analysis 37
9 Design Iteration and History **39**
10 Full-Scale Design **41**
10.1 Plate Sub-assembly 42
10.2 Hammer Sub-assembly 44
10.3 Frame Sub-assembly 47
10.4 Project Cost 49
11 Verification and Validation Plan **50**
12 Project Plan **50**

Planning Conclusion **51**
13 Final Build Validation **51**
13.1 Test Repeatability / Accelerometer Placement 54
13.2 Drop Height 55
13.3 Hammer Mass 57
13.4 Strike Plate Material 58
13.5 DUT Location 59
13.6 Boundary Conditions for IP Configuration 60
13.7 Impact Duration 64
13.8 Peak Acceleration Capabilities 65
14 User Guide **66**
14.1 DUT Setup 66
14.2 Hammer Setup 66
14.3 Test Setup 68
14.4 SRS Tuning 69
15 Reflection **70**
15.1 Public Health, Safety, and Welfare Implications 71
15.2 Global, Social and Environmental Considerations 71
15.3 Inclusion and Equity 71
15.4 Ethics 72
16 Discussion **72**
17 Recommendations **74**
18 Conclusion **75**
19 Acknowledgements **77**
References **78**
Appendix A: Team 21 Biographies **81**
Appendix B: Bill of Materials **83**
Appendix C: Supplementary CAD Views **92**
Appendix D: Engineering Drawings **106**
Appendix E: Impact Dynamics Model **113**
Appendix F: Concept Sketches and Ideas **115**

Note:

Text which appears in this color grey is carryover language from the DR1 or DR2 report

Text written in black is new content for DR3

Abstract

Mechanical shock testing is a valuable qualification step for space instrumentation, but the University of Michigan Space Physics Research Laboratory (SPRL) lacks the ability to conduct this testing in-house. This project aims to give SPRL shock test capability through the design, fabrication, and test of an affordable shock testing machine. The product must induce up to 3000 G peak accelerations under 25 ms on specimens up to 30 kg and measuring 50 cm in each dimension. After concept exploration, an architecture using a ringing plate struck by a hammer was determined to best achieve the design requirements for SPRL's application. A design has been developed and analyzed which utilizes a 40 inch square aluminum plate struck by a 60" hammer all supported and aligned in a t-slot aluminum frame.

1 Project Introduction and Background

The sponsor of our project is the Space Physics Research Laboratory (SPRL), who focuses on the development of instrumentation for space exploration organizations such as NASA and ESA [2]. SPRL's instruments are primarily used for mass spectrometry, which enables rovers to analyze the chemical composition of Mars and other planets. For example, the Curiosity rover, one of NASA's most famous rovers, was only able to make its breakthroughs with the power of mass spectrometry [16]. With this, NASA and similar organizations are able to extract a lot of information about other planets.

Since SPRL's instruments are transported on rockets, they must endure extreme conditions such as launch, separation and landing. Failure of a component on one of these missions can be catastrophic and unrecoverable, therefore rigorous testing is required to ensure their functionality and durability. Currently, SPRL lacks an in-house shock testing capability, instead relying on third-party testing facilities [2]. The primary problem that SPRL has with this method is that they face high costs, long lead times, and limited flexibility [2].

SPRL has previously done preliminary research into building their own mechanical shock testing machine, however they had to divert their attention elsewhere, leaving this project unfinished. They have also considered purchasing existing solutions such as the Lansmont Model 23D shock test system, which was priced at a high cost of around $40-55k depending on the additional tuning equipment they wanted to include [10] [2].

The primary objective of this project is to develop a fully functional mechanical shock testing machine that allows SPRL to conduct these tests in-house, while being in compliance with relevant engineering standards. A key standard to consider is NASA's General Environmental Verification Standards (GEVS), which all NASA instrumentation must meet to be qualified for space flight [11]. Furthermore, to ensure safe operation, the design must meet relevant requirements set by Occupational Safety and Health Administration (OSHA) and National

Electrical Code (NEC) [12]. A successful outcome of this project will be determined by whether or not our group is able to fabricate and verify a mechanical shock testing machine according to SPRL's requirements and specifications.

The scope of this project is captured below.

In-scope

- Verification of all requirements and specifications through analysis and experiments of the shock load capability of machine
- Design and fabrication of fully functional machine that meets all the requirements and specifications
- Accommodations for 3-axis testing of any DUT(Device Under Test) within given size and mass specifications
- Mount locations for accelerometers in locations which accurately capture the SRS
- Structural and harmonic analysis of the machine

Out-of-scope

- Calibration of accelerometers
- Tuning of fixture hardware for shock tests
- Shock tests on specific instrumentation
- Data acquisition system, which will be provided by SPRL
- Electronic/software user terminal, which will be provided by SPRL
- Tuning for specific waveform shape generation

Throughout the development of our project, we have and will be using a wide array of reliable information sources. Our primary information source would be interviews with the SPRL team. Our secondary sources include various standards documents, literature on shock response spectrum (SRS) and mechanical shock testing machines, and benchmarking data from existing similar products. Our team will utilize these information sources to strengthen our understanding while we continue to develop our project.

2 Design Context

Our largest stakeholder in this project is SPRL since they are our sponsors. Thus, we are designing this fixture to fit their specific needs for instrumentation testing. With that being said, complementary organizations at the University such as other research labs or student project teams oftentimes have a desire to test their parts for shock, so this project could benefit them even though it's not being designed for their requirements. Since the engineers at SPRL are experts in shock testing having conducted many tests in the past, we plan to utilize them as a resource to learn from and build off of throughout our project. Not only do we have SPRL, but we also have a plethora of other amazing teams at the school. With a dedicated machine shop in the ME building, many of the simple parts that we need can be made in house by us as students.

Further, we'll be able to utilize the machine shop as a resource as we develop more intricate drawings to help determine feasibility and manufacturability of our design.

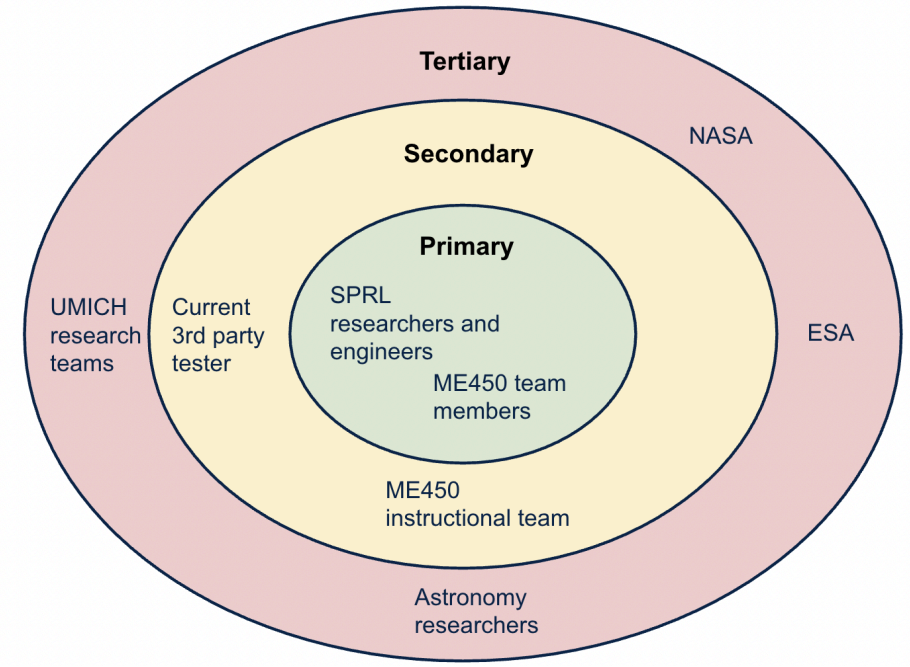


Figure 1. Stakeholder map

2.1 Public Health, Safety, and Welfare Implications

Safety is a top priority in the design of the shock testing machine. The system must be structurally robust, precisely controllable, and fully compliant with industry safety standards, including OSHA and ASME regulations, to protect operators and minimize risks. Given the high-force impacts involved, the design must incorporate protective enclosures, noise dampening, and vibration isolation to mitigate hazards such as flying debris, excessive noise, and unintended vibration transmission.

Beyond immediate safety concerns, this project also contributes to public welfare by improving the reliability and qualification of space instrumentation. SPRL's instruments are used in critical space missions, where component failure can lead to mission loss, scientific setbacks, and significant financial costs. Additionally, eliminating the need for external testing reduces environmental and noise pollution associated with transporting both instrumentation and personnel, further aligning the project with sustainable and responsible engineering practices.

2.2 Global and Social Considerations

This project aligns with global initiatives like advancing space exploration and its applications, championed by organizations such as NASA and ESA. These organizations strive to foster

technological innovation in the space exploration domain and by supporting SPRL's research, this project makes a contribution towards those global initiatives. The instrumentation developed by SPRL must be rigorously and thoroughly tested to ensure functionality on mission. Failed missions can have an impact on the governments(taxpayers) that fund the missions. The work done by these organizations, and supported by the shock testing machine, can impact society through scientific discoveries and inspire interest in STEM fields.

2.3 Environmental Considerations

The environmental impact of the shock testing machine should be relatively small if the design does not employ any toxic materials and utilizes primarily recyclable materials. One advantage to building a testing machine for SPRL to use at their facility is that the carbon emissions from transporting the instrumentation to and from the external test lab will be eliminated. However, the power consumed by the laboratory will increase, therefore putting more strain on the power generation capabilities on campus. In addition to the environmental impact of the power consumption, there are significant safety considerations that must be made for the design. The testing machine, should it fail to meet requirements, could pose a significant hazard to the operator of the machine. Steps will need to be taken to ensure that the machine meets requirements, can be safely operated and maintained, and cannot cause injury to anyone using it. Organizations such as ASME and OSHA have developed standards specifically written to ensure safety of all personnel during any dangerous testing [14].

2.4 Ethical Considerations

One ethical consideration surrounding this project is allowing SPRL to keep their technology private. Most technology developed by SPRL is ITAR controlled and therefore data from any specific instrumentation is also ITAR controlled. It would be a violation of the ITAR guidelines to allow non-US persons to access or view this data. When looking for an external testing vendor, SPRL had to take extra precautions to ensure they stay within ITAR guidelines. There are also concerns that the external parties may damage the technology or share information about the technology without SPRL's consent. These ethical considerations provide additional motivation to successfully complete this project.

2.5 Inclusivity and Power Dynamics

Working in a team environment on a complex project like this brings about some intricate power dynamics that will ultimately affect the final form of the solution. As a group of four students from four vastly different backgrounds, our personal identities will also be different which means that we each have a unique perspective on this problem. For example, as someone who worked

as a co-op developing lifting tools for large fabrications, I'll have a different perspective on the methods and important considerations going into the development of this fixture than many of my teammates. Further, my teammates will also have vastly different experience from me which shapes their views on this project. By including each of our unique perspectives, we'll ensure that we have considered a wide variety of different designs and fabrication methods which ensures that our final product will work for all the relevant stakeholders.

3 User Requirements and Engineering Specifications

This section outlines the user requirements for the project and how they have been translated into engineering specifications. These specifications serve as quantifiable targets for guiding and evaluating the final design.

The determination of engineering targets involved discussions with stakeholders, analysis of related products, and benchmarking against industry standards. Each requirement was assessed for necessity, feasibility, and compliance with relevant standards. The prioritization of requirements was based on criticality to function, safety, and project constraints.

3.1 Requirements Development Process

The engineering targets were derived through the following process:

- **Stakeholder Input:** Direct consultation with the sponsor (SPRL) and ME450 Instructional team.
- **Benchmarking:** Evaluation of existing shock testing requirements, including specifications from Rocket Lab, SpaceX Falcon User Guide, and NASA GEVS standard. Evaluation of shock testing machines available for purchase online.
- **Regulatory Compliance:** Consideration of OSHA, NFPA, NEC, and aerospace standards for safety and operability.

SPRL provided the baseline specifications which define the functional requirements of the testing machine. From these functional requirements, we developed several requirements that will need to be met to ensure that the designed machine can meet the functional requirements reliably and safely. Each requirement is classified based on its importance:

- **Must Have (Essential):** Requirements that are mandatory for the system to function as intended.

- **Nice to Have (Desirable):** Features that would enhance performance, usability, or longevity but are not critical.

3.2 List of Requirements and Specifications

Table 1. Design requirements and specifications for the mechanical shock testing machine (shock fixture), including a rating of priority, a brief justification, and a verification method.

Req ID	Requirement	Priority	Specification	Justification	Verification
1	**Accommodates test specimens**	Must have	Maximum specimen mass = 25 kg ± 5 kg	Given by SPRL	Finite element analysis
			Maximum specimen envelope = 50 x 50 x 50 cm ± 5 cm	Given by SPRL	By measurement in CAD
2	**Compact**	Must have	Equipment shall fit within a 3m x 3m x 5m box when assembled and a 2m x 2m x 5m box when stored	Maximum allocated space by SPRL for use and storage of the device	By measurement in CAD
3	**Capable of desired shock profile(s)**	Must have	Peak acceleration capability = 750-3000 G ± 100 G	Given by SPRL	Finite element analysis and proof testing with representative mass
			Shock response spectra (SRS) frequency range = 100-10,000 Hz		
			Shock duration < 25 ms ± 5 ms		
4	**Compliance with aerospace standards**	Must have	Shock fixture shall be able to reproduce a Shock Response Spectrum (SRS) for a known mass DUT conforming to NASA General Environmental Verification Standards (GEVS) GSFC-STD-7000A [11]	Specified testing capabilities, directly from SPRL	Proof testing of manufactured machine

Req ID	Requirement	Priority	Specification	Justification	Verification
			DUT shall be able to have shocks applied in all 3 axes	Specified testing capabilities, directly from SPRL	
5	**Compatible with DAQ system**	Must have	Machine shall be compatible with VR9500 DAQ system and capable of sampling at a minimum of 100 kHz	SPRL DAQ system is the VR9500 controller. Minimizes measurement errors due to insufficient sampling rate, "signal aliasing"	DAQ system datasheet; proof testing of manufactured machine
6	**Durable**	Nice to have	All components shall be fatigue rated for minimum of 4,000 cycles	Minimizes maintenance costs and labor	Finite Element Analysis; part finishing/coating
			All components shall not corrode within 15 years	Minimizes maintenance costs and labor	
			Any parts that require maintenance more frequently than mentioned shall have replacement or maintenance criteria	Minimizes maintenance costs and labor	
7	**Isolated**	Must have	Shock fixture shall not cause damage to any surrounding equipment in the laboratory or the building itself. Dynamic transmitted loads shall not exceed 1.5X the static transmitted loads.	Shocks induced outside the machine are undesirable	Finite Element Analysis
8	**Affordable**	Must have	Total project cost (materials and manufacturing) < $40,000	Low-end estimated price of a shock machine with similar specifications. Project is moot if the cost exceeds the price of equivalent machinery.	By project budget and accounting
		Nice to have	Total project cost (materials and manufacturing) < $16,000	Four year pay off period assuming $4,000 spent	

Req ID	Requirement	Priority	Specification	Justification	Verification
				yearly on 3rd party testing	
9	Safe	Must have	Operator shall be protected by hazards created at point of operation in compliance with OSHA 1910.212: General requirements for all machines [12]	Large forces and fast moving parts may present hazards such as pinch points	By inspection
		Nice to have	A standard operating procedure (SOP) will be provided identifying nominal user operation, hazards, maintenance, and required PPE for users.	Improper use of the machine may be hazardous and PPE such as hearing protection may be required for operation.	Approval of SOP by SPRL
		Must have	Machine shall not utilize pyrotechnics or explosives	Request of SPRL	By inspection
10	Portable	Nice to have	Machine total weight shall not exceed 5000 lbs	Maximum load rating for standard pallet jacks	By measurement in CAD
11	Reliable	Must have	All components must have a positive margin of safety with a SF of 2 to material yield strength	Component failure could destroy the machine or pose a hazard to operators	Finite Element Analysis
		Must have	Resonant response of the shock fixture to any frequency expected during a test must not compromise the integrity	To prevent damage to the test fixture itself	Finite Element Analysis

4 Concept Generation

The goal of concept generation was to fully explore the solution space for possible architectures which satisfy the design requirements. A functional decomposition of the shock testing machine facilitated idea generation by identifying the unique, concept-agnostic functions which the machine must accomplish. The functional decomposition is shown in Figure 2 and is organized chronologically from the start to end of a test.

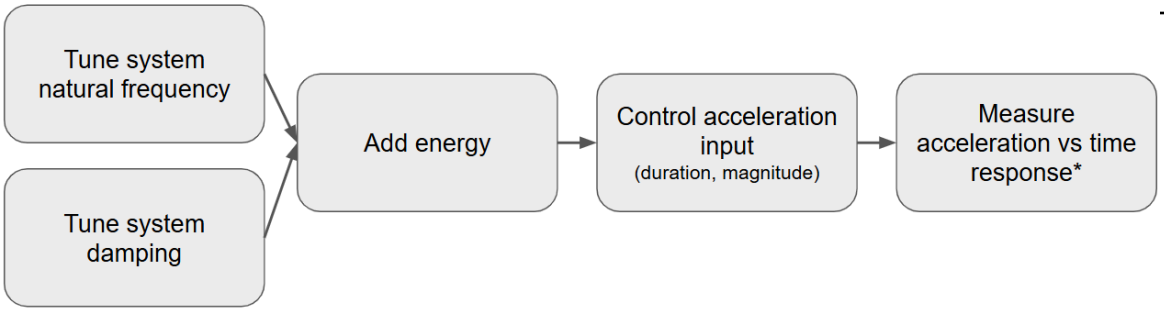


Figure 2. Functional decomposition of a shock testing machine for spacecraft instrumentation.
*Note: data acquisition is out of scope and will be handled by SPRL but included for thoroughness

Each member of the engineering team individually engaged in brainwriting to generate solutions for each function. For example, solutions to the function “add energy” included gravitational potential, pneumatic pressure, hydraulic pressure, springs/elastic materials, and electromechanical. Selecting one solution for each function yielded a complete concept for the shock testing machine and utilizing all possible combinations of solutions for each function produced a wide variety of concepts. A comprehensive collection of concepts is detailed in Appendix B. Over 80 potential solutions were generated between each team member at which point the focus transitioned from creating additional concepts to selecting the best one.

5 Concept Selection

Since the goal of the project is to deliver a functional, cost effective shock testing machine for SPRL, practicality of solutions far outweighs novelty. Ideas which would not feasibly meet the requirements (such as those involving pyrotechnics) and ideas which were complex with little or no existing documentation on their methods were cut. After coarse filtering for practicality and grouping similar ideas, five main concepts were identified for further evaluation.

The drop tower utilizes a carriage running on a vertical track which collides with a base in a controlled manner. Two derivatives of the drop tower were considered. The passive drop tower exclusively utilizes gravity to accelerate the carriage. The powered drop tower uses elastic bands or motors to accelerate the carriage beyond 1 G and achieve higher impact velocities without adding height to the machine. Figure 3a shows a commercially available passive drop tower.

The hammer or pendulum shock test machine architecture uses a mass on an arm of a fixed length which strikes a plate or a weldment which the device under test is rigidly attached to. Both a passive and a powered version of the hammer machine were considered where the rotating arm is accelerated beyond gravity in the latter. This architecture can take advantage of resonance in the plate or weldment to induce accelerations in the test specimen which are higher than the input magnitude. In the European Space Agency’s shock test bench shown in Figure 3b, a hammer strikes an aluminum plate.

A pneumatic machine uses a piston to precisely accelerate a carriage with the device under test attached. Although this piston can be used to directly induce the test accelerations of the device for lower G applications often referred to as a “bump” machine, for our application we consider an architecture where the carriage collides with a bumper to induce high magnitude acceleration. The machine shown in Figure 3c utilizes this architecture.



(a) (b) (c)

Figure 3. (a) Lansmont model 23D drop tower [22], (b) European Space Agency pendulum hammer shock test bench [23], and (c) CME model KRD15 pneumatic horizontal shock response spectrum test system [24]

The down-select process began by implementing a Pugh matrix with eleven categories derived from the requirements. Each category was assigned a weight between one and five where one indicates minimal importance and five indicates utmost importance. The passive drop architecture was used as a baseline and scored zero for all categories. Each concept was then scored against the passive drop. A negative one or two indicates slightly or much worse respectively, a positive one or two indicates slightly or much better respectively, and a zero indicates the concept is comparable to the baseline for that category. The Pugh matrix showing each concept's score for every category is shown in Table 2.

Table 2. Pugh Matrix comparing five concept architectures

Category	Weight (1-5)	Passive Drop	Powered Drop	Passive Hammer	Powered Hammer	Pneumatic
Cost	4	0	-1	2	1	-2
Full size	1	0	1	2	2	2
Collapsed size	3	0	1	2	2	2
Lead time	5	0	-2	0	-1	-2
Manufacturability	3	0	1	2	2	2
Complexity of assembling	1	0	-2	0	-2	-2
Complexity of testing (to use)	2	0	-1	-2	-2	1
Complexity of design	3	0	-1	0	-1	-2
Safety	3	0	0	-2	-2	-2
Reliability	3	0	0	0	0	-2
Technical expertise relevance	3	0	0	0	0	-2
Total	-	**0**	**-14**	**12**	**-2**	**-28**

The pneumatic architecture scored lowest primarily driven by the increased complexity and cost of the high pressure system. To facilitate repeatable tests, precise control is needed over the piston via valves and some kind of control system. Pressure vessels and a compressor to generate high pressure air would also need to be components of the design which bring with them cost and complexity. Additionally, the team does not have any prior experience working with pneumatic systems. For these reasons, the pneumatic architecture was cut.

The next lowest scoring concepts were the powered drop and powered hammer. They both scored lower than their passive counterparts due to the added cost and complexity of the acceleration systems. Adding elastic bands, a torsion spring, or motors introduces more parts which need to be purchased, manufactured, integrated, and/or assembled. The powered concepts offered some benefit by reducing the size of the machine compared to a passive concept, but this was outweighed by the downsides.
Between the passive drop tower and the passive hammer, the hammer proved the better concept. The cost of the hammer is primarily driven by raw materials for the weldment or plate and structure. The drop tower requires large precision rails and linear bearings which are relatively more expensive. Although the drop tower has a smaller footprint, it will need to be at least three meters tall to meet the acceleration requirements which is approaching the maximum allowable dimensions for the machine. The hammer architecture can be achieved in a table sized assembly and fits well within the specification when taking advantage of resonance in a “ringing plate” to amplify the output acceleration relative to the input. The lead time is believed to be comparable for both architectures as metal suppliers and McMaster Carr should cover most components. The manufacturability of the hammer is superior as the majority of the design will not require machining. The drop tower will likely require several custom brackets and parts to facilitate precise alignment. The complexity of assembly and design as well as the reliability and the team’s expertise are all comparable between the two architectures. The complexity of testing is considered worse for the hammer because in addition to the hammer height, the DUT positioning and plate boundary conditions also need to be manually configured by the test operator. Safety was also considered worse for the hammer concept because it will be harder to protect the pinch points of the hammer strike zone than the drop tower collision interface since the operator doesn’t have to access the drop tower interface to set up a test.

Ultimately, this process led the team to choose a passive hammer architecture. Specifically, the team chose a hammer striking a ringing plate as opposed to a weldment because a plate is simpler to model and analyze and there is existing technical documentation on the ringing plate method. SPRL was satisfied with the selection of this concept and the prevalence of this architecture in other space instrumentation testing applications reaffirms it is a viable choice.

6 Selected Concept: Hammer striking ringing plate

With the down-select process indicating that a hammer striking a ringing plate is the best solution to satisfy all requirements and engineering specifications of the project, detailed design and analysis was begun. Although much more design and analysis is yet to be complete, an “alpha design” or initial design serving as a starting point and framework for the final product is presented in this section.

6.1 Alpha Design

The alpha design is a generic version of the hammer striking a ringing plate but is inspired by the European Space Agency shock test bench [23] and a similar existing bench developed by a student at Chalmers University in Sweden [25]. The design is broken into nine subsystems identified in Figure 4, and achieves the functions from the functional decomposition in Figure 2.

The system damping and natural frequency are tuned by the (X,Y) coordinates of the DUT placement on the plate, the isolation material properties, and the boundary conditions of the plate (support location/type). Energy is added to the system by raising the hammer with the hoist and releasing it. The acceleration input denoted ẍ(t) is controlled by the variable drop height of the hammer, adjustable hammer mass, and hammer tip and strike plate materials. The acceleration response–denoted ÿ(t)–will be measured using provided equipment, specifically the VR9500 controller and accelerometers mounted at the fixture plate to DUT interface.

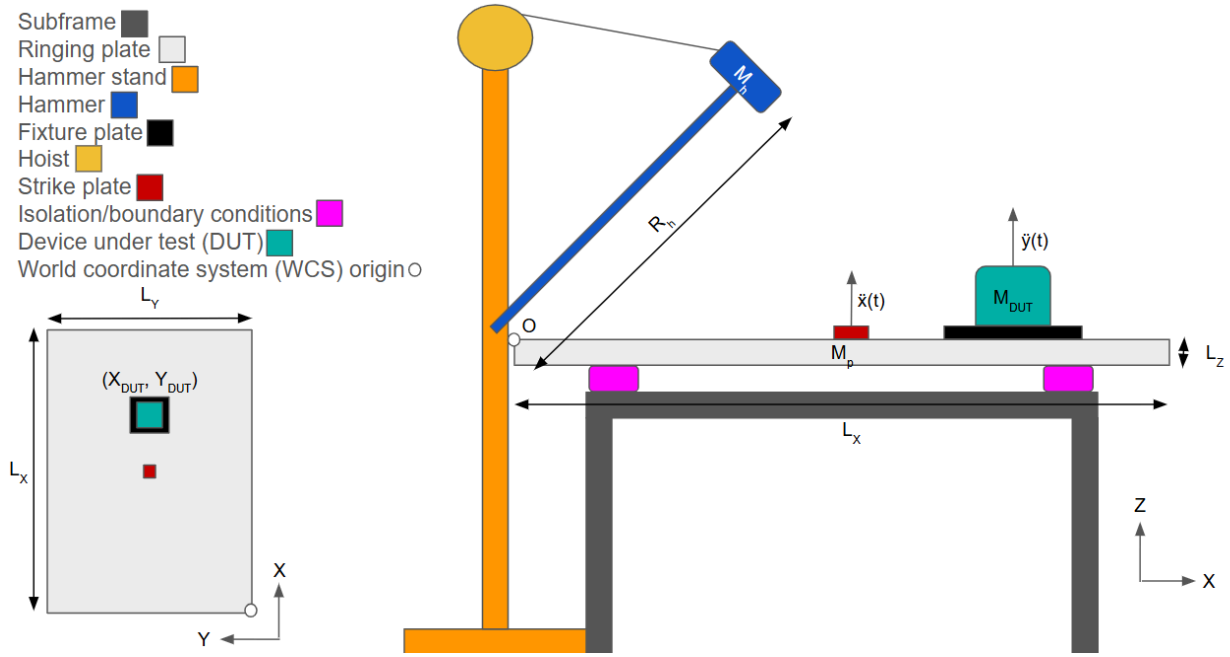


Figure 4. Alpha design and subsystems with labeled parameters

This version of the alpha design only includes parameterized values and dimensions as more rigorous engineering analysis is required to properly size components. Full-size CAD models, FEA models, and simpler MATLAB based physics models are all being employed to analyze the acceleration response of the design and its ability to meet the specifications. Because developing these models quickly relies on assumptions like the precise nature of the hammer on strike plate collision, which may have a non-negligible effect on the validity of the model, a small scale prototype is being designed, analyzed and fabricated in parallel to help validate the models.

6.2 Small-scale Prototype Shock Tester

The prototype shock tester is not designed to meet the specifications in place for the full size shock tester. The primary objectives of the prototype shock tester is to allow our team to explore

the effects of varying test parameters on the output SRS and to evaluate discrepancies between our simulations and experimental data. Achieving both of these objectives will greatly increase the robustness of the final shock tester design. Comparing various test parameters (setups) will be valuable because the team will have a stronger understanding of the "levers" in the design that can be adjusted to achieve the challenging specifications outlined for the full size tester. Additionally, these trends can be documented to expedite the tuning process for a specific SRS in future tests, therefore making the machine more usable for SPRL. Using the prototype shock tester to validate simulations is a critical step to ensure that the full size shock tester will be able to meet the specifications that it is designed to in the computer.

The driving principle in designing the prototype shock tester is minimizing time/effort to build. This is because the team has finite time and resources and must be able to produce the prototype tester very quickly in order to properly utilize it. A breakdown of the prototype shock tester is shown in Fig. 5.

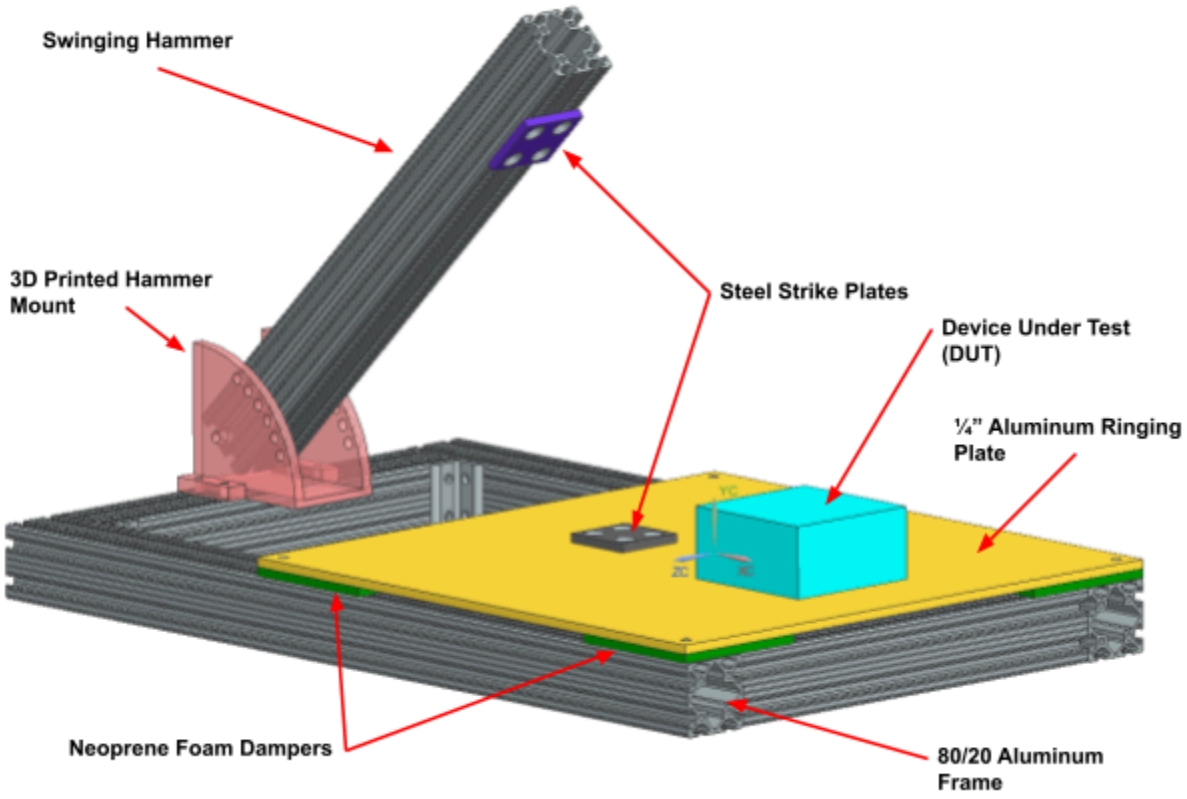


Figure 5. Diagram of the prototype shock tester

The prototype shock tester is built from primarily aluminum materials. The 80/20 aluminum frame was selected because it is easy to construct and minimizes the number of holes that need to be drilled to build the frame, since it can be assembled using T-slot nuts. Additionally, SPRL has this 80/20 in inventory, leftover from a previous project, therefore greatly reducing the BOM cost for the prototype shock tester. Steel was chosen as the material for the strike plates because the higher modulus (~210 GPa) of the steel compared to other material options, such as aluminum, will shorten the pulse duration of the shock, which should excite higher frequencies in the plate

and be allow the results to be more comparable to the full-size shock tester. The hammer is supported by a 3D printed mount (PLA) that allows it to be dropped from a variety of heights, providing adjustability in the amplitude of the input acceleration (Fig. 6). Holes in the mount accept a pin that will hold the hammer at a consistent drop height between tests. The hammer is supported by two bushings rotating on a shoulder bolt for consistent, smooth rotation.

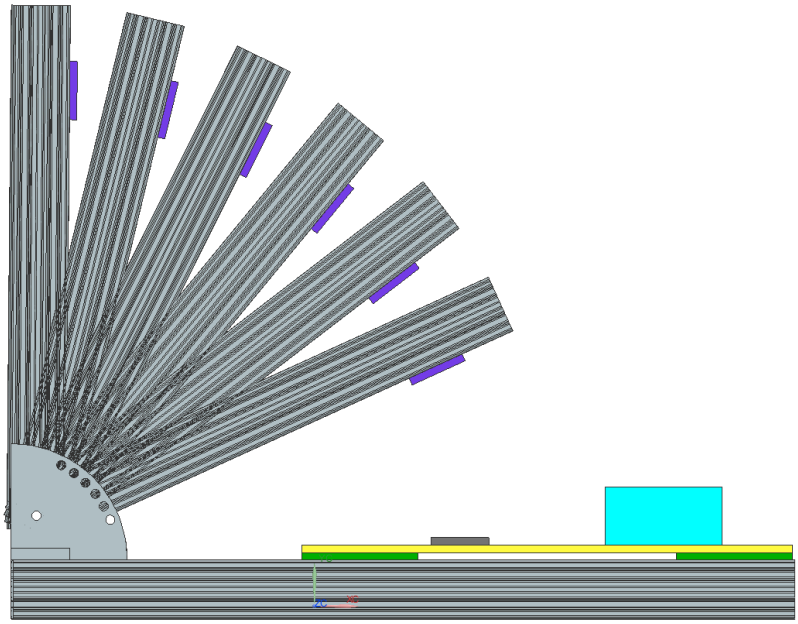


Figure 6. Hammer motion in the prototype shock tester

The total BOM cost of the prototype shock tester is less than $400 and it should take only a few days to build and assemble.

7 Problem Analysis and Future Engineering Work

Since DR1, our ultimate goal of delivering a fully-functional shock testing machine for SPRL has not been changed. At the end of the semester we intend to have a machine ready for SPRL to begin testing instrumentation. Before building the full-size version to the testing machine, we will build a miniature prototype shock tester that will guide our design decisions for the full-size version. Although we believe we are on the right track to developing a solution which meets all requirements and specifications, there are several areas of the design process which need further attention and engineering effort.

7.1 The Ringing Plate

The principal design driver of the ringing plate hammer shock test machine is of course the ringing plate. The ringing plate determines the frequencies that will be excited due to a given hammer strike, which is a key consideration in the design due to the 100-10,000Hz test capability requirement. The ringing plate also determines the transmissibility of the acceleration input to acceleration output, meaning that depending on the ringing plate and how it is mounted, we can adjust the peak acceleration on the DUT for a given hammer strike. Currently, the team

believes that the plate will be at least $1m^2$ x 1" thick, most likely aluminum. Plates of this size are accessible with a short lead time but come at a high cost (recent estimates put it around ~$3000-$4000), making the ringing plate the largest line-item of the whole machine.

The team's highest priority at this point in the design is to analyze the ringing plate to a sufficient amount of detail to determine the size and material of the plate, allowing the plate to be ordered and designed around. To tackle this problem, we have developed a Python script that interfaces with ANSYS Discovery and ANSYS Mechanical. It allows us to input parameters (dimensions of the plate, boundary conditions, meshing, etc.) and automatically generate a model that can determine the resonant frequencies of the plate via modal analysis in ANSYS Mechanical. We are working to extend this capability to perform a response spectrum analysis.

7.2 Information Gaps

Since DR1, our team's understanding of this problem has improved immensely. However, the problem is inherently very complex and utilizes principles that extend beyond typical undergraduate education. We have identified some information gaps that we are working to close soon. One information gap is how the machine can excite a wide range of frequencies with a single hammer strike. From literature, we have deduced that a single strike of the hammer can produce an SRS that spans the range of 100-10,000 Hz, but we do not understand how this is done and how the input acceleration needs to look in order to achieve this output.

Another information gap is the acceleration input from the hammer. We understand that the hammer will create an acceleration vs time input forcing function, but we are unsure of how to precisely characterize this function and utilize it in our analysis. We are working on modeling collision mechanics in MATLAB to generate this data and use it in ANSYS.

7.3 Anticipated Challenges

We are most concerned about the timeline to complete the machine and validate the design against the specifications. We need to design the machine quickly and efficiently in order to complete the BOM in time to send out parts and then subsequently build the machine before the end of the semester. If the full-size assembled machine does not perform as the models predict, there will be minimal time for corrective action. Our approach to solving this problem is rapid development of a simple, inexpensive representative physical system. We are developing the miniature shock tester in parallel with the full size shock tester and the analysis for both by allocating responsibilities on our team efficiently. We expect to learn a lot from the small-scale model in the coming two weeks before we finalize the design of the full-scale solution.

8 Engineering Analysis

The goal of the mechanical shock testing fixture is to generate a shock response spectrum which meets the specifications outlined in NASA's GEVS [11]. This was the most critical analysis that our group did since it determined the functionality of the fixture. The team's process behind generating the SRS consists of the following three steps:

1. Find the hammer's impact force onto the strike plate as a function of the hammer radius, hammer length, and drop angle (Section 8.1)
2. Simulate the ringing plate's response to the hammer input using ANSYS Explicit Dynamics modeling (Section 8.2)
3. Use the Smallwood Algorithm to turn the hammer and DUT response data into an SRS (Section 8.3)

In addition to the "SRS Analysis", the team conducted an experimental test to check our analysis and performed a structural analysis of the overall final structure to ensure that all the components will have a margin of safety to yield during operation.

8.1 Hammer Impact Force

Modeling the time domain acceleration induced in the ringing plate by the hammer is prerequisite to modeling the output acceleration and SRS experienced by the device under test. A model governing the interaction between the hammer and the ringing plate during impact is presented by Morais and Vasques in their 2016 paper, *Shock Environment Design for Space Equipment Testing* [26] and assumes a sphere colliding with an elastic half sphere based in Hertzian contact theory. The impact dynamics are modeled as the superposition of the rigid body dynamics and elastic properties of the colliding entities. While the bodies are in contact, the system is represented as an equivalent mass-spring system governed by a non-linear differential equation of motion and system properties given in Equations (1), (2) and (3).

$$m_s \ddot{x}_s(t) + k_{eq} x_s^{\alpha}(t) = 0 \qquad (1)\ [26]$$

$$\frac{1}{k_{eq}} = \frac{3}{4}\left(\frac{1-\nu_s^2}{E_s} + \frac{1-\nu_p^2}{E_p}\right)\frac{1}{\sqrt{r_{eq}}} \qquad (2)\ [26]$$

$$\frac{1}{r_{eq}} = \frac{1}{r_s} + \frac{1}{r_p} \approx \frac{1}{r_s} \qquad (3)\ [26]$$

where α = 3/2, E is the Young's modulus, ν is the Poisson's ratio, r is the radius of curvature, and the subscripts s and p refer to the hammer and plate respectively. Equations (1), (2), and (3) were

developed into MATLAB code which was used to solve the differential equation for defined system properties. The MATLAB code is presented in Appendix E. The script outputs position, velocity, acceleration, and force versus time data for a given hammer mass, radius, length, drop height, and material properties. Figure 7. shows an example motion and force profile generated from the MATLAB script. The model was used to generate acceleration and force data to be passed into ANSYS for further analysis.

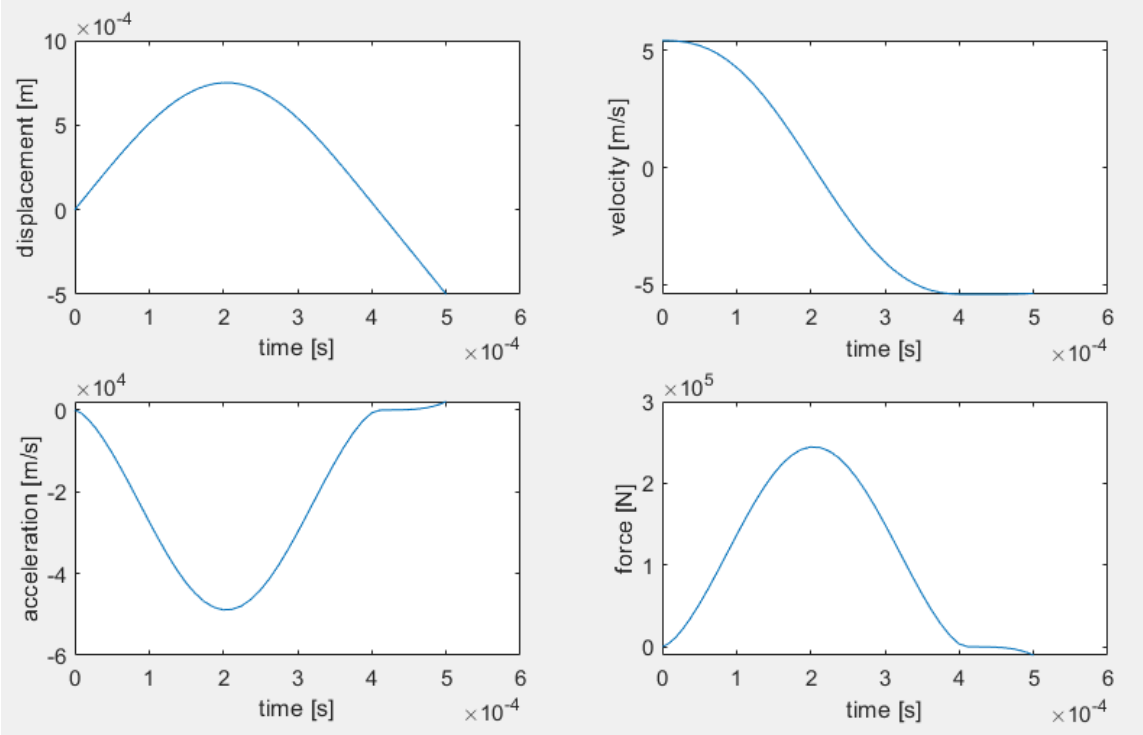


Figure 7. Motion and force profile for a 10 kg, 1.5 m long, 25 mm radius aluminum hammer dropped from 88 degrees onto a steel strike surface.

8.2 ANSYS Explicit Dynamics Model

The team used ANSYS to simulate the response of the ringing plate to a base excitation caused by this hammer. We were interested in the effect of the following tuning parameters on the output SRS of the system.

- Plate size
- Isolator stiffness
- Isolator location
- Hammer length
- Hammer mass
- Strike plate footprint
- Strike plate location
- DUT footprint
- DUT size
- DUT location

Since we are mainly interested in the response of the ringing plate, this is the only object which is modeled into ANSYS. The strike plate and DUT had remote points with rigid behavior scoped to them so that the plate cannot bend significantly at the mounting locations (both strike plate and DUT will be bolted to the ringing plate thereby constraining it), but not take up computational time unnecessarily modeling in two rectangular prisms. These areas are representative of the strike plate size and the expected DUT size respectively. Below the out-of-plane (OOP) configuration is shown, but the in-plane (IP) configuration was also simulated.

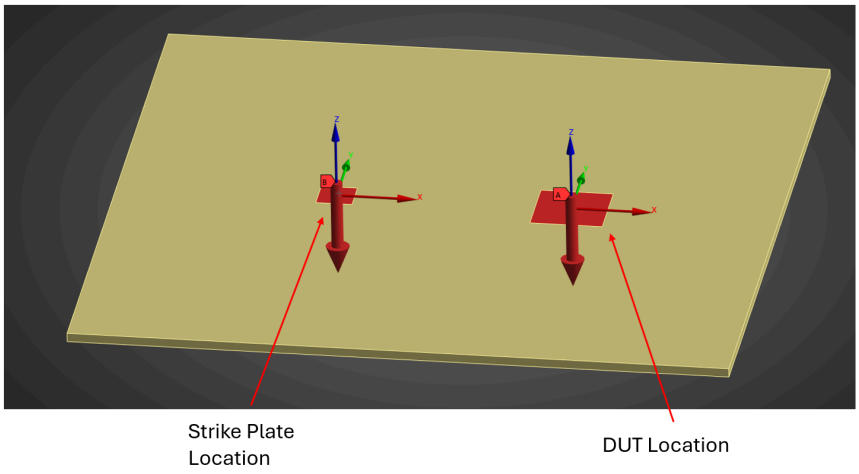


Figure 8. Explicit dynamics strike plate and DUT setup

To constrain this model, fixed remote displacement boundary conditions were used. This is done since it models the isolators which sit below the plate. While the below model only shows four isolators, models with six isolators were also used.

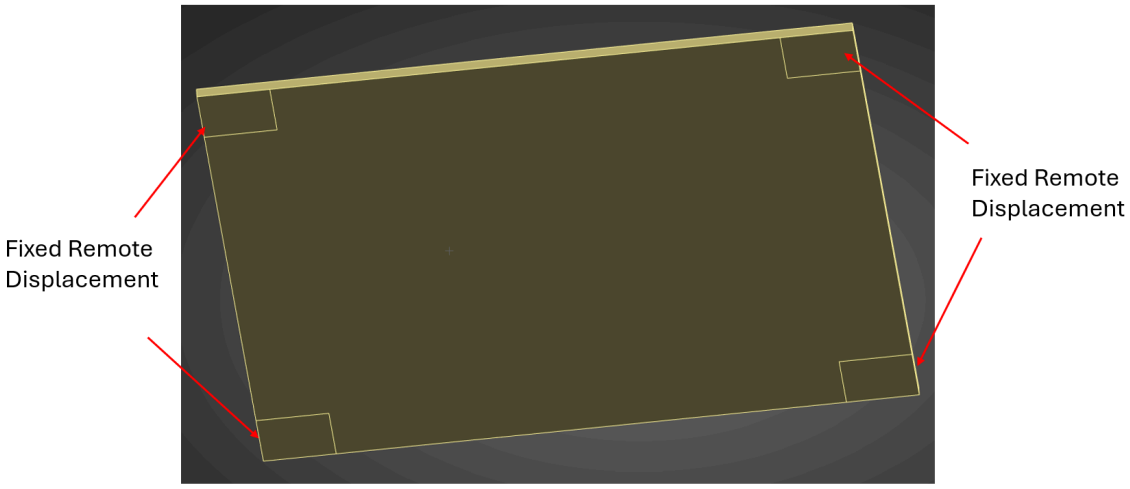


Figure 9. Explicit dynamics boundary conditions

At the start of the section, we laid out the variables which we wanted to understand the impact of. To do this effectively, we had to set up a series of ANSYS runs to quickly iterate through different designs. Thus, a parametrized model in ANSYS was set up. Using Discovery Scripting and Mechanical Scripting, we were able to turn the annoying set-up process (geometry import, imprinting, boundary conditions, mesh controls) into two scripts. See the following mini-presentation on the methodology behind the scripting used to set up each model.

Also, given the long run time of each model (~ 4 hours per model on Duderstadt CAEN computers) and the large size of each output file (~60 GB), the team had to be deliberate with the runs that were simulated and what information was extracted from each model. Thus, the team set up the following matrix to help control this. Table 3 shows a small snapshot of the series of runs which were simulated to quantify the impact of each variable.

Table 3. ANSYS Simulation Matrix

Variable	Run A	Run B	Run C	Run D	Run E
Plate xdim [mm]	1,200.0	1,000.0	1,000.0	1,200.0	1,000.0
DUT Weight [kg]	10.0	10.0	2.0	2.0	2.0
Isolator Count	4	4	4	4	6
Hammer Input [Excel]	"hammer_input_force"	"hammer_input_force"	"hammer_input_force"	"hammer_input_force"	"hammer_input_force"
Hammer Dead Weight on Strike [kg]	10	10	10	10	10
Single Mode Dominant?	Y	Y	Y	Y	Y
End Time [s]	0.05	0.05	0.05	0.05	0.05
Result Number of Points	50,000	50,000	5,000	5,000	5,000
Mesh Size [m]	0.014	0.014	0.014	0.014	0.014
Test Direction	OOP	OOP	OOP	OOP	OOP
Peak Stress [MPa]			187.8	175.8	184.8

The following data is extracted from each ANSYS model of the ringing plate

- Modes and Participation Factors (modal run)
- Strike plate position
- Strike plate velocity
- Strike plate acceleration
- DUT position
- DUT velocity
- DUT acceleration
- Maximum ringing plate stress over time

The strike plate position and DUT accelerations are then used in the Smallwood algorithm to calculate the system's SRS (detailed in Section 8.3).

8.3 Smallwood Algorithm

To give a brief summary of what the shock response spectrum (SRS) is, it calculates the peak acceleration in either the positive or negative direction (often called the maximax acceleration) of the output at a wide range of natural frequencies. As shown in Figure 10, for a given input, a single degree of freedom (SDOF) system with a predefined natural frequency will have a quantifiable output. With a known input, we can use the SDOF mathematical model across a wide range of natural frequencies to find the maximax acceleration as a function of the natural frequency of the system. However, in practice it's not feasible to build a series of systems with a series of natural frequencies (or continuously tune a system to vary the frequencies). Plus, we do not want to test the DUT for fatigue failure by subjecting it to a battery of tests. For those reasons, we require a few mathematical tricks (i.e. the Smallwood algorithm) to turn our measured acceleration data from a single test into a continuous SRS.

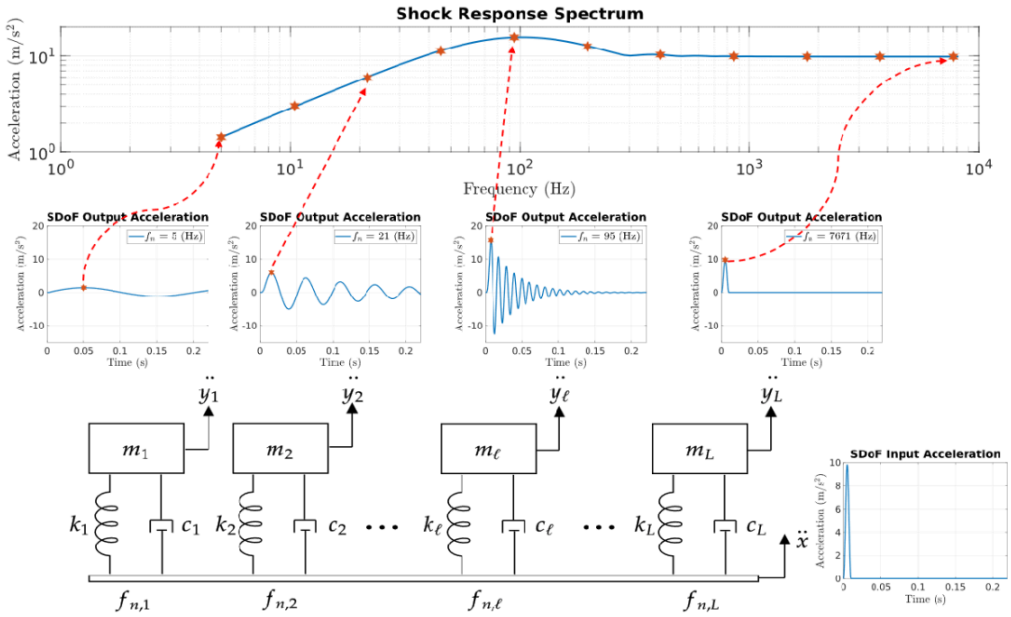


Figure 10. Methodology demonstrating SRS generation [28]

We predict the SRS using the simulation data from ANSYS described in Section 8.2. From the ANSYS runs, we have the time response of both the strike plate and the DUT. The basic premise of the SRS is detailed in "Principles and Techniques of Shock Data Analysis" by Ronald D. Kelly and George Richman. [27] It relies on the calculation of the response of the SDOF system to a forced input.

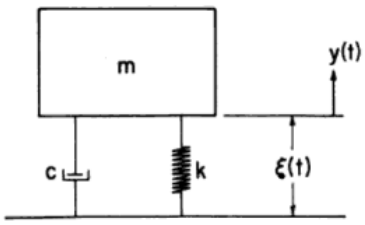


Fig. 4.11. A simple mechanical oscillator with damping.

Figure 11. Single degree of freedom system assumed in SRS generation [27]

As was shown earlier, the model assumes there is a base excitation x that causes a response y in this SDOF system. In our case, this will describe the hammer's base excitation (x) that causes the DUT (y) to vibrate on the ringing plate. Within this model, the displacement of the DUT relative to the hammer is denoted as xi. This relative displacement xi is directly related to a common measurement in shock analysis known as the pseudo velocity (shown in Equation 4.17). While this is a useful measurement in analyzing the severity of a shock, it is not in scope per the requirements laid out by NASA GEVS [11] and by SPRL to quantify the pseudo velocity of the DUT. However, xi is also used when calculating the shock response spectrum as will be shown later, so it's useful to describe its meaning here.

In actual practice, two other responses are also used. The first of these is the pseudovelocity $V(t)$ defined by

$$V(t) = 2\pi f_n \xi(t), \qquad (4.17)$$

[27]

For an unforced and underdamped single-degree-of-freedom system, the system's response can be described with Equation (4). However, the SDOF system being used for our shock fixture cannot be approximated as a single base excitation. In fact, it has a forced input throughout the duration of the shock. Thus, it's necessary to use the Duhamel integral. This is an integral (outlined in the "Principles and Techniques of Shock Data Analysis") which is simply a convolution of the acceleration of the input function x with the general response to the base excitation (Equation 4) to find the output response of the system (see Equation 4.30).

$$x(t) = e^{-\zeta\omega_n t}\left(A\cos(\omega_d t) + B\sin(\omega_d t)\right) \qquad (4)$$

$$\ddot{y}(t) = 2\zeta\omega_n \int_0^t \dot{x}(\tau) e^{-\zeta\omega_n(t-\tau)} \cos\,\omega_d(t-\tau)\,d\tau + (2\zeta^2 - 1)\omega_n^2 \xi(t). \qquad (4.30)$$

[27]

Put differently, from acceleration data for the strike plate (x) and the DUT (y), we can now use the Duhamel integral to find xi (a measure of the shock severity as a function of time). As inputs to this equation, we need to know the natural frequency of the system (ω_n) and the damping ratio (ζ). The natural frequency is important since it dictates the response of the system itself. On the

other hand, since the shock is so transient (<100 ms), the damping of the system has a negligible effect on the response. In these calculations, 5% is assumed.

From xi, we can find the input acceleration to the system using Equation 4.23. Again, it relies on convolving the input with the unforced natural response of the SDOF system. Through some algebraic manipulation, the time response of the input acceleration can be found using the relative displacement.

$$\xi(t) = -\frac{1}{\omega_d}\int_0^t \ddot{x}(\tau) e^{-\zeta\omega_n(t-\tau)} \sin \omega_d(t-\tau)\, d\tau. \qquad (4.23)$$ [27]

The first question that arises is why we used the input and output acceleration data to then find the input acceleration data. At first glance, it seems counterintuitive and unnecessary. Put simply, the reason behind this is that the underlying equation behind this model (called the "relative displacement model") relies on Equation 4.20. This means that the relative displacement of the DUT relative to the strike plate is used as the measure of the intensity of the shock. Though we don't measure the relative displacement directly, we want to ensure that the data used for the relative displacement (the measure of the intensity of the shock) is accurate, then use this "intensity measurement" across a wide range of different natural frequencies.

$$\ddot{\xi}(t) + 2\zeta\omega_n\dot{\xi}(t) + \omega_n^2\xi(t) = -\ddot{x}(t), \qquad (4.20)$$ [27]

The second question that arises is whether the SDOF model really applies to this data. Looking at the modal participation factors in the ringing plate, we cannot make the assumption that it rings with a single dominant frequency. However, we can break away from saying that this system is a single SDOF system and move to say that it's multiple SDOF systems in parallel. To do this, we can take a Fast Fourier Transform (FFT) of the input and output responses to find the constituent frequency responses of the system. The figure below shows the original input acceleration (measured form ANSYS) compared to the reconstructed signal after the FFT is performed and added. From the FFT, we now know the time history response of each mode of the plate. Thus, instead of putting in the total acceleration response, we can use superposition to add each response and "natural frequency" (really mode in this case) to find an effective xi.

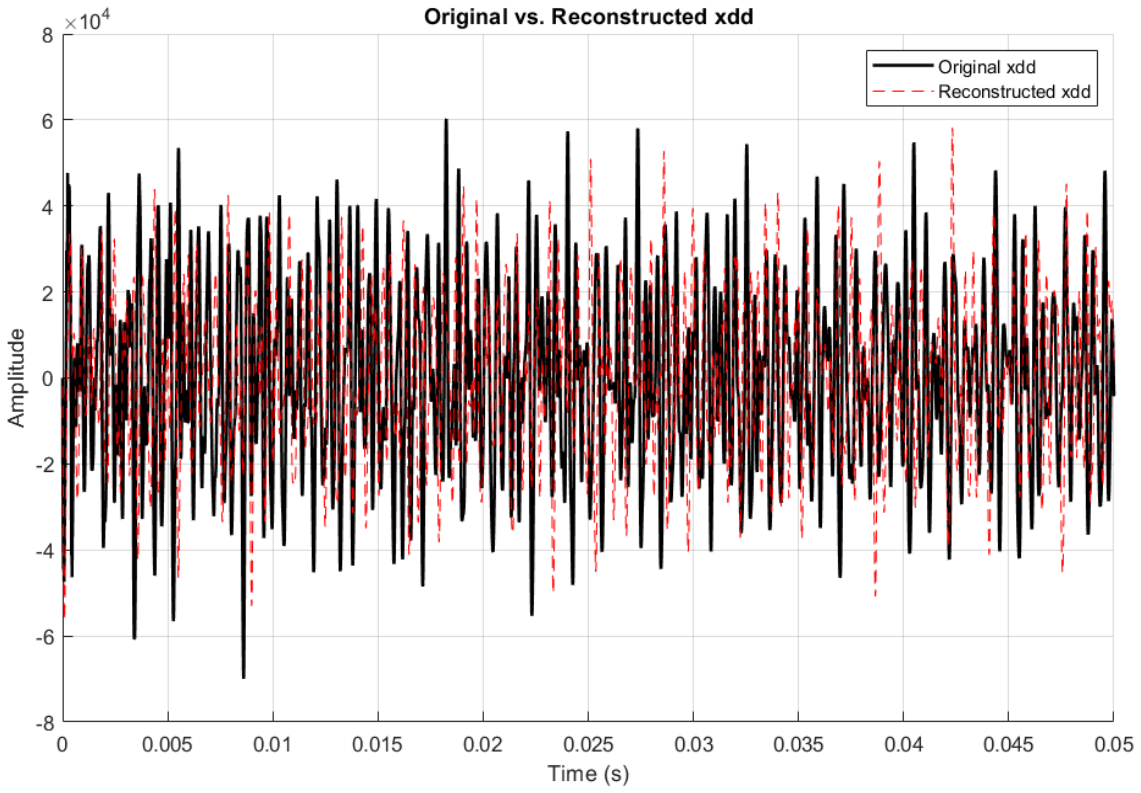


Figure 12. Reconstruction of acceleration time history using an FFT

The other piece of information which the FFT tells us is the constituent frequencies of the signal. These constituent frequencies match (with some error) the modes of the plate with the dominant modes in the plate. This gives confidence that this plate can be modeled with a multitude of SDOF systems in parallel meaning that this methodology holds.

Now that we have an "accurate" input acceleration time history, we can now abstract this across a range of system natural frequencies. In other words, we will use the input acceleration we just calculated and use Equations 4.23 and 4.30 to find the output acceleration, but iterate across a wide range of natural frequencies (not just those of the physical system). With the response acceleration time histories, we can then find the maximum acceleration and create the SRS.

Below is a recap of the mathematical steps taken in MATLAB to go from the output acceleration data from ANSYS to a generated SRS.

1. Perform an FFT of the input and output data to break up the total response into its constituent frequencies
2. Use Equation 4.30 to find xi (the displacement of the DUT relative to the strike plate) from the input and response acceleration time histories. This is done for each constituent frequency.

3. Use Equation 4.23 to find the input acceleration from xi. Again, this is done for each constituent frequency.
4. Add each input acceleration together using superposition. We assumed this was a bunch of SDOF systems in parallel, so to find the total input, we must add each input to each SDOF system together.
5. Normalize the signal energy with respect to the input. There is a lot of numerical error introduced from the numerical convolutions and FFTs, so this just ensures that the input to the SRS has the same energy (kinetic energy in this case) as was predicted in ANSYS.
6. With the input acceleration that was just generated, use Equations 4.23 and 4.30 (again) to find the maximax acceleration across the range of natural frequencies desired. In the case of this analysis, we care about 100 Hz to 10 kHz.

8.4 Empirical Shock Response Spectra with Small Scale Prototype Shock Tester

Going back to Section 6.2, the group chose to conduct a trial test on a small scale prototype of our model. The main purposes of this test were to validate the analytical model for SRS generation detailed from Sections 8.1 to 8.3 and to serve as a training tool for our team to learn how to do this empirically before assembling the full-scale tester. Figure 13 shows the physical model that is shown in the CAD by Figure 6. We used a 1 lb weight plate that was hot glued to the ringing plate to represent the rigidly attached DUT. There was also an attachable weight plate adapter (not shown) which lets the user attach weights to the hammer. The hammer mount (the black 3D printed piece that holds the hammer) has slots in the side which are used to control the drop height of the hammer into the ringing plate. Two accelerometers were attached to the shock tester — one to the hammer and another to the DUT. These two accelerometers were rated for 500G and 2000G respectively.

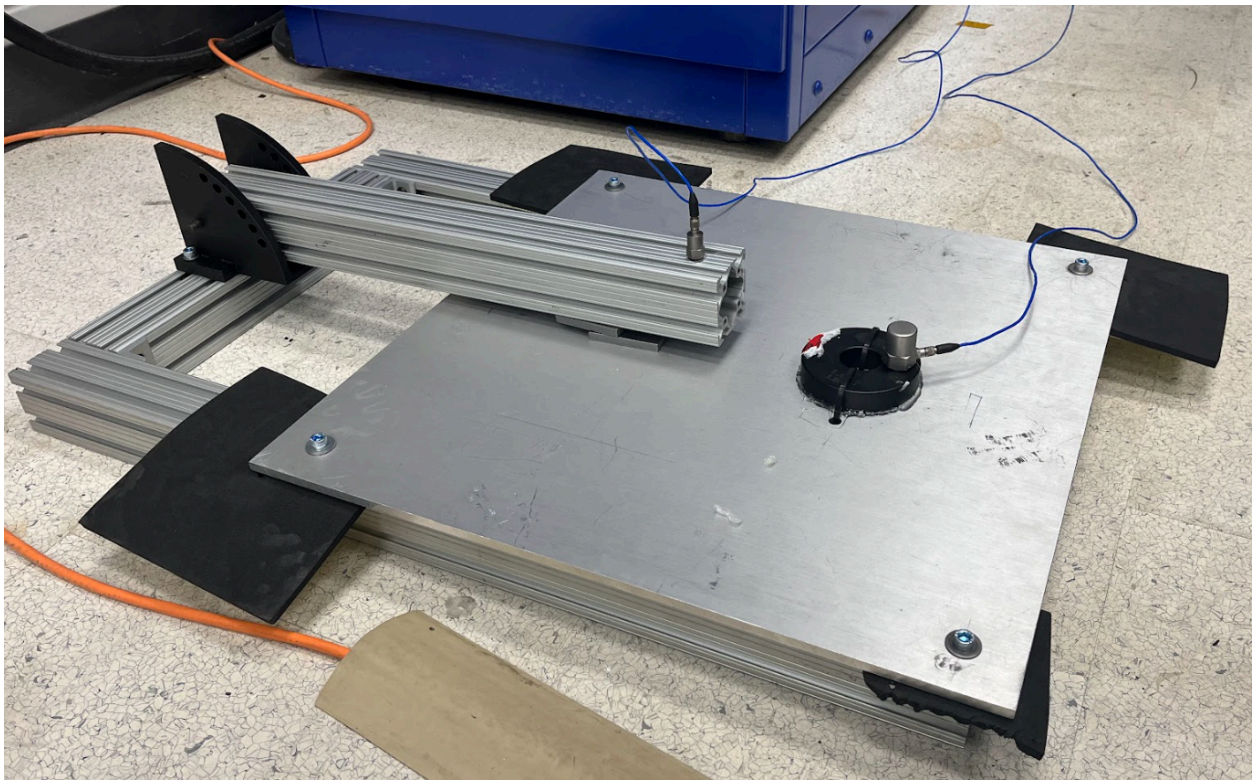


Figure 13. Small scale, “mini” shock test fixture

During testing, five unique runs with three trials each were conducted. These runs are described in Table 4. The two variables which were measured during this preliminary testing were the effects of the drop height and hammer weight on the DUT’s response.

Table 4. Small Scale Test Matrix

	Run 1	Run 2	Run 6	Run 7	Run 8
Hammer Weight Added [lb]	1	1	0	0	0
DUT Weight [kg]	0.5	0.5	0.5	0.5	0.5
Unique Isolator Positions	4	4	4	4	4
Isolator Dim [in]	2	2	2	2	2
Isolators in z direction used	1	1	1	1	1
Slot Dropped	1	2	1	2	3

To process the accelerometer data and create the SRS’s from the empirical data, VibrationVIEW was used. Figure 14 shows the SRS’s generated for Runs 6, 7 and 8. This demonstrates the impact of drop height on the shock response spectrum. As expected, increasing the drop height shifts the SRS up vertically.



Figure 14. Experimental SRS results of varying drop height

Further, Runs 1 and 2 were conducted with a 1 lb mass attached to the hammer while Runs 6-8 were not. In Figure 15, the runs with an added mass are represented with solid lines while those without the added mass are represented with dashed lines. Figure 15 shows that the added mass also shifts the SRS up.

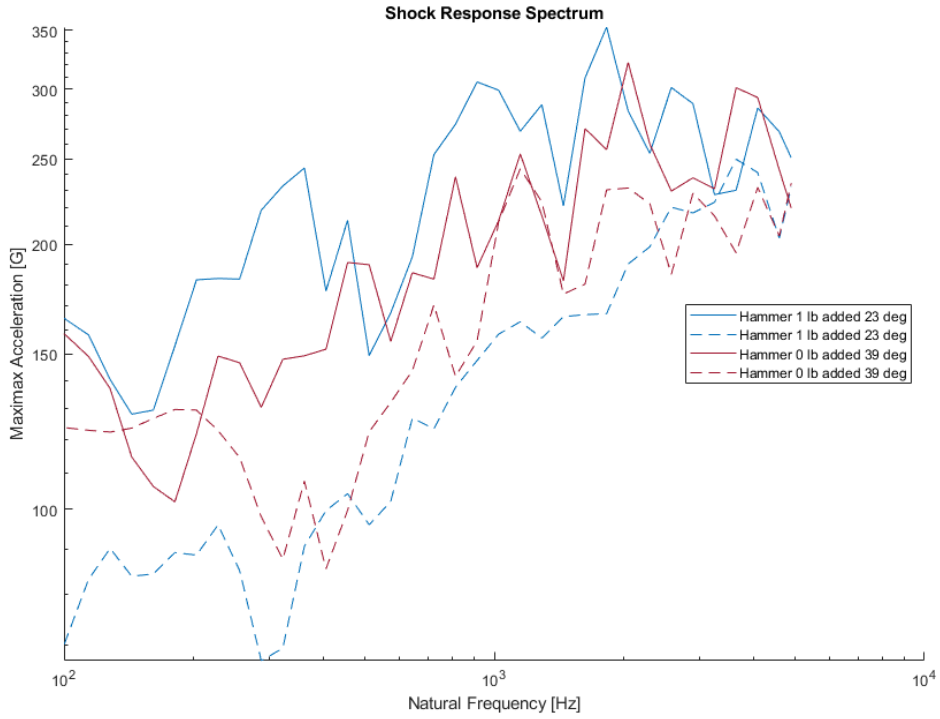


Figure 15. Experimental SRS results of varying hammer mass

When conducting the prototype testing, we were limited by the strength of the hot glue in this mounting configuration. For any slot higher than the fourth (or drop angles above 50 degrees), the hot glue between the accelerometers and the mounting location would break. Thus, we weren't able to get data at high accelerations. To remedy this, we could drill a clearance hole into the DUT and the hammer since the accelerometers do have internal threads, but the team believes that the data collected from the test is enough to satisfy both purposes of the test — to train us in using VibrationView and to use as a comparison point ot the analytical model (discussed in Section 8.5).

From this testing, two lessons were used to improve our analysis methods. First, comparing the FFT of the analytical data to that of the empirical data proved to be surprisingly different. Looking at Figure 16, the constituent frequencies of the analytical model are significantly higher than those in the experiment.

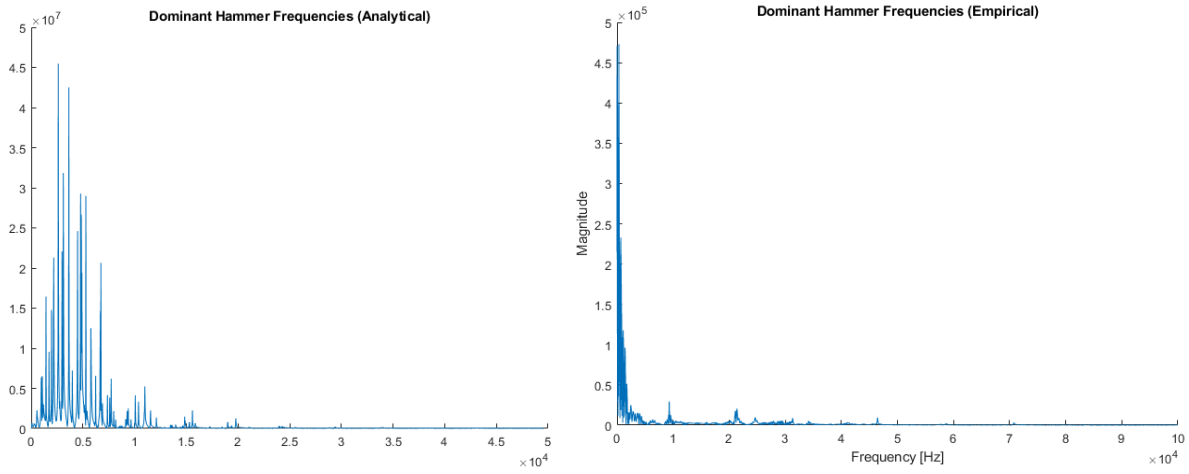


Figure 16: Comparison of FFT for the Hammer between Analytical Model (left) and Experimental Results (right) in the Prototype Shock Tester (0.5 kg hammer, 23 degree drop angle)

To correct this, a low-pass first-order Butterworth filter with a cutoff frequency of 1200 Hz was implemented in MATLAB on the output acceleration data from ANSYS. This cutoff frequency was derived from looking at the participation factors of the modal response of the plate. The majority of the plate's frequencies with high participation factors out of plane were below 1200 Hz. Thus, we believe by neglecting these higher frequency signals which are not representative of reality (low frequency modes dominate the modal response), the SRS will be more accurate. The low-pass filter significantly reduced the magnitude of the SRS at higher frequencies as shown in Figure 17. As shown in Section 8.6, the SRS with the filter is significantly closer in magnitude to that generated from VibrationView experimentally.

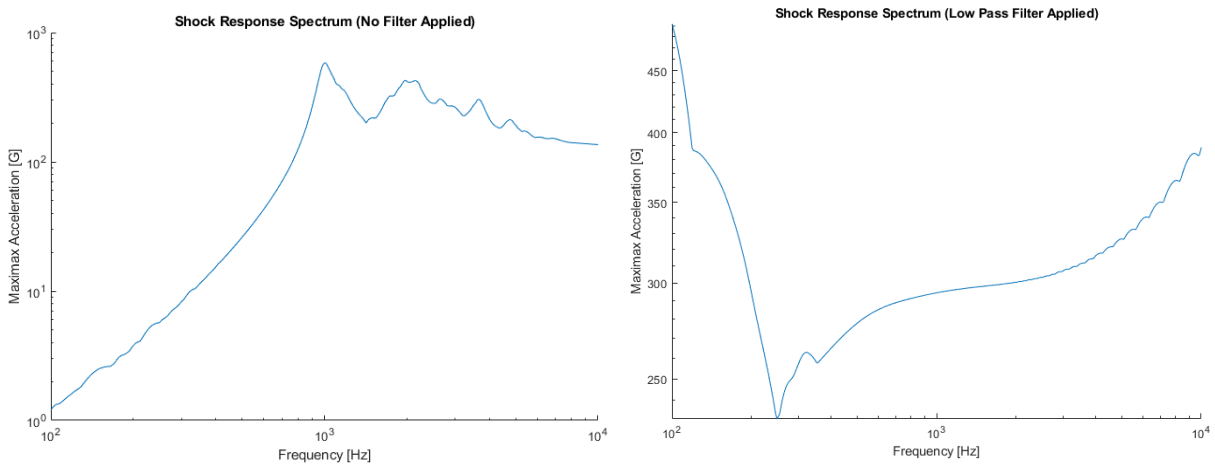


Figure 17: Comparison of Shock Response Spectra without a low-pass filter (left) and with a low pass filter (right)

The second lesson learned is that the stiffness and damping of the isolators play an important role in the response of the system. For some of the tests conducted, the isolators would compress upon first impact from the hammer, then spring up after that first impact with a force such that the whole prototype would momentarily jump off the ground. Though this specifically isn't a concern with the full-sized model since it is significantly heavier, it speaks to the point that the isolator's ability to store energy and dampen vibrations cannot be neglected in our analysis. As is detailed in Section 8.2, the isolators in all models up until the experiments had assumed perfectly stiff isolators. However, as an outcome of this testing, the boundary conditions of the ANSYS model have been updated with isolator stiffnesses representative of the neoprene used (all analytical SRS's shown in Sections 8.4 and 8.5 have a non-infinite isolator stiffness).

8.5 Comparison of Analytical to Empirical Shock Response Spectra

Due to long computation times for ANSYS models and long lead times on receiving accelerometers, we were only able to develop and compare SRS's for the mini with a 1 lb mass being dropped from 23 degrees. Ideally, we would have a range of SRS's to compare and truly validate our design with, but time limitations prevent us from doing so. Figure 18 compares the analytical SRS's generated using the process outlined from Section 8.1 to 8.3 with the prototype small-scale tester shown in Section 8.4.

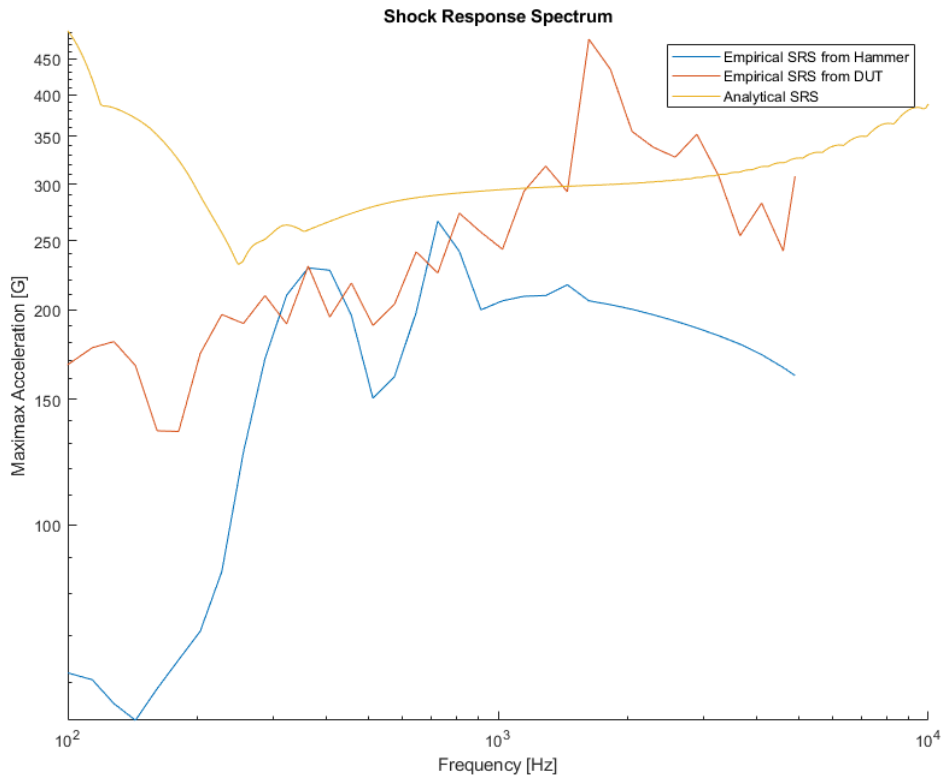


Figure 18: Comparison of shock response spectra between analytical and experimental tests

Though there is some level of congruence between the spectra, this should not be taken as a final conclusion that our process is perfect. The SPRL team will need to do some analysis (likely through experimentation) to generate the SRS's that they want for their DUT's.

8.6 Subframe Structural Analysis

To model the geometry, the parasolid was pulled from NX into ANSYS Spaceclaim and converted into a 1D beam model. Figure 19 compares the current NX model to the 1D model set up in ANSYS. Though this geometry does not exactly match the final design (see Section 10 for finalized design), we are confident that the newer design is stronger than this one which already passes all test cases. Thus, we did not think it was necessary to redo the structural analysis.

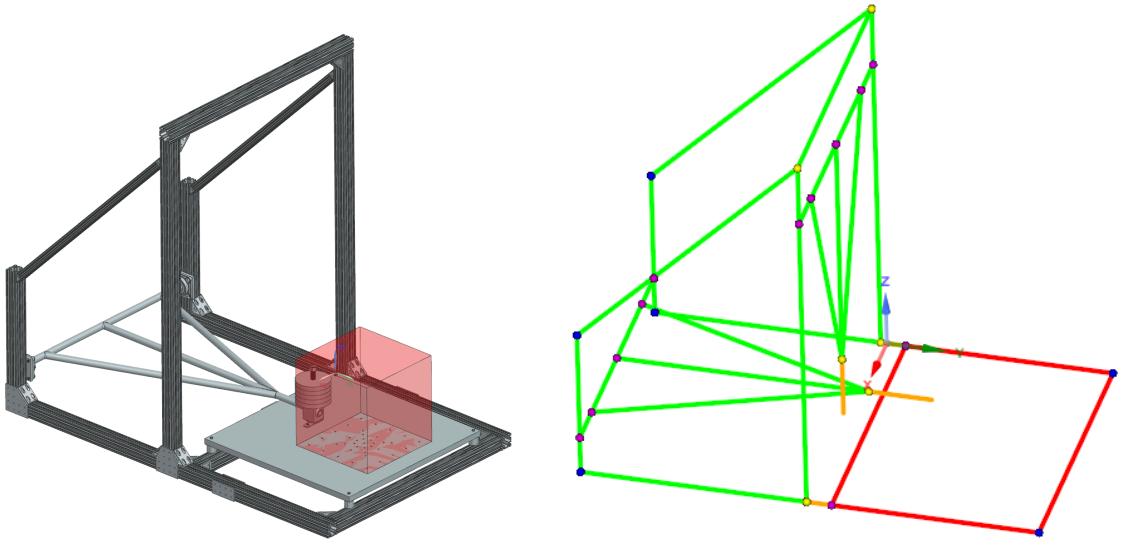


Figure 19. Comparison of NX model to 1D ANSYS beam model of full size structure

The purpose of this FEA is to show that the subframe and hammer stand will be structural during testing. The ringing plate itself has its stresses modeled in the Explicit Dynamics models, so it is not represented in this model. Since the transient hammer force is completely transferred from the hammer into the ringing plate, that transient force can be neglected in this model (again, this is captured in the Explicit Dynamics models explained in Section 8.2). Thus, this subframe is only loaded with gravity with fixed boundary conditions at the bottom of the structure to model the ground.

Figures 20 and 21 show the stress plots for the OOP and IP configuration respectively. With a peak stress of 1.7 MPa across both models compared to a yield strength for Aluminum 6061 of 55 MPa, we can confidently conclude that the subframe assembly will be able to withstand all loading conditions.

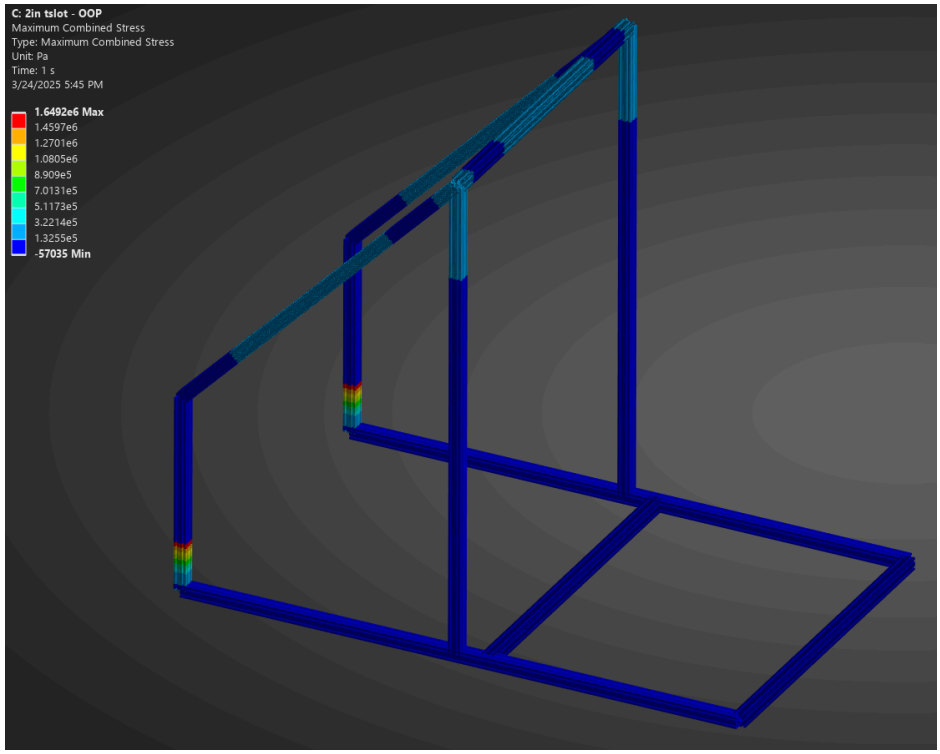


Figure 20: OOP subframe and hammer stand stress plots (gravity loading)

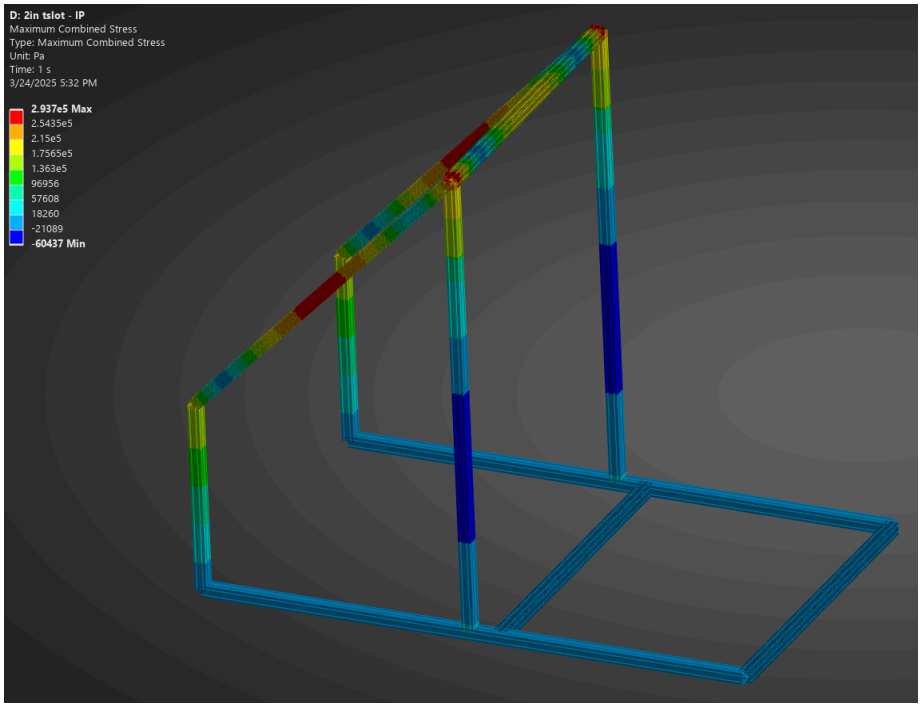


Figure 21: IP subframe and hammer stand stress plots (gravity loading)

8.7 Hammer Structural Analysis

The hammer is a simple pendulum that rotates about two ball bearings. The relevant loads for the hammer are:

1. Hammer cantilevered on the release pin (bending load)
2. Hammer striking the plate (compressive load)

For case 1, the shear and moment diagram is shown below, with the weight of the plates and the weight of the hammer weldment providing downward force. The hammer is supported by a pin 4” from the axis of rotation. The loads are highest when the hammer is supported at the full 90 degrees with maximum weight (~20lbs). To simplify the calculation and to generate a more conservative maximum moment, it is assumed all of the weight is at the tip of the hammer. The maximum bending moment is 4800 lb-in. This yields a safety factor of 5.5 against yield for ⅛” wall tube section and 3.2 for 1/16” wall tube section.

$$\sigma = (4800\ lb - in) * (0.75\ in) / (0.21184\ in^4) = 5700\ psi$$

For the shear pin, the maximum shear force is calculated based on the moment balance, and is 1200lb, resulting in a max shear stress of 2716 psi. The yield strength of 1215 carbon steel (used for the pin) is 60000 psi, therefore the maximum shear stress should not yield the pin. Typical shear strengths for ⅜” bolts is 5000-10000 psi.

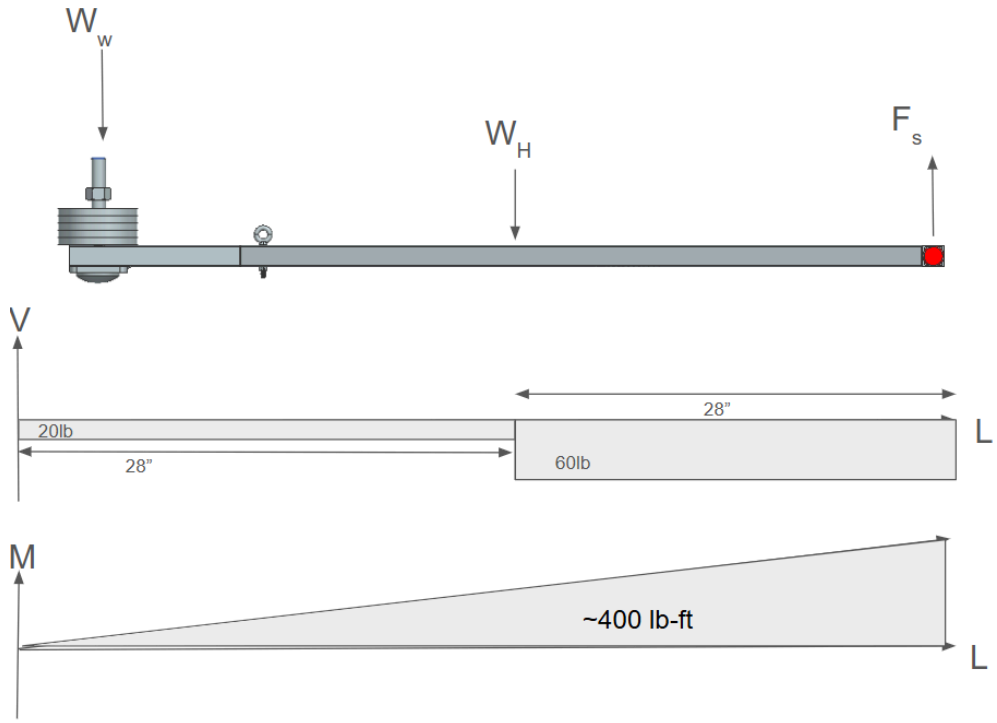


Figure 22: Hammer weldment FBD and shear and moment diagrams

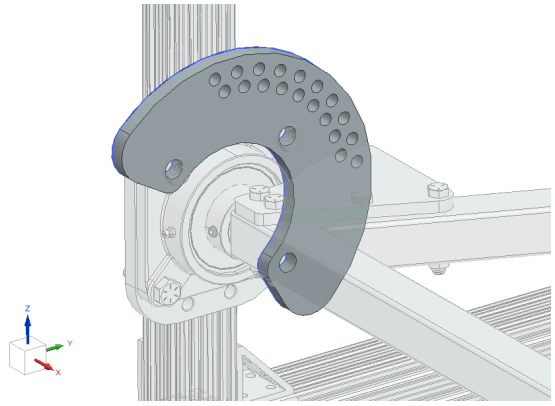


Figure 23: Angle gauge plate



Figure 24: Angle gauge plate integrated with hammer and frame structures

For case 2, we look at the local compressive strength of the tube stock between the weight plates and the hammer tip to ensure it will not be locally crushed by the mass deceleration of the weight plates upon impact. It is unknown what exactly this deceleration rate is, we have not successfully calculated it. The max load is determined for a ⅛” wall and 1/16” wall section, considering the load distribution of the plate.

- Yield strength = 31,000 psi
- 4” section of .12” wall
- Cross-section = (4*.12*2) = .96 in2
- Max load = ~30,000 lbs
- For .0625” wall
- Max load = ~15,000 lbs

9 Design Iteration and History

From the alpha design and concept sketch of Figure 4 in section 6.1, the design has undergone several additional iterations and developments prior to arrival at the final design. These intermediate designs are covered briefly to give additional context to the considerations and challenges which influence the ultimate design.

One of the first CAD designs shown in Figure 25, features a prefabricated table supporting a 1 meter by 2 meter aluminum plate. A smaller fixture plate sits atop the ringing plate and the pendulum hammer is supported by a freestanding frame. Although the prefabricated table provides some convenience, it was ultimately scrapped due to concerns about precisely aligning the hammer and strike points and the overall height of the machine with the plate supported at 36 inches.

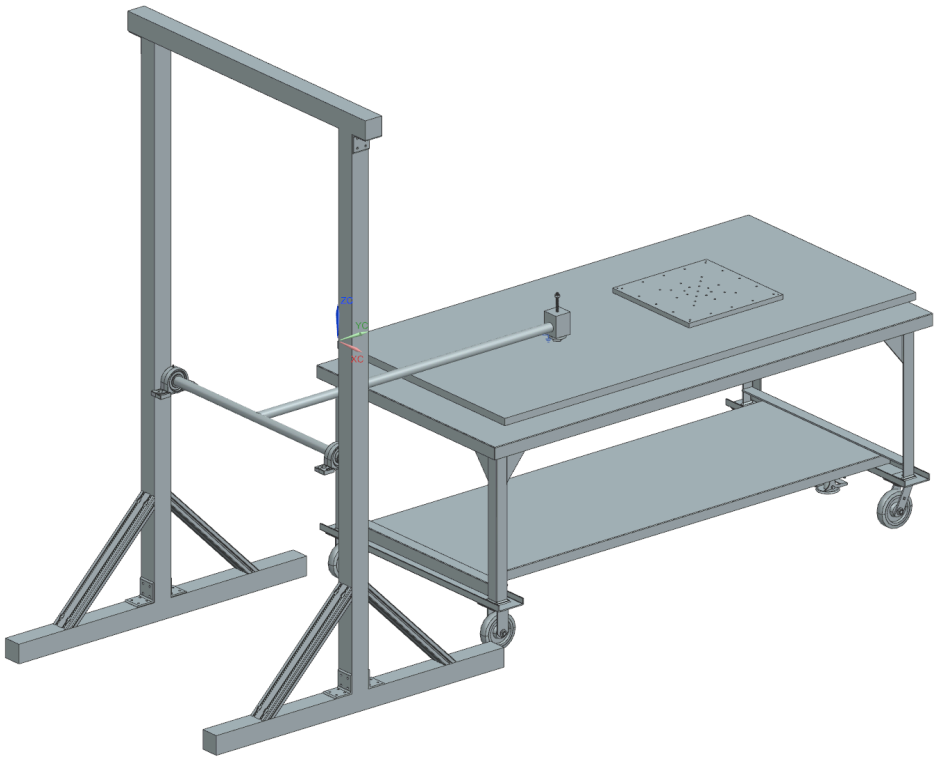
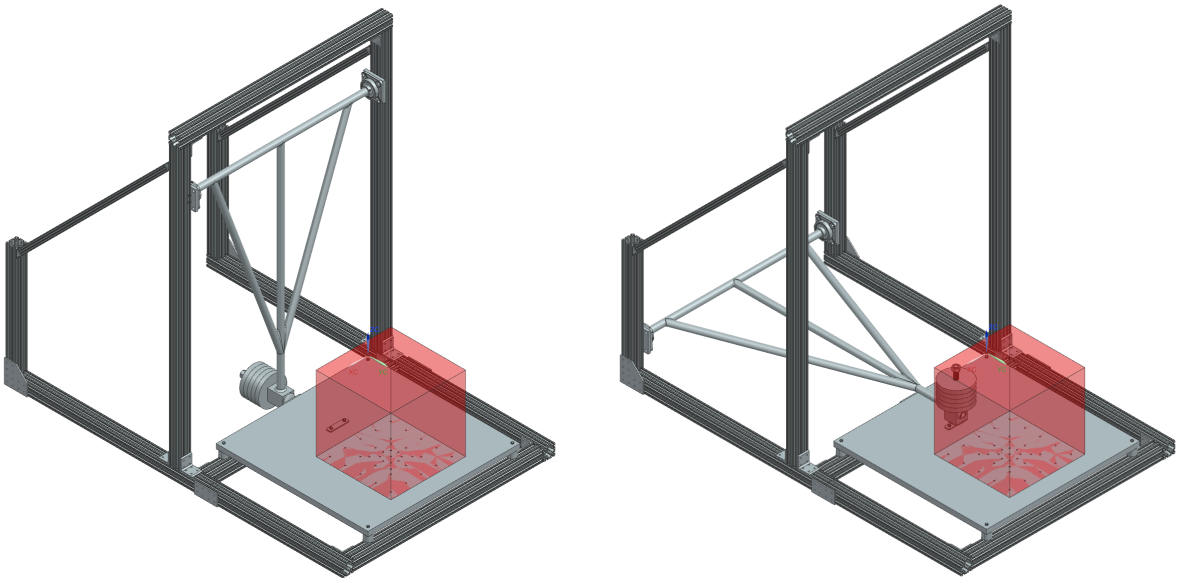


Figure 25. Early CAD design utilizing a prefabricated table and 1m x 2m plate

The next iteration of the design integrated the support for the plate and the hammer into one t-slot aluminum structure. It also eliminated the stand-alone fixture plate in favor of mounting the DUT directly onto the ringing plate. Analysis proved the plate size could be reduced to 40” square and the hammer assembly was made more robust and properly integrated into the t-slot framing. Figure 26 shows the in-plane and out-of-plane configurations of the design.



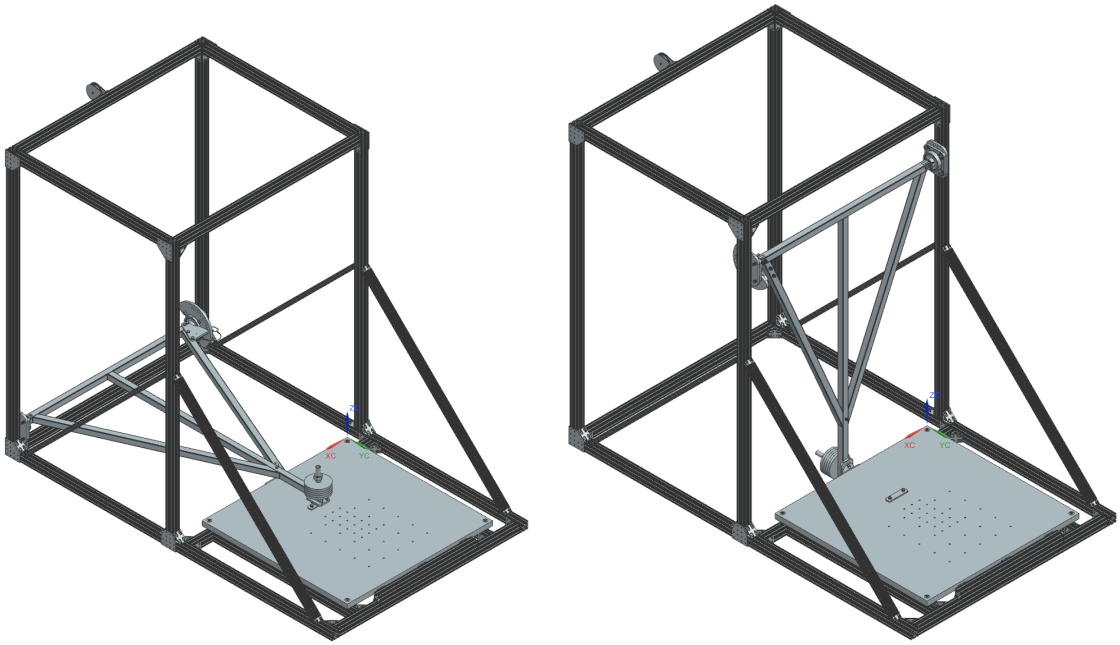
(a) (b)

Figure 26. In-plane (a) and out-of-plane configurations for the intermediate design

Although this design marked a vast improvement over the early design, additional changes were needed to improve the structural integrity of the frame, increase manufacturability, and add mechanisms to lift and control the angle of the pendulum hammer.

10 Full-Scale Design

The full-scale design consists of a 2-inch quad T-slot aluminum structure that supports a configurable pendulum hammer that can be oriented in either an out-of-plane (OOP) or in-plane (IP) configuration (Figure 27). The structure consists of three main subassemblies: the plate subassembly, the hammer subassembly, and the frame subassembly (Figure 28).



(a) (b)

Isometric view of the final design in the out-of-plane (a) and in-plane (b) configurations

Full-size CAD images are provided in Appendix D.

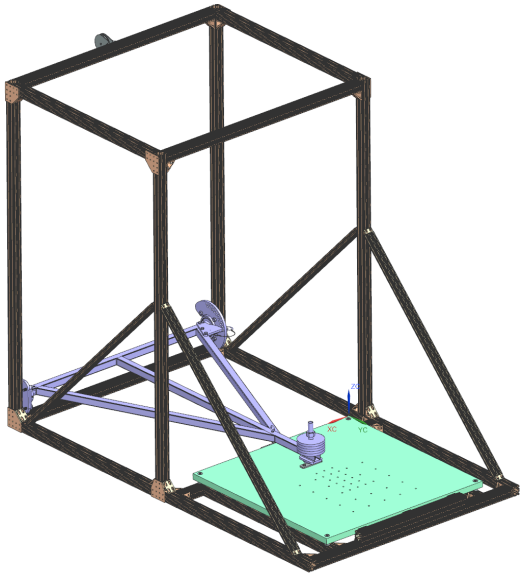


Figure 28. Structure divided into plate (green), hammer (purple) and frame (tan) subassemblies.

10.1 Plate Sub-assembly

The plate sub-assembly provides a mounting surface for the device under test (DUT), a strike surface to transfer energy from the hammer into the plate, and isolation between the ringing plate and the frame. The plate is square aluminum 6061 with a side length of 40 inches and a thickness of 1.25 inches. The design accommodates a 50 cm x 50 cm x 50 cm test envelope as specified in the requirements (Figure 29).

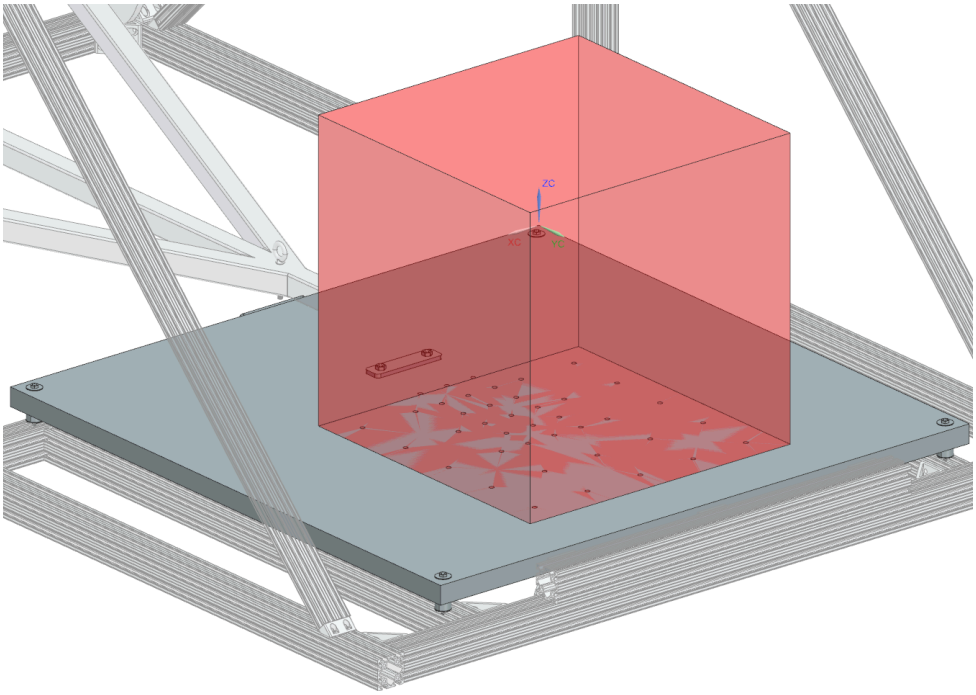


Figure 29. Plate sub-assembly accommodates 50 x 50 x 50 cm DUT envelope shown in red

The plate has two overlapping bolt patterns for mounting the DUT, those being a square 5 x 5 - 4” on center pattern and a rectangular 6 x 3 - 2” on center pattern. All holes for mounting the DUT are thru holes with 3/8-16 UNC helicoil inserts. The hole layout is shown in Figure 30. The inserts protect the plate from wear when fasteners are installed and removed. Helicoil inserts are also used to provide mounting locations for the strike plates. The OOP strike point uses thru holes in the same manner as the bolt patterns. The IP strike point also uses two 3/8-16 UNC helicoil inserts but set into blindly tapped holes. There is a 3/8” clearance hole offset 1” on center from each corner of the plate for mounting to the frame. Free fit nylon sleeve bearings adapt the 3/8“ hole to 1/4-20 hardware used to interface with neoprene vibration isolators. These sleeves also serve as a layer of protection and sacrificial material between the steel mounting hardware and aluminum plate, particularly against bearing failure of the holes in the aluminum plate when striking in the in-plane configuration. The isolators are blindly threaded on one end and feature a 1/4-20 standoff on the other. The standoff threads into t-slot nuts in the subframe as shown in

Figure 31. Detailed engineering drawings of the ringing plate and strike plate are provided in Appendix D.

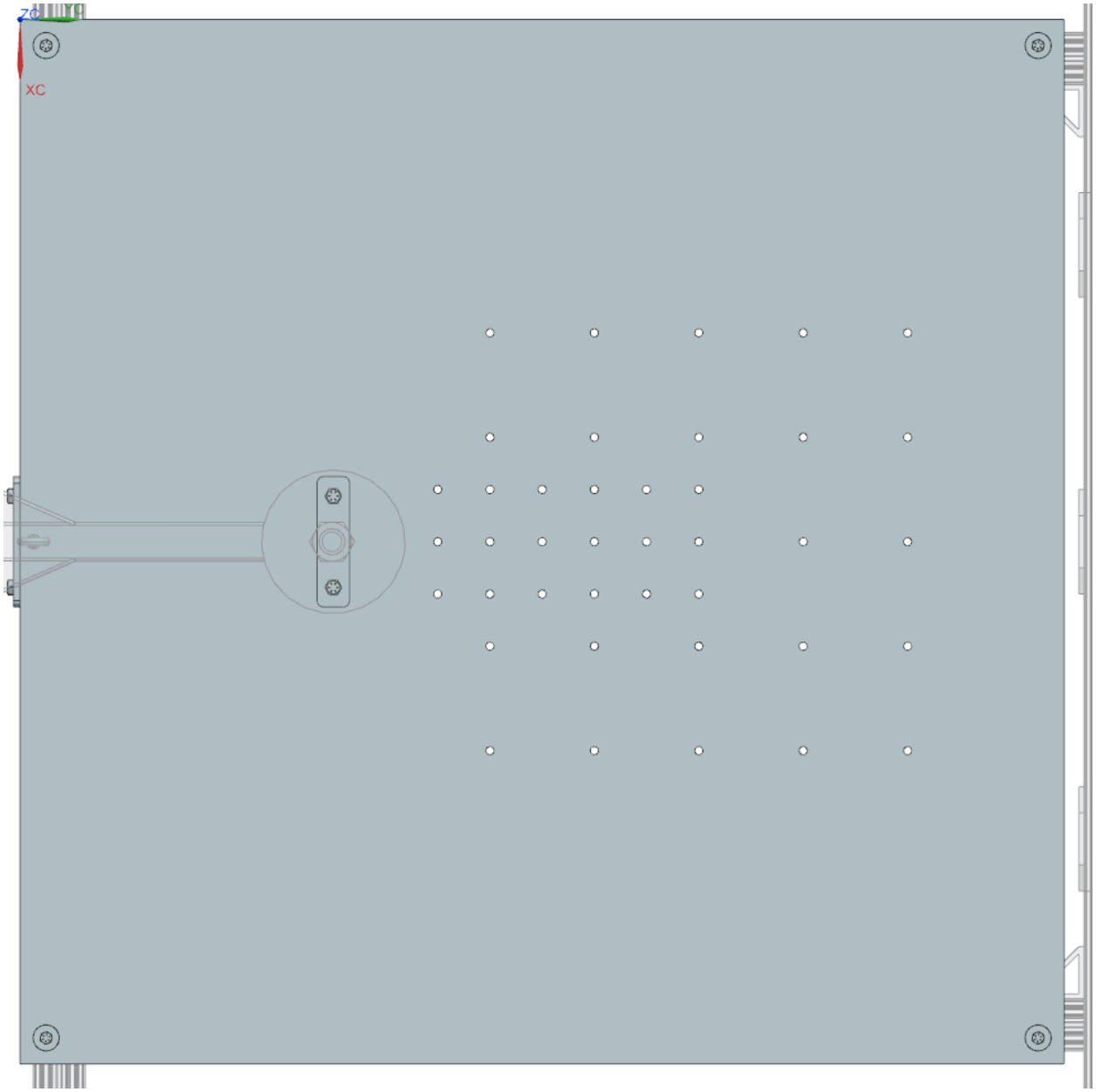


Figure 30. Top view of plate sub-assembly showing mounting hole layout and strike plate locations for IP and OOP configurations

Strike plates are interchangeable between steel and aluminum as a tuning parameter during testing. Additionally, the strike plates protect the ringing plate from damage caused by the impact of the hammer and can be easily replaced.



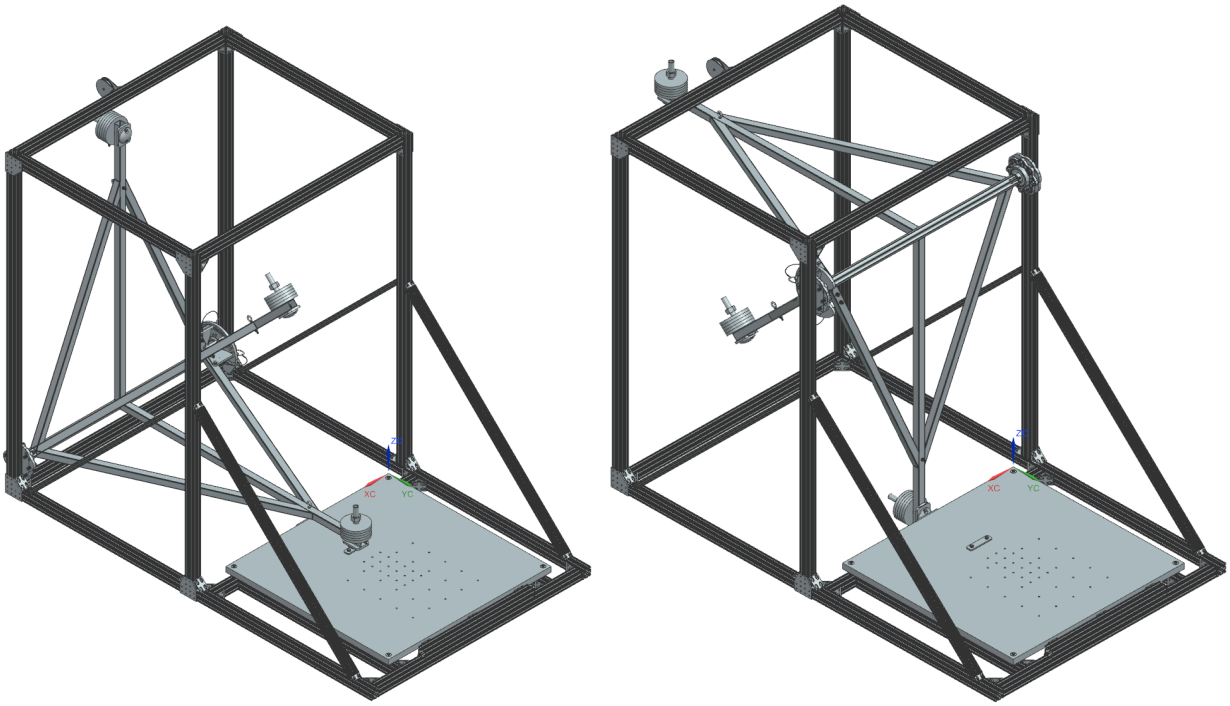
Figure 31. The ringing plate is bolted into four neoprene isolators which are threaded into the t-slot frame

The plate sub-assembly is composed of custom and off-the-shelf components. The ringing plate and strike plate are custom while all other hardware is sourced from McMaster-Carr. The ringing plate manufacturing is being outsourced to ProCam Services in Zeeland, MI. ProCam will be sourcing stock material and hardware; milling, drilling, and tapping the plate; and installing the helicoil inserts. The ringing plate will be picked up in Zeeland and brought back to Ann Arbor for assembly into the structure at SPRL. The strike plates will be waterjet from 1/4" plate. A complete bill of materials for the plate sub-assembly is provided in Appendix B.

The sub-assembly can be put together with basic shop tools which are available in SPRL's lab. Care will need to be taken when moving the 200 lb ringing plate. The plate will be palletized for transport but final assembly will require a minimum of four people.

10.2 Hammer Sub-assembly

The pendulum hammer has 90 degrees of rotation from the strike plane in both configurations. Rotating on 2 flange mounted ball bearings, the pendulum will have minimal friction during rotation. The body of the hammer is constructed from 1.5" square steel tubes and it is welded together into one piece, the square tubes were chosen because they will be easiest to cut, fixture, and weld together. The tip of the hammer is a hard 4140 alloy steel machined into a 50mm radius to ensure a repeatable contact between the hammer and the ringing plate, it is bolted onto the hammer to ensure it is replaceable if damaged. The hammer has 2 adapters that fit to the flange bearing for a better tolerance and enabling the usage of square tubes. There is a steel plate between the hammer body and the hammer tip to distribute the compressive load across a larger surface area. The hammer weighs 25 - 30 lbs unladen. It can carry up to 20 lbs of weight on a threaded rod at the tip of the hammer, to adequately accelerate heavy DUTs. The hammer can be hoisted to a designated angle via a rope and pulley, and there is an angle gauge at the base of the hammer to allow repeatable drop heights.



(a) (b)

Figure 32. Hammer motion sweep through OOP (a) and IP (b) configurations

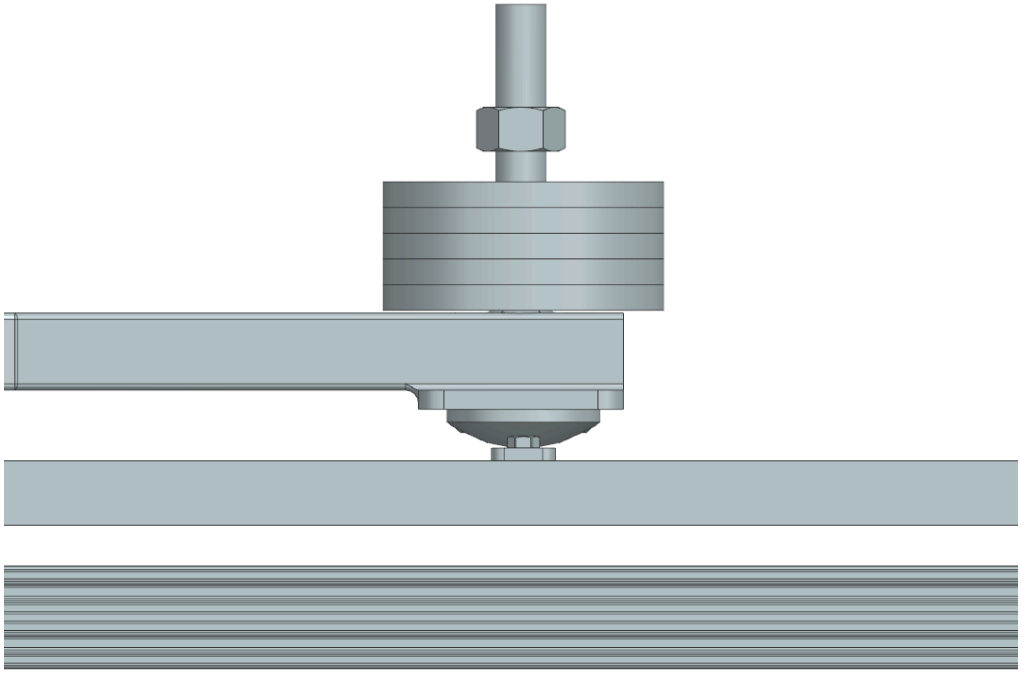


Figure 33. Hammer tip and weights

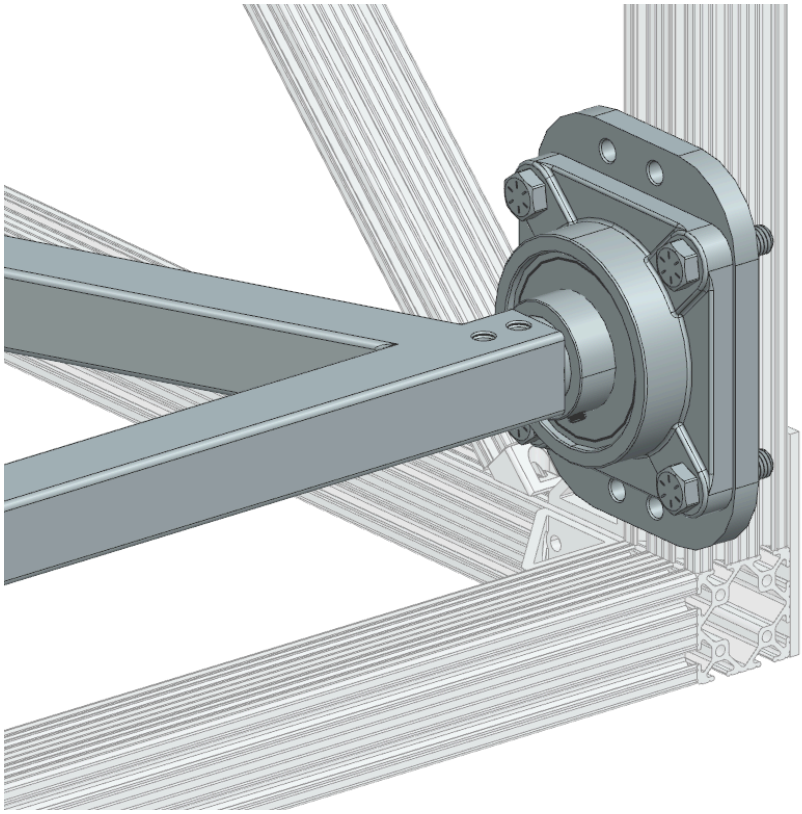


Figure 34. Pillow block bearing and frame integration via custom adapter plates

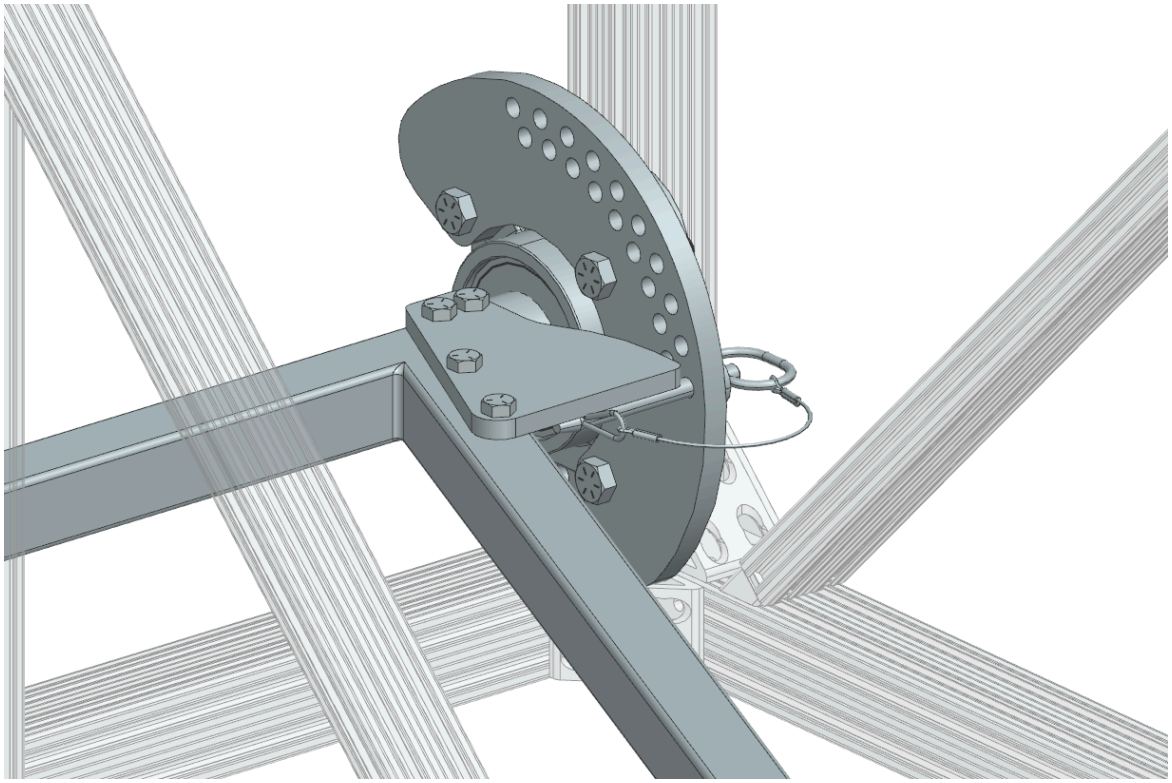


Figure 35. Angle gauge and safety pin to control drop height

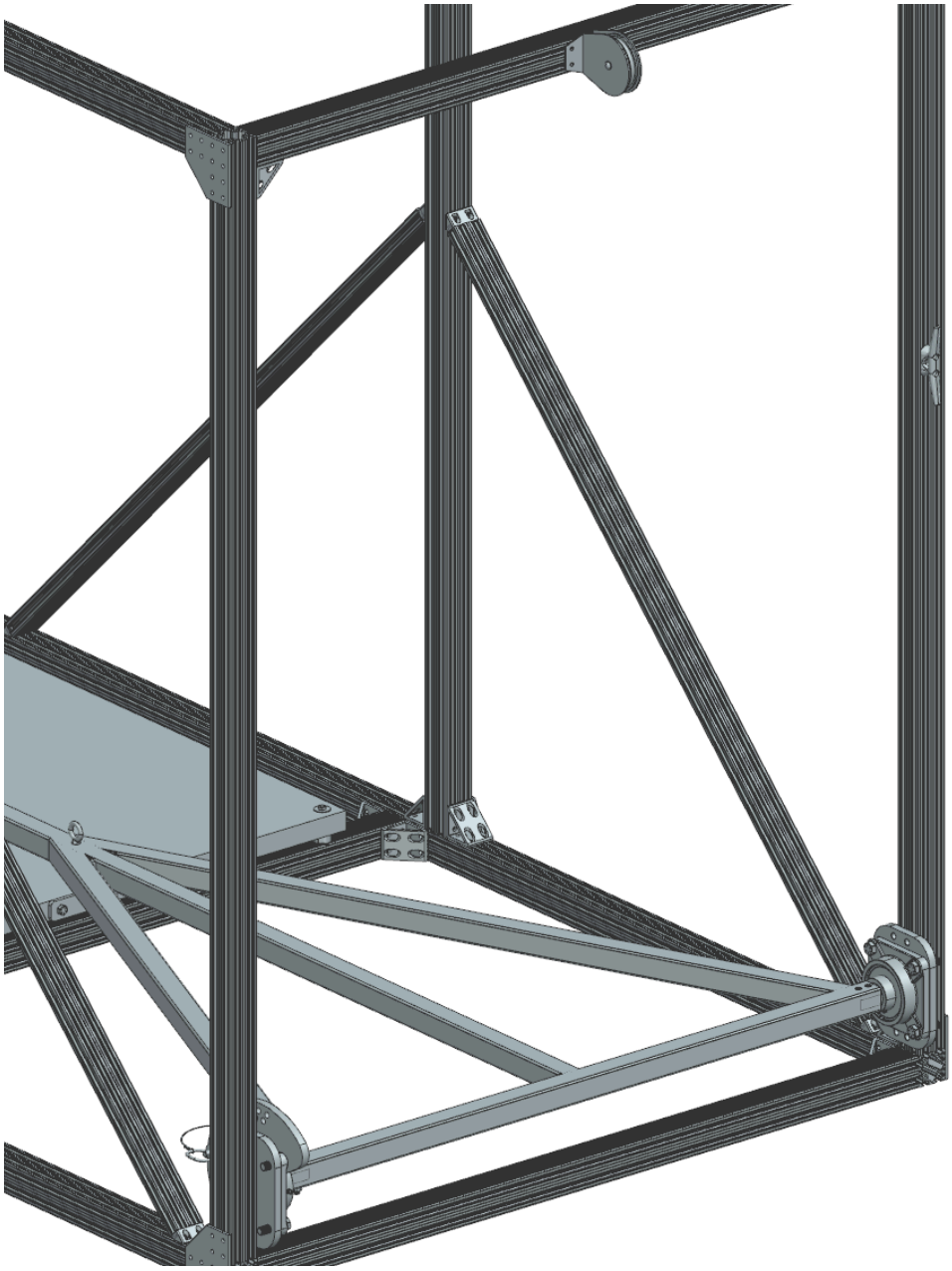
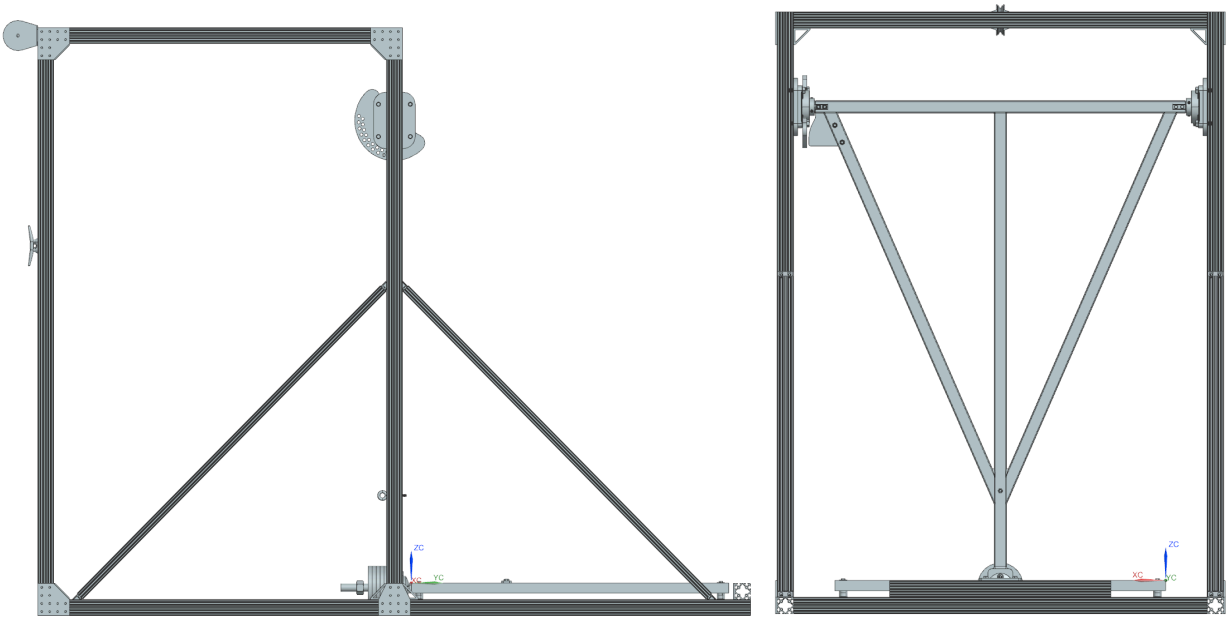


Figure 36. The hoist system consists of an eye bolt on the hammer weldment, a pulley at the top rear of the frame, and a cleat to tie down the rope on the rear right upright.

10.3 Frame Sub-assembly

The frame sub-assembly provides structure to support the weight of the plate and hammer, react the impact loads, and align all components together. The frame is assembled from lengths of 2 inch “quad” t-slot aluminum (Figure 37). The t-slot aluminum frame provides ease of assembly and modularity compared to a ground-up custom fixture such as welded tube steel frame. The system is compatible with 1/4-20 and M6 hardware but 1/4-20 will be used preferentially. All

components of the frame are off-the-shelf, but the aluminum will need to be cut to length using a bandsaw in the ME X50 shop or Wilson Center. The frame lengths are assembled together using OTS angle brackets and supplied hardware (Figure 38) which will be assembled at SPRL using simple tools.



(a) (b)

Figure 37. Side (a) and front (b) view of the frame

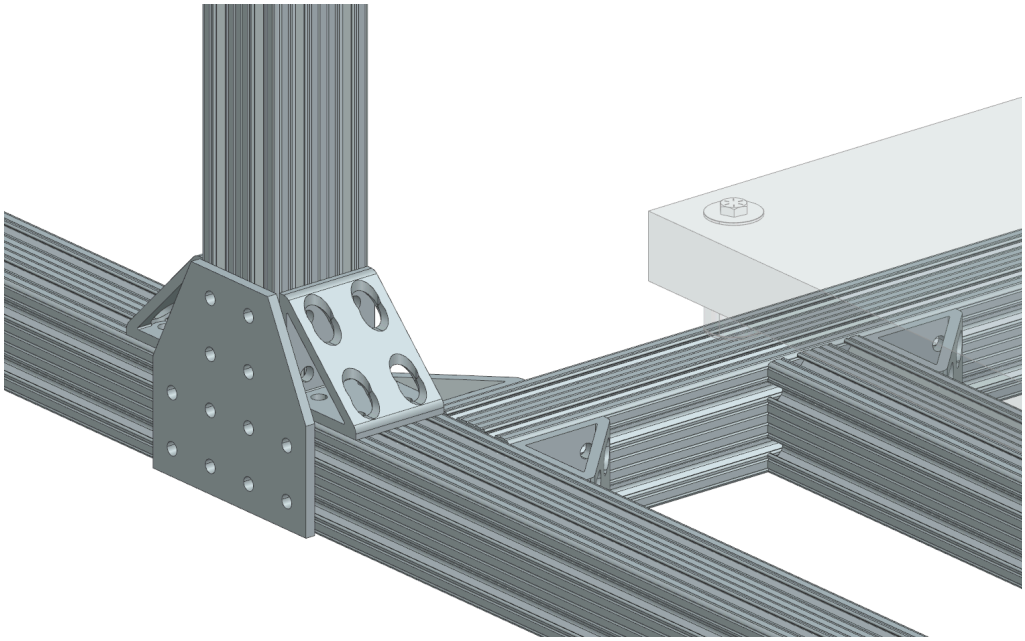


Figure 38. Face mount and angle brackets join the cut lengths of the frame. Note the 1/4-20 bolts which thread into t-slot nuts are not shown in this image

SPRL has a collection of 2 inch quad t-slot aluminum which is available for use (Figure 39). Although this is not sufficient to build the entire frame, the supply will be utilized to its fullest extent and is reflected in the bill of materials in Appendix B. Repurposing this pre-existing supply of material reduces project cost and environmental impact from purchasing and shipping new stock.

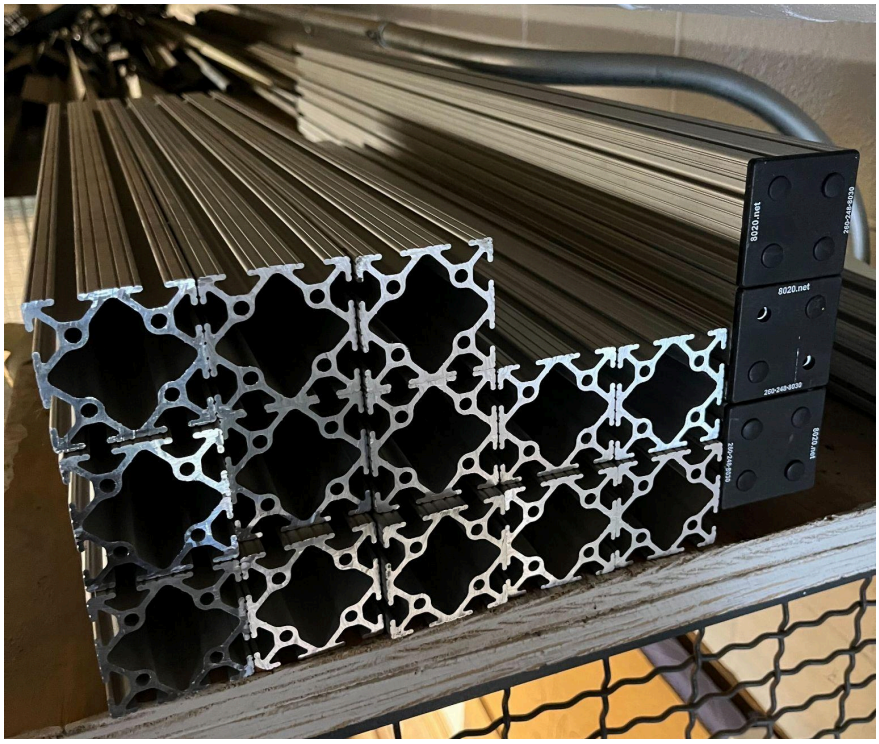


Figure 39. Stockpile of SPRL 2” t-slot aluminum in storage

10.4 Project Cost

The current bill of materials which includes all raw materials, machining services, and OTS parts indicates the total project cost will be $4,982.57. Costs not represented in that number are plate stock assumed to be available at SPRL which would need to be purchased otherwise and shipping of McMaster-Carr hardware. Neither of these line items are expected to substantially increase the project cost. Spare parts are being ordered only for components deemed high risk for loss or need of replacement such as spare t-slot nuts and strike plates. The anticipated project total is well under the project requirement of less than $40,000 and goal of less than $16,000. Remaining project budget will be reserved for additional spare parts, software licensing, or reworking if needed.

11 Verification and Validation Plan

To verify the functionality of the full-size tester, a similar approach will be taken as was used to to test the small-scale prototype. This means that we will set up a test matrix with the important test parameters (hammer weight, drop angle, etc.), then use VibrationView to measure the acceleration data and generate the SRS. However, there are two important distinctions between prototype testing and full-size testing. The first is that SPRL will be acquiring 10,000 G accelerometers for the full-size which were not available for the prototype testing. Second, both the hammer and DUT will have clearance holes on them such that we will be able to thread into the accelerometers that SPRL will be getting. This means that we will no longer need to rely on hot glue to attach the accelerometers and, thus, will allow us to conduct shock testing at those high G loads per our specifications.

12 Project Plan

The project plan to the end of the semester is to fabricate the shock tester. Thankfully, the components of the machine do not have long lead times, otherwise we would not be able to design and build it within one semester. Since this is not the case, the team has scheduled out time to build the machine over the next 2-3 weeks. Between 3/31 and 4/4, the structure of the tester will be built out of 8020 aluminum that is already in hand at SPRL. The ringing plate will be machined at our vendor ProCam. We will machine parts for the hammer on a rolling basis between 4/3 and 4/10. The weldment will be done in house and is expected to take 4-5 hours to complete. The timeline for the rest of the semester is shown in the table below:

Table 5. Project Plan for March and April

3/13 - 3/18	3/18-3/22	3/22 - 3/31	3/31 - 4/4	4/4-4/8	4/8-4/10	4/10-4/15	4/15-4/20	4/20-4/28
Build mini tester	Finish mini tester build	**BEGIN TESTING WINDOW**						**END TESTING WINDOW**
		Mini testing				**SRS testing full-size, small masses**	SRS testing full-size, large masses	
Finalize SRS predication for mini tester	SRS predictions for plate sizes and DUT masses	Install VibrationView				Debugging full size		
		Install accelerometers				Tuning handbook		
Freeze ringing plate size	Freeze ringing plate size							
		Order ringing plate		**Ringing plate arrival**	**Final assembly**			
Finalize full size CAD	Finalize full size CAD							
		Create drawings for custom fab parts	Begin hammer head fab (machining)	Finish hammer head	Attach hammer head and arm			
			Begin hammer stand fab (cutting 8020)	Finish hammer stand	Setup hoist and hammer on stand			
			Begin subframe fab (cutting 8020)	Finish subframe	Attach ringing plate to subframe			
			Begin hammer arm fab (cutting and welding steel tube)	Finish hammer arm				
Create initial BOM	Create initial BOM							
		Finalize BOM						
		Order parts and materials	8020 in hand, steel in hand					
			Order all fasteners					
			All COTS parts ordered					
DR3 Presentation - 3/18						DR4 Presentation - 4/10		Final Report - 4/27

The biggest challenge to keeping this schedule will be:

- ME450 team time spent in the machine shop in between classes and jobs
- Rework required for any parts

If we can overcome these two challenges, we should be able to finish the machine before the end of the semester, with time to test and tune.

Planning Conclusion

This ME450 project aims to deliver a fully functional shock testing machine to be used by the Space Physics Research Laboratory within the Winter 2025 semester. SPRL has provided functionalities that they need the machine to have and we have developed a comprehensive set of design requirements and specifications for a design to achieve those functionalities. Through a thorough concept generation and selection process, a hammer striking a ringing plate was determined to be the best architecture for the given application. A design has been developed and analyzed which is believed to meet the design requirements. The remaining project tasks are to fabricate, assemble, and test the design to validate it against the specifications and models.

13 Final Build Validation

Over 100 tests were conducted on the machine, ranging from the highest to lowest loading conditions in various hammer and test configurations. Generally, the machine held up quite well and the data gathered from the tests indicate that the machine meets the specifications. Nothing on the machine broke during testing, a sign that the design is robust. However, the hammer was dented after repeated testing at the maximum loading condition. Modifications to the hammer to mitigate future damage and robustify it for repeated testing cycles are in the pipeline and expected to be implemented in the week of 4/27/25.

The data collected on the machine showed that the capability of the machine exceeds predicted peak acceleration in the out-of-plane configuration and the knee frequency is not as distinct as predicted in the analysis. For the in-plane configuration, the machine is not producing peak accelerations as high as expected and the knee frequency is right in line with expectations. The discrepancy between peak accelerations in the in-plane configuration analysis vs testing are believed to be due to the stiffness of the boundary conditions. Stiffening the boundary conditions of the in-plane configuration is predicted to increase the peak acceleration in that configuration. Many of the SRS's generated do not have as distinct of a knee frequency as predicted, this is potentially due to discrepancies in the damping characteristics of the machine that is not reflected in the analysis. Additionally, we were not able to evaluate results at frequencies >4900Hz so it is unclear whether the behavior of the SRS is as expected in this frequency range.

The final build in the out-of-plane configuration is shown in Figure X.



Figure X. Final Build in OOP Configuration

To validate the requirements set for this project, our team conducted mock shock tests to determine the capabilities of the fixture itself. To do this, we set masses on the ringing plate while representing a DUT, then attached accelerometers (capable of measuring up to 5000G) to it to measure the response of the system. Using VibrationView, we turned the accelerometer data into an SRS which we then compared to our specifications.

From the initial set of requirements detailed in Section 3.2, we validated the capabilities of the fixture through experimentation. Table X shows the key requirements and describes how they were validated.

Table X. Requirements Validated through Testing at SPRL

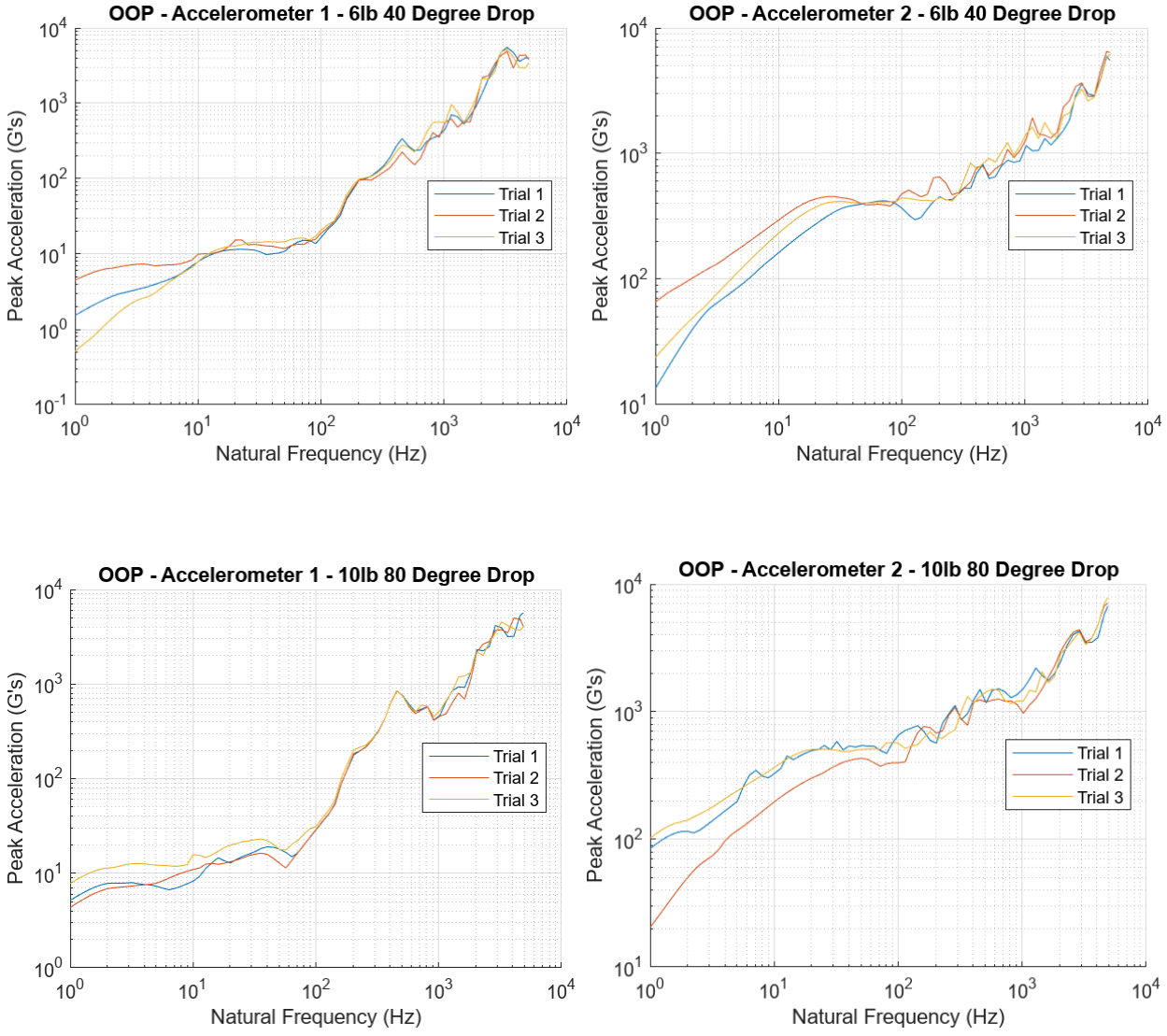
Req ID	Requirement	Specification	Validation	Outcome
3	**Capable of desired shock profile(s)**	Peak acceleration capability = 750-3000 G ± 100 G	Data collected on the fully built and assembled machine. Dependent on test configuration, the machine can exceed 3000G in the high frequency band and can be tuned to a specific peak acceleration. Maximum tested DUT mass was ~15kg, with shocks well over 3000G applied to the 15kg mass, we are confident that the machine can test a 25kg DUT.	
		Shock response spectra (SRS) frequency range = 100-10,000 Hz	Data collected on the fully built and assembled machine. The machine is expected to be capable of inducing shocks up to 10,000Hz, but this could not be verified due to software limitations.	
		Shock duration < 25 ms ± 5 ms	Time domain acceleration data collected for over 100 tests on the fully built and assembled machine. See Section 13.7.	
4	**Compliance with aerospace standards**	Shock fixture shall be able to reproduce a Shock Response Spectrum (SRS) for a known mass DUT conforming to NASA General Environmental Verification Standards (GEVS) GSFC-STD-7000A [11]	Data collected on the fully built and assembled machine. No specific test was tuned to meet GEVS within the tolerance band. However, several tests were close to complying with the tolerance band and the machine is proven to have high adjustability/tunability to ensure GEVS can be met.	
		DUT shall be able to have shocks applied in all 3 axes	Machine was built and proven to be capable of inducing a shock in all 3 axes of a DUT.	

Although requirement 3.2 specifies that we must validate from a frequency range of 100 to 10,000 Hz, the temporary VibrationView license given to us by SPRL only permitted us to measure from 100 to 4,900 Hz. Despite this limitation, we are confident that the data collected is sufficient to say that we've met these requirements.

Sections 13.1 through 13.6 detail the findings of the tunability and repeatability of the tests. Sections 13.7 and 13.8 discuss the compliance of our results with the aforementioned requirements.

13.1 Test Repeatability / Accelerometer Placement

2 accelerometers were placed on the DUT at opposite corners. Accelerometer 2 is closer to the strike point and accelerometer 1 is farther from the strike point. There are some discrepancies between the accelerometer readings, indicating that the shock is not uniform across the DUT. For official tests, an average of the two shock environments would likely be most representative of the shock environment on the device. Across both mass/angle settings the shock test machine demonstrates excellent repeatability—better than ±3 % (≈±0.25 dB) through the bulk of the spectrum.



6 lb hammer – 40 ° drop

Low-band (100 Hz – 1 kHz) – curves are practically indistinguishable; point-to-point differences stay within ±3 % (≈0.25 dB).

High-band (> 1 kHz) – a slight divergence appears, rising to ~5 % at the extreme knee (~3–4 kHz). This is typical of contact-time jitter between hammer and anvil and limits of the accelerometer resonant frequency, not a systemic repeatability flaw.

Cross-channel agreement – At every frequency decade the two accelerometers match within approximately ±5 % despite being mounted at different locations, indicating both spatial uniformity of the shock and good sensor correlation.

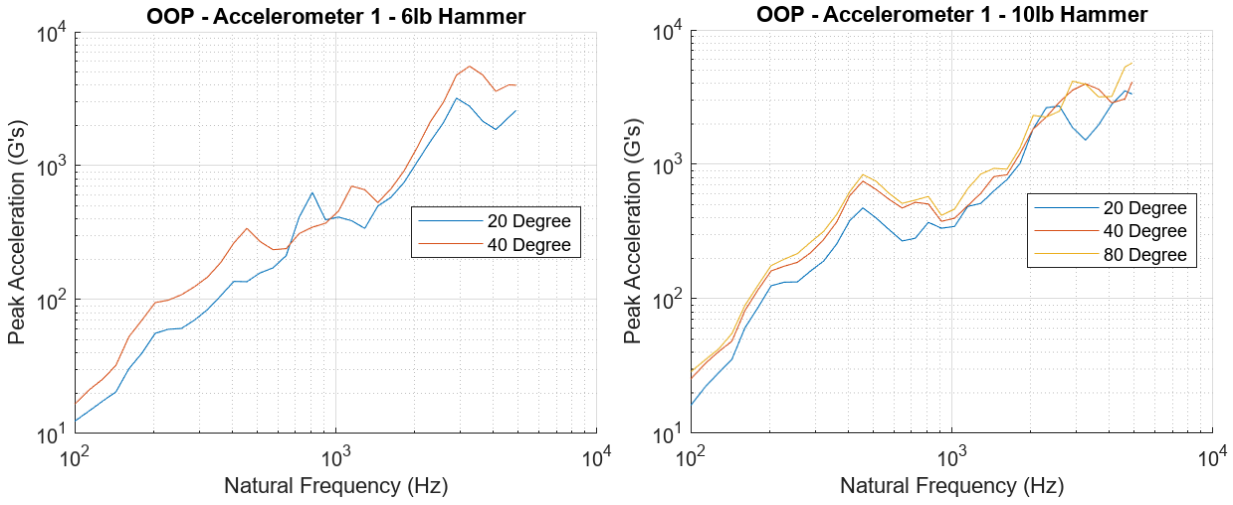
10 lb hammer– 80 ° drop

Entire band (10 Hz – 5 kHz) – trial-to-trial spread rarely exceeds 2 %, and the two channels track each other even more closely than in the lighter-drop case. The heavier, steeper-angle impact yields a broader high-frequency plateau (~600 Hz–2 kHz) but does not introduce additional scatter, evidence that the fixture system scales well with impact severity.

Key takeaways:

- The machine delivers repeatable shock environments.
- Reasonable agreement between accelerometers confirms that mounting stiffness and mass loading are adequate; no localized ringing is observed.
- An average of the two shock environments would likely be most representative of the shock environment on the device.
- High-frequency scatter can likely be reduced further by refining hammer rebound damping.
- There is a significant difference between the SRS of accelerometer 1 and accelerometer 2 in the 1-100 Hz range.

13.2 Drop Height

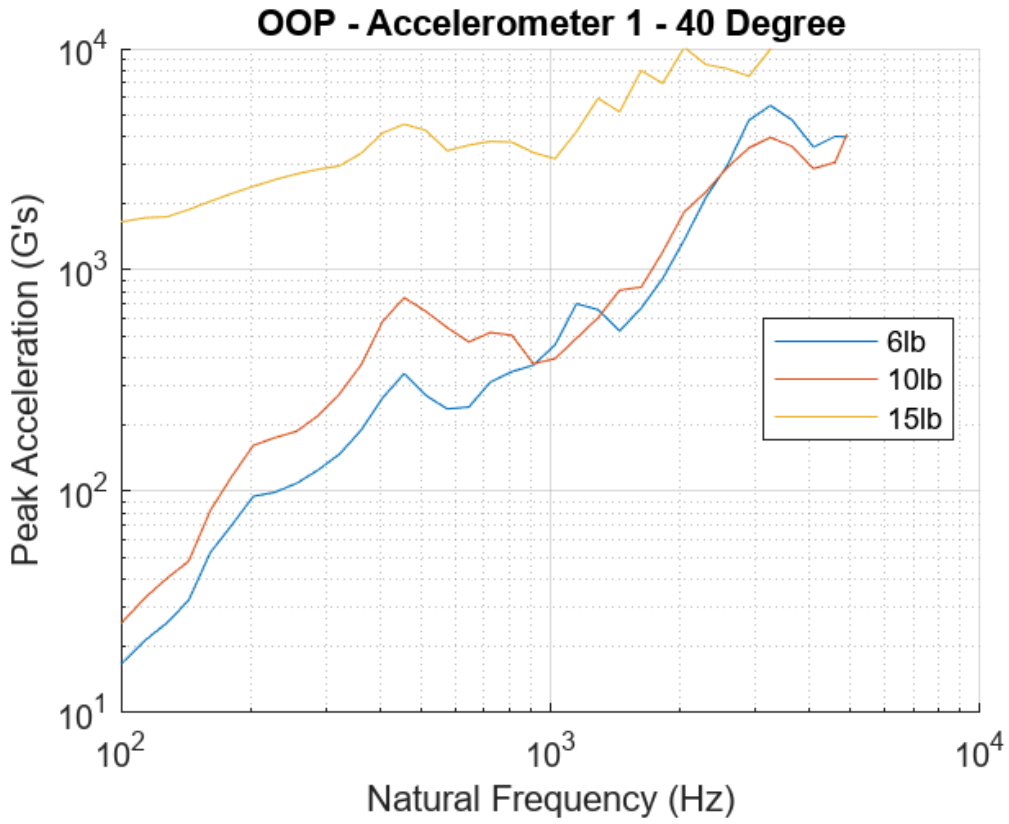


For the out of plane configuration, the drop height was varied for 2 different hammer masses to investigate the effects on the resultant SRS.
6 lb hammer (left panel) – Raising the swing from 20 ° to 40 ° roughly doubles the available potential energy. That translates to a steeper velocity at impact and a uniform 2–3 dB rise in the spectrum between 200 Hz and 2 kHz. Above ~2 kHz the two curves converge, indicating that fixture compliance or sensor resonance, not input energy, now governs the response ceiling. Peak-G at the primary knee (~2.5 kHz) climbs from ≈3.0 ×10³ G to ≈3.6 ×10³ G—a ~20 % gain that tracks well with the √h scaling expected for drop tests.

10 lb hammer (right panel) – The heavier striker preserves this trend but with diminishing returns. Going from 20 °→40 ° gains ≤3 dB below 400 Hz; the extra jump to 80 ° yields only another 1–1.5 dB except in the first decade. Above 1 kHz all three traces collapse into a tight band (<±1 dB), suggesting the fixture has reached a stiffness-limited plateau where added impact energy no longer couples efficiently into higher natural-frequency modes.

Key takeaway – Increasing drop height is an effective way to lift the low- and mid-frequency portions of the SRS, but the benefit tapers once the input energy exceeds the mechanical bandwidth of the test setup. For out-of-plane shocks on this rig, 40 ° appears to be the inflection point beyond which higher swings return marginal spectral gains, especially with the 10 lb hammer.

13.3 Hammer Mass



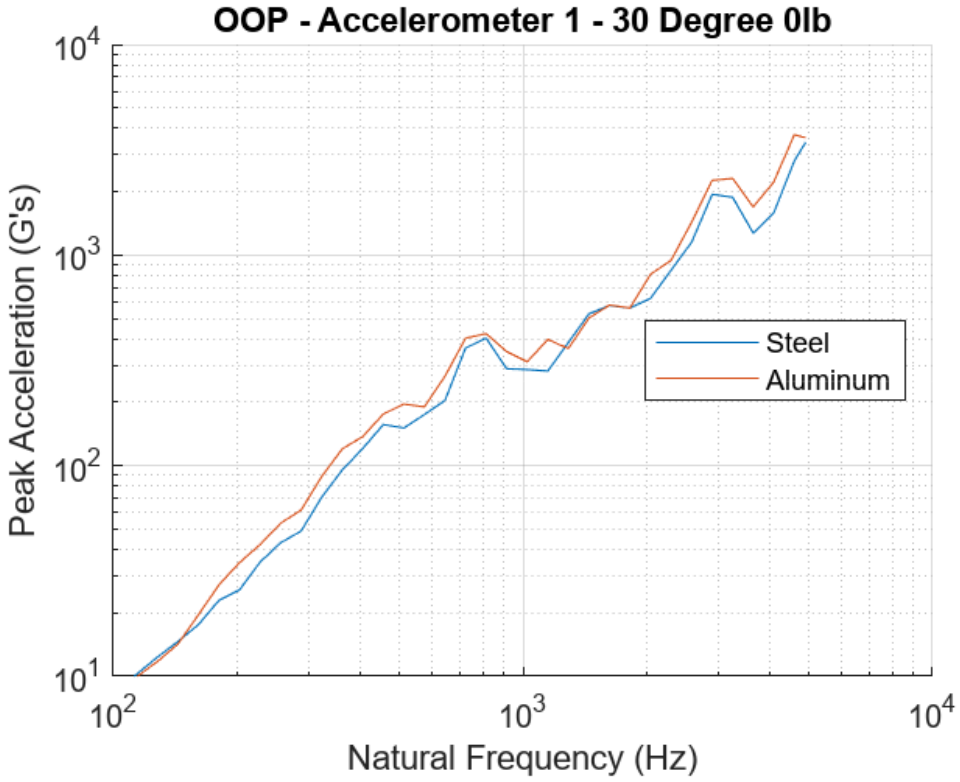
At a fixed drop angle the only variable is impact momentum; doubling the hammer mass doubles the input energy for a given release height.

6 lb → 10 lb (≈ +67 % mass) – Raises the SRS by ~3 dB (×1.4) below 600 Hz. Beyond 1 kHz the two curves converge, showing the fixture becomes stiffness-limited and additional mass no longer couples efficiently into the higher modes.

10 lb → 15 lb (+50 % mass) – Produces a further 5–6 dB lift across the entire 100–2 kHz band, pushing peak acceleration into the 5–10 k G range. Little change in slope: the response scales almost uniformly rather than shifting resonant knees, indicating that mass chiefly affects overall impulse magnitude, not system dynamics.

Key takeaway – Heavier hammers are an effective lever for boosting low- and mid-frequency SRS levels, but the gain is sub-linear: every additional pound yields progressively smaller spectral increases. Above ~2 kHz all masses approach the same ceiling, suggesting fixture rigidity or sensor bandwidth—not input energy—governs the high-frequency limit.

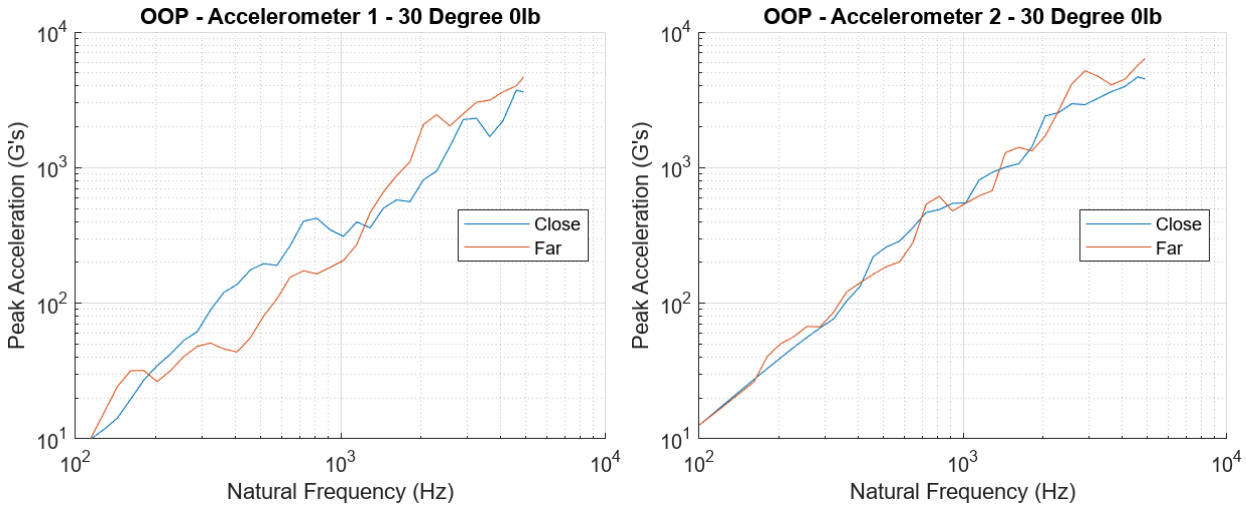
13.4 Strike Plate Material



With the modest 30 ° drop the steel and aluminum plates generate virtually identical SRS traces across the entire 100 Hz – 5 kHz band; point-wise differences stay below ~1 dB, i.e., within sensor repeatability. At this lower impact energy the contact pulse is long enough that the plate's elastic modulus (70 GPa vs 200 GPa) no longer governs the spectral content; fixture dynamics and hammer compliance dominate instead. Interface stiffness only becomes a tuning lever once the impulse is short enough—seen in the higher-energy (40 °) test where steel gained 2–4 dB in the mid-band.

Key takeaway – For calibration or low-severity shocks, either plate material may be used interchangeably; material selection matters chiefly when the drop height (or hammer momentum) is large enough to approach the plate's elastic time constant. Since the impact to the resultant SRS is negligible, it is recommended to use the steel strike plate since it is more durable and less likely to break than the aluminum.

13.5 DUT Location



The fixture distributes shock energy very uniformly, even at the resonant peaks the close-vs-far spread stays within ±3 dB. The second accelerometer's minimal variation implies that, for most DUT placements on this platform, location-dependent mismatch will be smaller than sensor-to-sensor repeatability.

Key takeaway – For qualification at this energy level, DUT placement anywhere on the mounting rail should experience essentially the same shock environment. Only if a specification calls for tighter than ±3 dB in the 1–4 kHz region would relocation or fixture tuning be necessary. This trend likely does not hold true for the in-plane configuration since the damping of the ringing plate will have a more significant effect on the SRS for the in-plane.

13.6 Boundary Conditions for IP Configuration

To understand the impact of the boundary conditions on the SRS, we varied the way in which the ringing plate was mounted to the ground. For the IP test (and the OOP test), there are four ¼”-28 bolts along the four corners of the ringing plate which are torqued down onto neoprene isolators. For the IP configuration, there is a backstop at the end of the plate which transmits the force into the 80/20 frame. Further, we investigated the use of c-clamps along the edges of the plate to quantify the impact on the SRS.

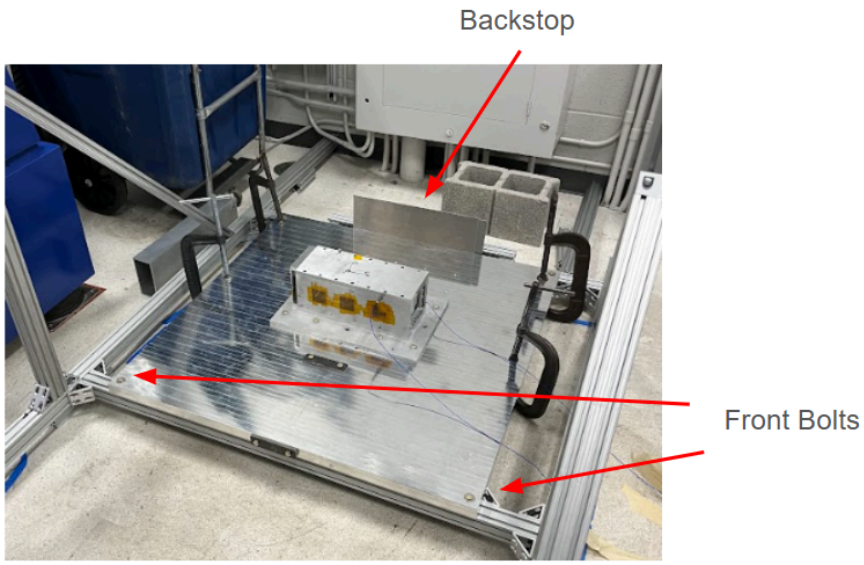


Figure X. Labeled Picture of Backstop for IP Testing and Front Bolts. Clamps are in Positions 3 and 4 during this test.

First, we looked at the impact of the c-clamps. As shown in Figure Y, we looked at the use of c-clamps in four positions: close to the strike plate, close to the front corner, close to the middle of the plate, and close to the back corner. All c-clamps were positioned symmetrically about the centerline of the plate (clamps were always placed on both sides when used). With the c-clamps, three tests were conducted in three different configurations. For these tests, the hammer was dropped without added mass with a DUT weighing 32 lbs (same DUT as shown in Figure X). Figure Z shows the resultant SRS from these tests.

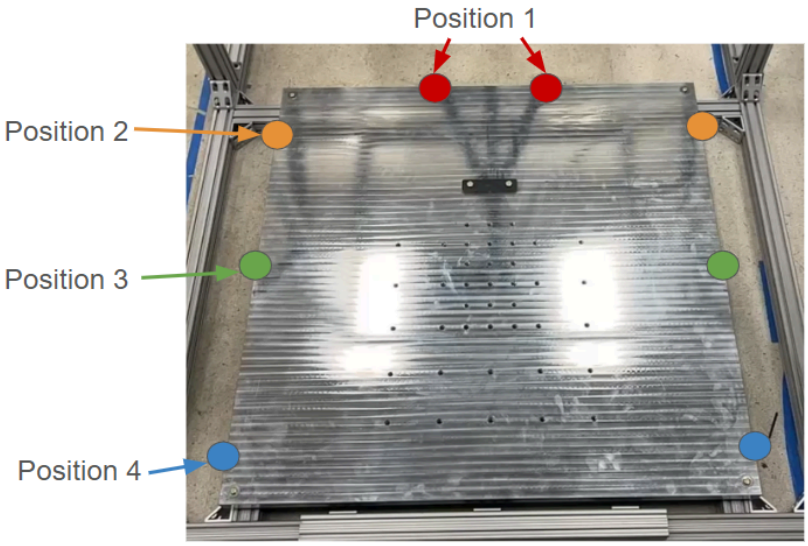


Figure Y. Locations for C-Clamps Tested for IP Configuration
Red - Position 1, Orange - Position 2, Green - Position 3, Blue - Position 4



Figure Z. C-clamp Location Impact on SRS

From Figure Z, it seems that constraining the plate closer to the strike point shifts the SRS above the knee frequency up. However, our data analysis is limited since SRS data is only collected up until 4900 Hz and the data at this point is very noisy, so more testing would be necessary to definitively conclude this.

To investigate the impact of the bolts on the side of the ringing plate, we compared the SRS generated when those bolts were in-place and torqued down to completely removed. Figure X shows the results of these two tests.

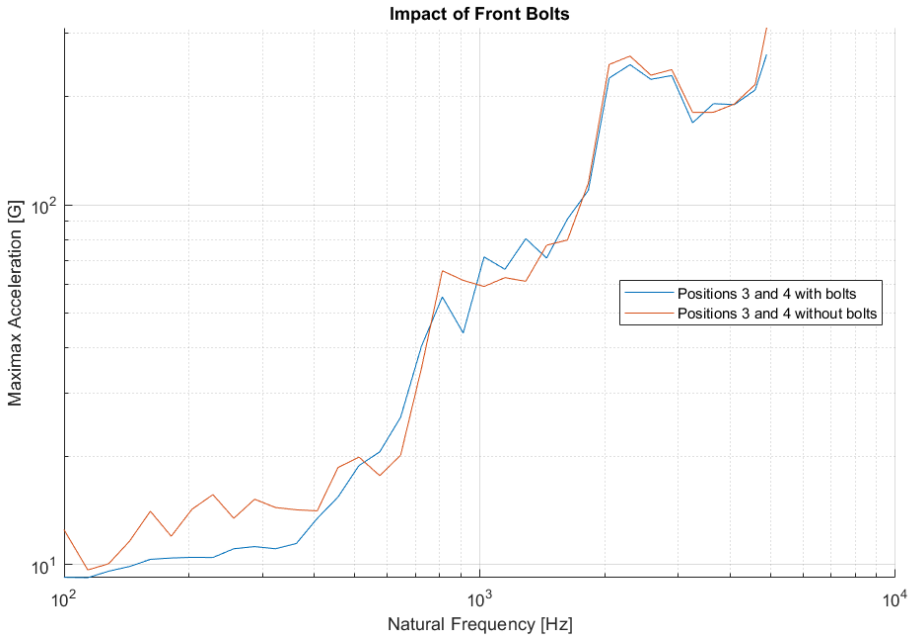


Figure X. Impact on Using Front Bolts on SRS

The change from the use of the front bolts to not using was not appreciable.

After varying the boundary conditions, we wanted to see if the material choices for both the strike plate and the backstop would have a noticeable impact. Figure X compares the use of an aluminum to a steel strike plate while Figure Y compares the use of a steel to a neoprene backstop.

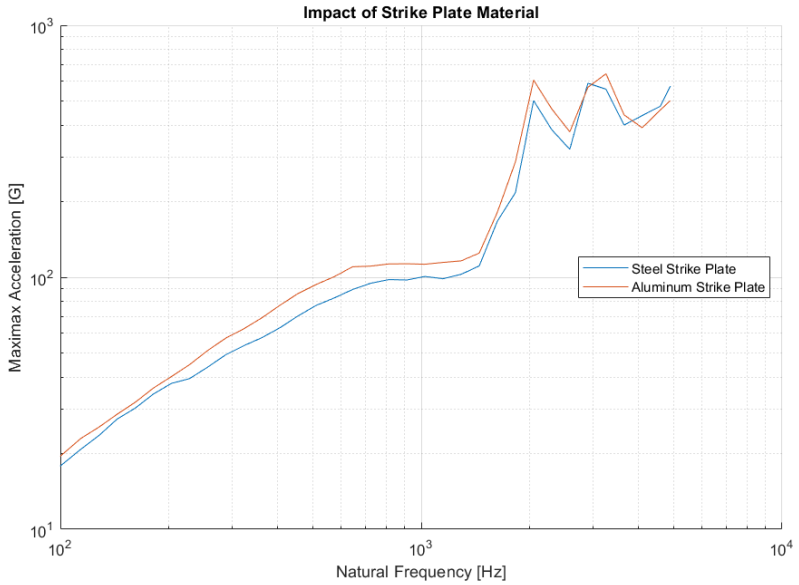


Figure X. Impact of Strike Plate on SRS

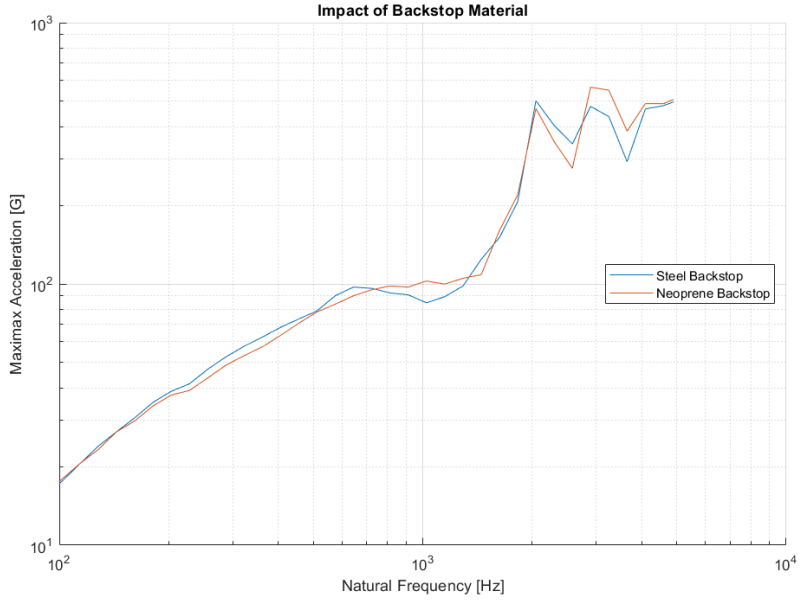


Figure Y. Impact of Backstop Material on SRS

For both of these tests, the material choice did not make a noticeable difference on the SRS.

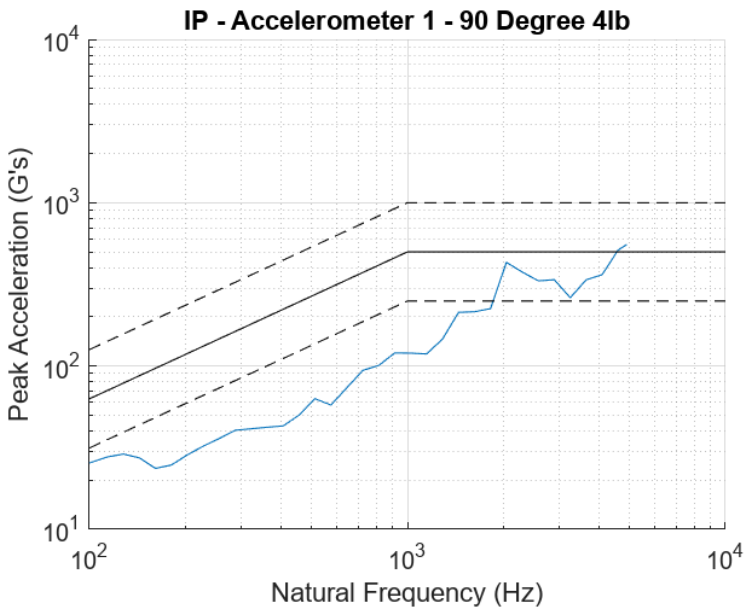


Figure #. Comparison between an in-plane SRS and the NASA GEVS specification SRS, with tolerance band shown.

13.7 Impact Duration

Requirement 3.3 states that the duration of the pulse must last less than 25 ms. To verify this, we looked at the acceleration time history over a variety of the pulses. For the wide variety of test configurations we tested, the principal impact was nearly entirely dissipated by 25 ms after the initial impact. The machine comfortably meets the 25ms +-5ms impact time requirement. It should be noted that due to the elasticity of the collision, the hammer will sometimes induce a secondary shock into the ringing plate. This can be seen in Fig. X. Magnitude of the secondary shock is dependent on the mass and configuration of the hammer. A well-trained user of the machine is able to eliminate the secondary shock by pulling the rope at the right moment.

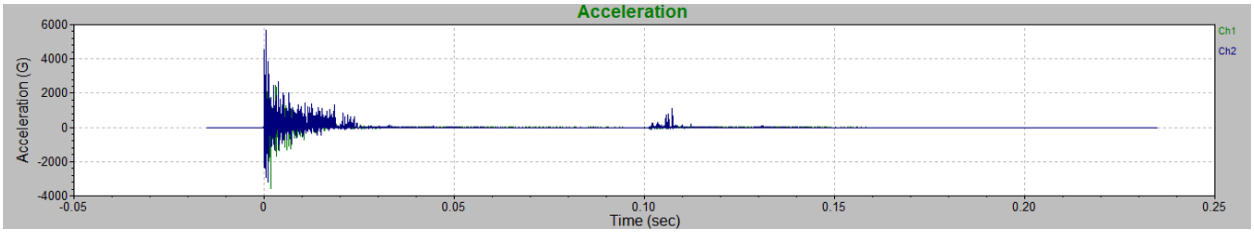


Figure X. Acceleration Time History for OOP test with 6lb additional hammer mass and 40 degree drop

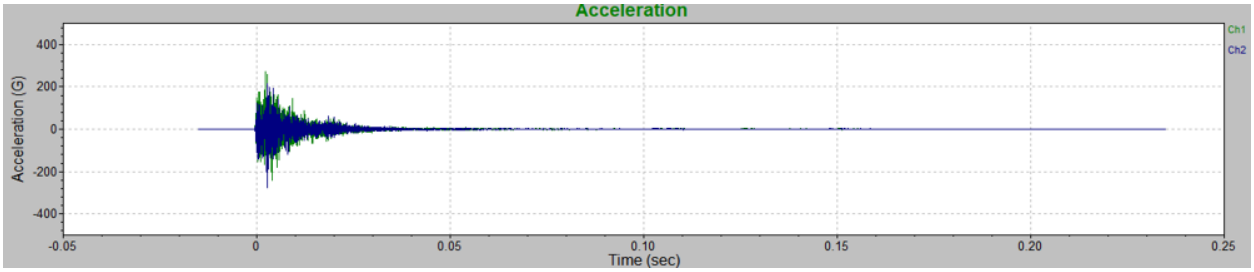


Figure Y. Acceleration Time History for IP test with 0lb additional hammer mass and 90 degree drop

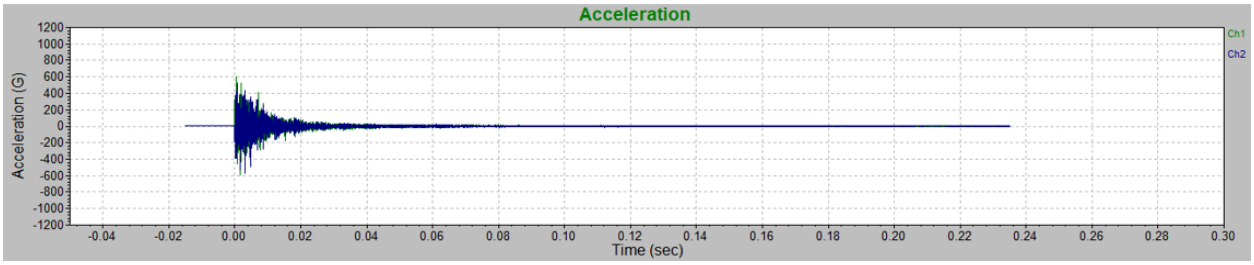


Figure Z. Acceleration Time History for IP test with 4lb additional hammer mass and 90 degree drop

13.8 Peak Acceleration Capabilities

The peak acceleration of the machine is dependent on a variety of factors and is not a clear-cut measure. Generally, the peak accelerations for the machine are noticeably higher in the out-of-plane configuration than the in-plane configuration. In the out-of-plane configuration we were able to achieve peak accelerations of ~5000G in the high frequency band (>1000Hz) on a DUT of 15kg. The peak acceleration can be tuned to be lower by adjusting the hammer drop height, mass, and strike plate material. For the in-plane configuration, the maximum peak acceleration achieved across all tests was ~1000G, which is lower than the specification. This can be amended with further testing, exploring different ways to stiffen the boundary conditions of the plate and the structure. Testing was not as thorough on the in-plane configuration due to time constraints. Some potential modifications that could yield higher peak accelerations in the in-plane configuration are listed below:

1. Adjust the structure so the hammer can be dropped from higher than 90 degrees in the in-plane configuration.
2. Adjust the mounting of the DUT so that all 3 axes can be tested using the out-of-plane configuration.
3. Adjust the mounting of the DUT to move it closer to the in-plane strike point
4. Stabilize the structure with sandbags or ballast of some type to reduce energy lost to motion of the machine
5. Adjust the mass distribution of the plate to amplify vibration modes at the DUT mount point

14 User Guide

To support the handoff from our team to SPRL, we've put together a user guide which details how SPRL can use the fixture to conduct their shock tests.

14.1 DUT Setup

The DUT shall be bolted down to the ringing plate, using the any of the ⅜"-16 blindly threaded holes, before any shock tests are conducted. In our tests, we've found that the difference between using a torque wrench compared to a socket wrench did not have a meaningful impact on the SRS. Either the DUT itself or the custom fixture plate between the DUT and ringing plate will need tapped holes according to the thread size and pitch of the accelerometers (¼"-28 for the PCB Piezotronic 350C04 model) used during the test. Figures X and Y show two setups used to test the OOP and IP configurations respectively for the shock test. The accelerometers are mounted such that their main axis is normal to the direction of the shock since the accelerometers are typically single-axis.

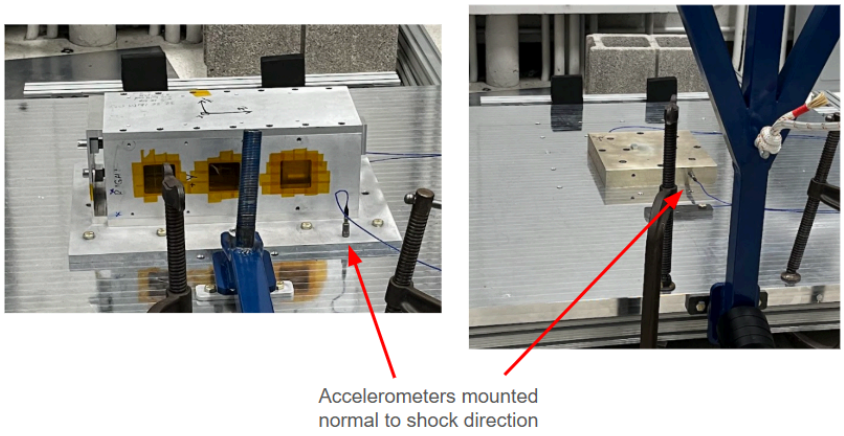


Figure X. Sample Setup of DUT and Accelerometers for OOP (left) and IP (right) configurations

14.2 Hammer Setup

The hammer is attached to an adapter plate which fits into the slots of the 80/20. There are four adapter plates on the current fixture in SPRL: two are set up for the height of the OOP configuration and two are set up for the height of the IP configuration. However, if SPRL needs to adjust the height of the hammer itself, they should start by moving the adapter plate and making sure that it's in the correct position. See Figure X for a labeled figure of the setup.

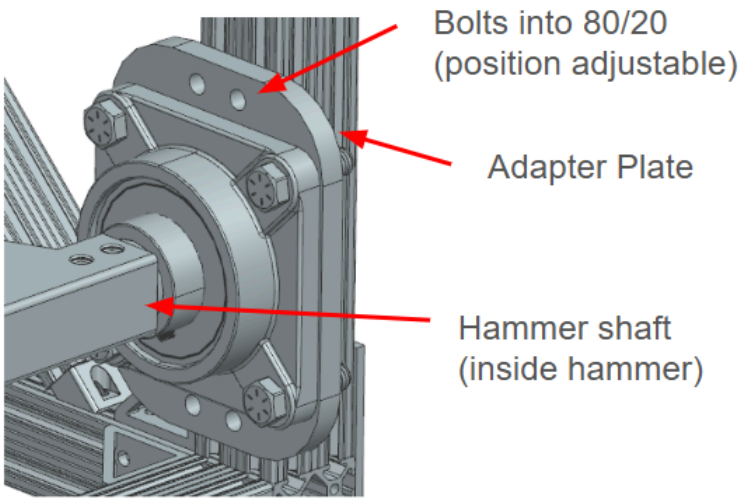


FIgure X. Labeled Diagram of Hammer Mounting Configuration (OOP shown)

Once the adapter plate position is finalized, the hammer shall be attached on both ends simultaneously. To do this, the hammer shaft and bearing should be placed into the hammer, then the entire assembly should be slid into place on the adapter plate. See Figure X for a visualization of this process in the OOP configuration (similar process for the IP configuration). This operation likely requires two people: one to hold and maneuver the hammer while the other inserts the bolts. Once the bolts are placed, the hammer can be set down then properly torqued.

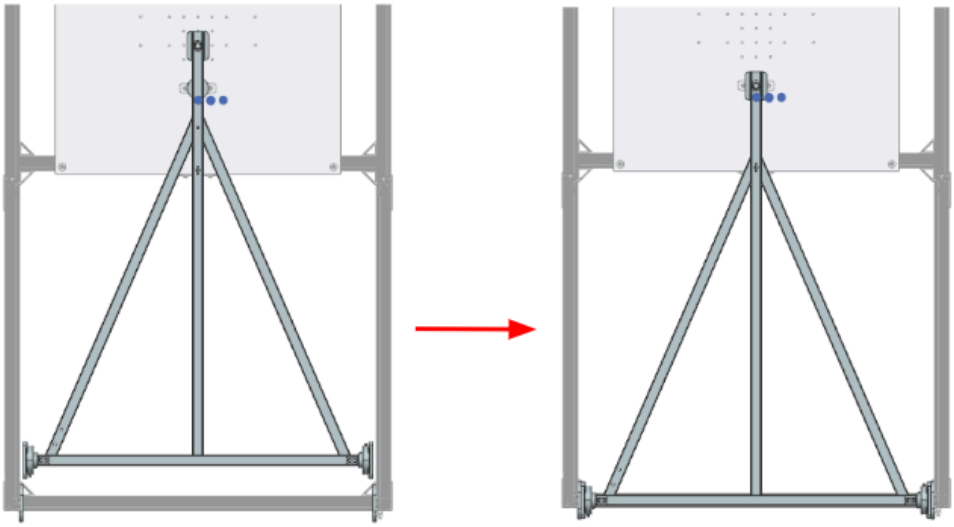


Figure X. Hammer Installation onto Adapter Plates (OOP Configuration)

Bear in mind that the pillow block bearing is not rigidly attached to the hammer. Thus, when the hammer is being moved during installation, the user must be careful that the bearing and hammer shaft do not fall out of the side of the hammer. Also, the hammer tip should be held up at all

times during hammer movement to ensure that the hammer tip doesn't scratch the plate or vice versa.

While the current setup in SPRL should not require any adjustments, there is potential that the hammer tip does not make square contact with the strike plate. However, this can be adjusted by moving the ringing plate itself. Figure X shows that the 80/20 underneath can be moved axially thereby changing the position of the ringing plate. Though the CAD does not reflect this, the 80/20 on the outside are oversized so that these adjustments can be moved.

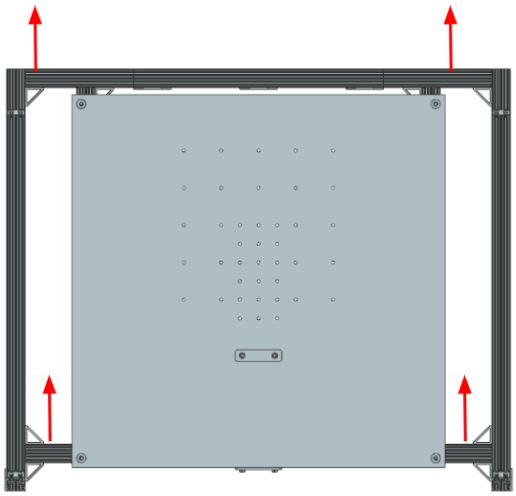


Figure X. Strike Plate Alignment with Hammer Tip

14.3 Test Setup

To conduct the shock test, the hammer should be picked up using the rope to the desired angle. To control the angle, the hammer can be lifted until the prong makes contact with the pin. This ensures repeatability between tests. See Figure X for a visual of the hammer drop angle control.

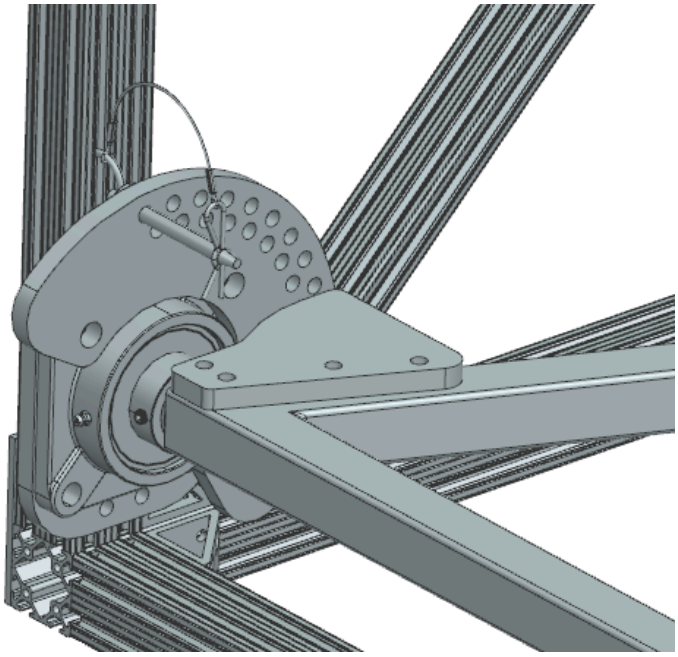


Figure X. Hammer Drop Angle Control

Once the hammer is at the desired angle, the user can simply drop the hammer.

14.4 SRS Tuning

The shock-fixture can be "dialed-in" to almost any NASA-GEVS-style SRS by judiciously changing a handful of mechanical levers that were quantified during final-build validation (Sec. 13). The practical tuning sequence below starts with the variables that shift the spectrum the most and ends with the secondary refinements. Between adjustments, always run a short three-shot repeatability check and average the two on-board accelerometers to confirm the spectrum is moving in the intended direction and that trial-to-trial spread remains within ±3 % (≈0.25 dB). References [25] and [29] contain insightful information about tuning SRS's. It is recommended to develop a data handling script that will quickly allow the test operator to compare the test result SRS to the specification and tolerance band.

1. **Set a baseline strike.**
   Begin with the steel strike-plate, a 10 lb hammer, and a 40 ° drop. That combination reliably produces a smooth, broadband spectrum whose mid-band knee sits near 2.5 kHz, giving ample head-room to tune both upward and downward.
2. **Shape the low- and mid-frequency levels with drop height.**
   Raising the swing from 20 ° → 40 ° lifts the spectrum uniformly by 2–3 dB between 200 Hz and 2 kHz; beyond ~2 kHz the curves converge because fixture stiffness—not input energy—limits the response. Above 40 ° the returns diminish, so use smaller increments (10 °) to avoid overshoot.

3. **Adjust the overall amplitude with hammer mass.**
   At a fixed angle, adding mass scales the spectrum almost uniformly below ~1 kHz (≈3 dB per 67 % mass increase). Gains taper at higher frequencies and become negligible above 2 kHz where plate rigidity governs the ceiling. Use the threaded nose-rod to fine-tune in 1-lb steps; expect sub-linear returns beyond 15 lb.
4. **Swap strike-plate material for mid-band fine tuning.**
   Steel and aluminium plates behave identically at gentle impacts, but at higher energies steel adds 2–4 dB in the 1–3 kHz band thanks to its higher elastic modulus. Keep the steel plate installed for severe shocks; substitute aluminium when a softer mid-band is required or to protect delicate DUTs.
5. **Refine high-frequency content with boundary conditions.**
   In the in-plane (IP) set-up, adding C-clamps closer to the strike point or torquing the corner bolts harder stiffens the plate and nudges the spectrum above the knee upward by 1–2 dB. Conversely, loosening the front bolts or moving the clamps outward softens the response. For the out-of-plane (OOP) configuration the four neoprene isolators dominate; replacing worn isolators or temporarily shimming them with harder rubber pads lowers damping and restores lost high-frequency energy.
6. **Verify pulse duration and eliminate secondary hits.**
   The primary impact should decay within 25 ms; if a secondary spike appears, pull the hoist rope immediately after the rebound to arrest the hammer before it re-contacts the plate. A lingering second hit usually exaggerates the first decade (<100 Hz) and should be avoided for qualification tests.
7. **Account for DUT position only for tight tolerances.**
   In OOP shocks the fixture delivers spatially uniform energy—placement anywhere on the mounting grid stays within ±3 dB across the spectrum. Relocation becomes useful only when a specification calls for tighter than ±3 dB in the 1–4 kHz range or when an IP test shows location-sensitive scatter.
8. **Confirm peak-G and iterate.**
   After each tuning cycle, compare the live SRS against the target template in VibrationVIEW. If the entire trace sits high, shorten the drop or shed hammer weight; if only the first decade is low, raise the angle a further 5-10 °. For IP tests that still fall short of high-frequency targets, consider adding ballast to the frame or elevating the hammer above 90 ° as outlined in Sec. 13.8.

15 Reflection

Our team, much like the UM Mechanical Engineering Department, is committed to making the world work better. Throughout the course of this project, we continually reflected on how our design impacts public welfare, the global context, and ethical and social dynamics.

15.1 Public Health, Safety, and Welfare Implications

As mentioned previously, safety remained a top priority due to the high force impacts involved in mechanical shock testing. Our final design incorporated OSHA and ASME standards by emphasizing structural robustness, noise dampening, and vibration isolation. We reinforced the importance of safety through the addition of a pin secured by a hairpin cotter to the design, which acts as a two step release mechanism, ensuring safe operation. Additionally, the machine contributes to public welfare by ensuring the reliability of spaceflight instrumentation, helping prevent mission failures that can lead to significant financial losses.

15.2 Global, Social and Environmental Considerations

Our design benefits the global marketplace by providing a cost effective, in house shock testing solution. Firstly, this allows SPRL to ensure reliability and safety in space missions, benefiting space exploration missions globally. Additionally, our design could also benefit other universities, research organizations, laboratories, and aerospace companies globally by providing a more affordable option to expensive commercial shock testing machines. Our machine creates a positive societal impact by giving access to better testing capabilities as well as scientific research. Potential negative social impacts may be caused from the manufacturing process of our machine, including materials sourcing, production, and disposal. However, by using recyclable materials, and local machining and manufacturing, we minimize these negative impacts while supporting the local economy. Over its lifetime, the machine would save SPRL thousands of dollars annually by reducing their reliance on third party testing. Furthermore, the machine's use of a modular aluminum structure enables easy and low cost maintenance that extends the lifetime of the product, leading to better economic impacts. Throughout the development process, stakeholder maps were used to help us better understand the societal impacts, and life cycle costing analysis to understand the economic impacts.

15.3 Inclusion and Equity

Our team brought diverse differences regarding cultural backgrounds, engineering experiences, and working styles. Each member brought unique perspectives, from industry and co-op experience to international viewpoints, to the team. These differences influenced many things throughout the design process such as priorities, safety considerations and communication styles during team meetings. Furthermore, working with our sponsor SPRL added another layer of complexity to our design process and final design. We considered SPRL as experts in this topic, which led us to place a lot of weight on their opinion and feedback. However, by being aware of these similarities and differences, we made sure to encourage open discussion where no single person dominates the team’s discussion and decision.

15.4 Ethics

One ethical dilemma that we faced was whether to prioritize cost savings or safety margins. At one point during our design process, we were faced with the decision to choose between using 3-inch or 2-inch T-slot aluminum sections. This was because a design that uses less material would significantly reduce the total cost, and SPRL already had spare 2-inch sections available, further incentivizing us to use the smaller size. This raised concerns about whether prioritizing cost savings would negatively affect the safety and structural integrity of the machine. However, we mitigated this by performing proper safety factor calculations to ensure that the structure will be stable. Although we didn't directly handle sensitive data, another ethical dilemma that we faced was to stay respectful and mindful of SPRL's ITAR controlled information. If this mechanical machine were to enter the marketplace and be sold commercially, some ethical concerns could arise, including ensuring user safety through proper training and user guide, being transparent about the system's capabilities and limitations, and promoting responsible end of life disposal methods.

Our team's personal ethics aligns closely with the professional ethics held by the University of Michigan, including but not limited to ensuring public safety and health, honest communication, and the responsible use of resources. These principles guided our decision making throughout the whole semester and will continue to do so throughout our future careers.

16 Discussion

While our team was able to successfully design, build, and validate a mechanical shock testing machine that met SPRL's requirements, there are still several areas for improvement. With additional time and resources, we would be able to explore and refine more aspects of the design to better define the problem. One area of improvement surrounds a more in-depth characterization of how different DUT characteristics influence the required shock spectrum. The approach chosen did not consider any DUT characteristics beyond mass but stiffness of the DUT and its mounting conditions likely impact SRS shape. Including these considerations would help mitigate performance variation between representative masses and real instruments. Nevertheless, the chosen approach considering only mass is felt to be successful given the time constraints of the project.

There are several strengths to our design. Firstly, our machine is highly cost effective, with the total cost coming in at just under $5,000, which is significantly lower than comparable commercial shock testing machines. For comparison, one machine that SPRL was considering purchasing was priced between $40,000 and $55,000. We also prioritized manufacturability by using standard, readily available materials and parts. For instance, we used a T-slot aluminum frame, which not only made construction easier but also provided high modularity, allowing for simple reconfiguration between in-plane and out-of-plane setups, as well as future modifications.

Furthermore, the machine is designed for intuitive operation by using a straightforward hammer release mechanism and simple procedures for adjusting mass and height. This minimizes overall machine operation complexity and helps reduce the risk of user error and potential safety risks. Lastly, the system is highly repeatable across different mass and angle settings, achieving better than ±3 % (≈±0.25 dB) across most of the SRS spectrum.

On the other hand, we recognize that there are also weaknesses to the design. One weakness is that overtime, we noticed that the neoprene vibration isolators became slightly squished, which may affect their long term effectiveness and the reliability of the machine. Additionally, we put less thought into the damping design for the in plane configuration when compared to the out of plane configuration. While the neoprene isolators were made for absorbing axial loads in the out of plane setup, they were not suited for shear loads in the in plane setup. We attempted to address this issue by adding backstops with foam between them and the ringing plate to help absorb the load, as well as installing clamps to help distribute load. However, these additions felt more like a patchwork solution than a fully integrated design. Additionally, improving the hammer release mechanism would improve both the consistency and safety. Currently, the rope and pulley hammer release mechanism relies on a human operator manually letting go of the rope, which can potentially have slight variability in the hammer drop speed if the release is not completely clean. Having an operator hold the rope also introduces a small safety risk, as there is a possibility of a hand becoming entangled during release. Lastly, we were unable to validate the SRS up to the full 10 kHz because we were limited by the version of the software we were provided. There was little we could've done about this, nevertheless this was still a big weakness.

In hindsight, several changes can be made to mitigate the weaknesses highlighted previously. One change would be to find more durable shock absorbers that can better maintain their performance over repeated impacts. We recognize that the eventual degradation of the absorbers is unavoidable, so we can address this by having multiple sets of replacement absorbers. Additionally, designing a more dedicated in-plane shock absorbing system would improve the design. We can do this by integrating additional shear rubber mounts specifically designed to handle shear loads, which are readily available for purchase online. An alternative solution would be to install additional neoprene isolators, similar to those currently used, onto the backstops to help absorb the load. Furthermore, to address the problem with the hammer release mechanism, we can improve this by implementing a quick release mechanism instead of the current rope and pulley mechanism. This would create a more consistent release and improve the overall safety. Finally, purchasing the full capability version of the data acquisition software would allow measurement of the SRS up to 10 kHz, providing a more complete data set.

One challenge we faced was dealing with long lead time items. Custom machined and welded parts had by far the longest lead times, and considering our limited project timeline, we

prioritized avoiding these components as much as possible. By using T-slot aluminum for the structure, we avoided machining in the student machine shop, saving a big portion of time. Similarly, by intentionally using as many off the shelf parts as possible and limiting the custom machined and welded part to only the ringing plate and the hammer arm, we were able to significantly reduce the total lead time and help keep the project on schedule. Another challenge we faced was getting a solid understanding of how the system would react to shock. We had little prior experience with shock, so there were many aspects that were unfamiliar to us. Since a solid understanding of shock behavior was crucial to the success of this project, we addressed this risk by running simulations in ANSYS and comparing our results through real life experimental data collected from our mini shock tester. This helped us to gain a better understanding and confidence, and allowed us to make more informed design choices for the full scale design. A risk to end users of our machine is the extremely loud noise level during the impact of the hammer with the ringing plate, requiring the use of hearing protection. There is also a risk of crush injuries during the setting up and operation phases. To address this risk, a two step hairpin cotter release mechanism is used to help prevent those injuries. Additionally, due to the high shock nature of the system, there is a risk of fatigue failure in the long term. This issue can be addressed by performing regular maintenance and inspections of the machine and replacing parts when necessary. Finally, to reduce the risk of misuse of the machine, we have included a user guide to help ensure proper operation and prevent potential damage to the system.

17 Recommendations

1. Broaden high frequency capability
    a. Purchase the high frequency (10kHz) VibrationView license so SPRL can verify compliance with the entire NASA-GEVS envelope without extrapolation.
    b. Replace the neoprene corner mounts with off-the-shelf shear mounts rated for a high maximum load.
2. Increase in-plane energy transfer into the DUT
    a. Add additional back-stop material or extra shear mounts under the plate edge opposite the strike point.
    b. Re-drill the hammer hinge plates with an additional row of holes to allow drops up to 120 ° and remove the hoist bar of the structure to unblock the hammer drop. This simple change yields a 30 % velocity increase without lengthening the frame.
3. Spare hardware
    a. Extra aluminum and steel strike plates, pillow-block bearings, isolators, and hammer tips.
4. Documentation and training
    a. Create a laminated “quick-start” sheet that pairs common GEVS spectra with hammer settings validated during our campaign.

5. Stability
    a. Fix the machine to the floor with sandbags or ballast of some type
    b. Loctite all fasteners of the frame and plate to ensure the bolts do not loosen over time

18 Conclusion

Over the course of 15 weeks, we successfully designed, analyzed, and fabricated a mechanical shock testing machine for the University of Michigan's Space Physics Research Laboratory (SPRL). This system allows SPRL to conduct in-house mechanical shock qualification of their flight hardware, eliminating dependence on external testing facilities, reducing cost, and increasing flexibility. Through careful requirements development, concept generation, and selection processes, we arrived at a hammer-striking ringing plate architecture. Extensive modeling and simulations, verified by small-scale prototype testing, validated the expected performance of the full-size system.

The mechanical shock testing machine meets or exceeds every primary requirement, delivering repeatable shocks from 750 g to over 5,000 g, spanning 100 Hz to 5 kHz (software-limited), and confining the main pulse to under 25 milliseconds. It provides three-axis testing capability, with out-of-plane shocks already satisfying the full NASA GEVS envelope and only minor stiffening needed in the in-plane configuration to achieve equivalent peak levels. The final system was produced at a total cost of $4,983—below the $40,000 project ceiling—and more than 60% of its parts were sourced from off-the-shelf components or repurposed SPRL inventory, making it highly cost-effective at less than one-eighth the price of a comparable commercial machine. The design is reconfigurable, with the t-slot frame, modular hammer mass, and interchangeable strike plates allowing extensive tunability of the shock spectrum using only basic tools. Finally, the machine was thoroughly validated both analytically and experimentally: results from ANSYS explicit dynamics simulations, MATLAB-based Smallwood SRS synthesis, and over 100 physical drops showed agreement within ±2 dB across the critical 200 Hz–3 kHz band, providing strong confidence in the system's predictive models for future testing.

With the recommendations in §17, the fixture will remain reliable for 10 000+ cycles, expand to the full 10 kHz bandwidth, and streamline day-to-day operation. Most importantly, SPRL now controls its own mechanical-shock qualification schedule—reducing external test costs, protecting ITAR-sensitive hardware, and accelerating instrument delivery for upcoming space missions.

19 Acknowledgements

We would like to sincerely thank Louis Marr, Fernando Saca, Frank Palumbo, Jonathan Van Noord, and the rest of the SPRL team for their support and guidance. Additionally, thank you to Vibration Research for providing VibrationVIEW software for data analysis. Finally, we would like to thank Professor Shorya Awtar for his expertise and mentorship through the course of this project and for serving as our advisor.

References

[1] Ansys. Performing Response Spectrum Analysis Using Ansys Mechanical — Lesson 1 YouTube, 28 Mar. 2017, youtu.be/5DYMvfEUJNc.

[2] Harrington, Joseph, et al. “ME450 Shock Testing Machine.” Received by Louis Marr, Fernando Saca, 14 Jan. 2025.

[3] Harrington, Joseph, Kalen O’Connor, et al. “ME450 Team 21 and SPRL Meeting.” 17 Jan. 2025.

[4] “High Speed Shock Testing System HDST Series: Shock Tower.” Shinyei Corporation of America, www.sca-shinyei.com/drop/shock_hdst. Accessed 30 Jan. 2025.

[5] “Home.” Spectral Dynamics Inc., www.spectraldynamics.com/index.php/shakers/shock-test-machines. Accessed 30 Jan. 2025.

[6] How to Perform Response Spectrum Analysis - Lesson 1 | Ansys Innovation Courses, innovationspace.ansys.com/courses/courses/single-point-response-spectrum-analysis-using-ansys-mechanical/lessons/how-to-perform-response-spectrum-analysis-lesson-1/. Accessed 31 Jan. 2025.

[7] International Electrotechnical Commission (IEC). IEC 60068-2-27: Environmental Testing – Part 2-27: Tests – Test Ea and Guidance: Shock. IEC, 2008.

[8] Irvine, Tom. An Introduction to Shock and Vibration Response Spectra, Revision A. Vibrationdata, 2005.

[9] MathWorks. Practical Introduction to Shock Waveform and Shock Response Spectrum. MathWorks,www.mathworks.com/help/signal/ug/practical-introduction-to-shock-waveform-and-shock-response-spectrum.html. Accessed 30 Jan. 2025.

[10] “Model 23D.” Lansmont, www.lansmont.com/products/shock/standard/model-23d. Accessed 30 Jan. 2025.

[11] NASA Goddard Space Flight Center, "GSFC-STD-7000A: General Environmental Verification Standard (GEVS) For GSFC Flight Programs and Projects," Approved April 22, 2013, Accessed January 30, 2025.

[12] National Fire Protection Association (NFPA). NFPA 70: National Electrical Code. 2023 ed., NFPA, 2023 www.nfpa.org/codes-and-standards/all-codes-and-standards/list-of-codes-and-standards/detail?code=70. Accessed January 30, 2025.

[13] National Fire Protection Association (NFPA). NFPA 79: Electrical Standard for Industrial Machinery. 2024 ed., NFPA, 2024, www.nfpa.org/codes-and-standards/all-codes-and-standards/list-of-codes-and-standards/detail?code=79. Accessed January 30, 2025.

[14] Occupational Safety and Health Administration (OSHA). “General Requirements for All Machines (29 CFR 1910.212). United States Department of Labor,” Approved October 30, 1978, www.osha.gov/laws-regs/regulations/standardnumber/1910/1910.212. Accessed January 30, 2025.

[15] Rocket Lab USA. 2002337G CSD Data Sheet. Rocket Lab, www.rocketlabusa.com/assets/Uploads/2002337G-CSD-Data-Sheet-compressed.pdf. Accessed January 30, 2025.

[16] “Sam: Sample Analysis at Mars on the Rover ‘Curiosity.’” *NASA*, NASA, ssed.gsfc.nasa.gov/sam/curiosity.html. Accessed 30 Jan. 2025.

[17] “Space Physics Research Laboratory.” Climate and Space Sciences and Engineering, 19 Mar. 2024,clasp.engin.umich.edu/research/instrumentation-observational-methods/space-physics-research-laboratory/.

[18] SpaceX. Falcon 9 and Falcon Heavy Users' Guide. Sept. 2021, SpaceX, www.spacex.com/media/falcon-users-guide-2021-09.pdf. Accessed January 30, 2025.

[19] United States Air Force Space and Missile Systems Center (SMC). SMC-S-016: Test Requirements for Launch, Upper-Stage, and Space Vehicles. 5 Sept. 2014, NASA, explorers.larc.nasa.gov/2019APSMEX/MO/pdf_files/SMC-S-016_05SEP2014.pdf. Accessed January 30, 2025.

[20] United States Department of Defense. MIL-STD-883: Test Method Standard – Microcircuits. U.S. Department of Defense, 1996. Accessed January 30, 2025.

[21] “Vibration Controllers - Control Hardware & Software.” Vibration Research, 14 Oct. 2024, vibrationresearch.com/products/vibrationview/?gad_source=1&gclid=Cj0KCQiA4-y8BhC3ARIsAHmjC_HCmL7a64rXSSbAdVyrNLYBlIKEUXa2pBjBSCRw6HoA36_nRFqYQ3gaAp4qEALw_wcB

[22] Lansmont. (n.d.). *Model 23D shock test system*. Accessed March 3, 2025. https://www.lansmont.com/products/shock/standard/model-23d

[23] European Space Agency. (n.d.). *Shock test bench*. Accessed March 3, 2025. https://technology.esa.int/page/shock-test-bench

[24] CME Technology. (n.d.). *KRD15 pneumatic horizontal shock response spectrum test system*. Accessed March 3, 2025. https://www.cmetechnology.com/products/krd15-pneumatic-horizontal-shock-response-spectrum-test-system/

[25] Jonsson, M. (2012). *Development of a shock test facility for qualification of space equipment* (Master’s thesis). Chalmers University of Technology, Department of Applied Mechanics, Division of Dynamics.

https://odr.chalmers.se/server/api/core/bitstreams/afe6af89-96db-4c0d-9626-665b709b1871/content

[26] Morais, T., & Vasques, C. M. (2016). Shock environment design for space equipment testing. *Journal of Aerospace Engineering, 231*(6), 1154–1167. https://doi.org/10.1177/0954410016648998

[27] Richman, S. J., & Kelly, J. J. (1997). *Principles and techniques of shock data analysis*. The Shock and Vibration Information Center, Naval Research Laboratory.

[28] MathWorks. (n.d.). *Practical introduction to shock waveform and shock response spectrum*. Retrieved March 30th, 2025 from https://www.mathworks.com/help/signal/ug/practical-introduction-to-shock-waveform-and-shock-response-spectrum.html

[29] Kelly, Ronald D., and George Richman. "Principles and Techniques of Shock Data Analysis." *Proceedings of the 9th European Conference on Spacecraft Structures, Materials & Mechanical Testing* (ESA SP-581), edited by K. Fletcher, European Space Agency, 2005, pp. 125-132. NASA ADS, https://adsabs.harvard.edu/full/2005ESASP.581E.125K.

Appendix A: Team 21 Biographies

Kalen:

My name is Kalen O'Connor. I was born and raised in New Jersey. Ever since I was young, I had a fascination with puzzles. Whether it was playing minesweeper on my dad's iPad to my high school obsession solving Leetcode challenges, I was continuously finding new puzzles to solve and constantly pushing myself to learn and think critically. This passion for problem solving led me to study engineering at UM.

As a freshman looking to get involved in engineering, I joined the UM Solar Car Team where I quickly realized how much I had to learn. Stepping into such a fast-paced environment was daunting. Despite being an inexperienced freshman, I stuck with the team for two years, gaining lots of invaluable experience. I learned a ton not just about engineering, but about how to work in a team-based environment.

Now, as a senior in ME 450, I'm excited to apply my knowledge to another real-world issue—creating a shock fixture for the Space Physics Research Laboratory (SPRL for short) to test space instrumentation. I'm excited to make a contribution, though indirectly, to space exploration and the intriguing work that SPRL does.

Looking ahead, I'm lucky enough to say that I'll be working as a mechanical engineer at Leonardo DRS in the defense sector once I graduate. I'm eager to continue taking on challenging problems and develop innovative solutions to problems.

Joey:

I'm Joey Harrington and I hail from the great city of Pittsburgh, Pennsylvania. A self declared yinzer, I love all things Pittsburgh, especially the Steelers, Penguins, and Heinz ketchup. I always have and continue to love building stuff and solving problems. I grew up on Legos and that passion has transformed into solar cars, normal cars, weather balloons, and a handful of other big "toys" that I keep myself entertained with now. Engineering is an artform to me as much as it is a science. There is beauty in simple designs that solve actual problems and bringing those solutions to life while working alongside and learning from other talented engineers is a deeply satisfying profession.

After graduating, I intend to enter the workforce full-time in either the automotive or aerospace industry. I am currently in the interview process for several positions.

Nate:

I am Nathan Gustafson, I am from Edwardsburg, Michigan in the southwest corner of the state. My interest in mechanical engineering stems from an interest in building and designing ideas. I have chosen to pursue a career in engineering because I believe that engineers are capable of doing great things for the world and accomplishing astonishing things, like putting humans on the moon, connecting people around the globe, and harnessing energy from a star from on top of our homes.

This is my 5th year at UM, I took my 4th year off to race with the UM Solar Car Team and work in industry. After graduation I will be starting full-time work. I am interviewing for positions in the space industry.

Ice:

My name is Ice Kulsetsophon, and I am an international student from Thailand. Ever since I was young, I have always loved mathematics, physics, astronomy, and building things with my hands. I was always building toys or anything that I thought was cool for myself, and had a lot of fun doing it! One of my favorite things I remember building was an air pressure rocket in 5th grade made out of PVC pipes, where I copied the idea from a youtube video. Eventually my passion for building things led me to choosing to pursue mechanical engineering at UofM. An interesting fact about me is that I love photography, which I recently got into in recent years. As for my future plans, I am still currently in the process of finding full time positions, both in the USA and Thailand.

Appendix B: Bill of Materials

Link to spreadsheet

Plate Subassembly						
Item	**Vendor**	**Link**	**Qty**	**Price (unit)**	**Price (total)**	**Comment**
					$1,933.69	
Ringing Plate	ProCam Services		1	$1,852.26	$1,852.26	To be picked up 4/4
Aluminum strike plate	SPRL?		3		$0.00	Check if SPRL has stock 6"x6"
Steel strike plate	SPRL?		3		0	Check if SPRL has stock 6"x6"
Isolators	McMaster-Carr	https://www.mcmaster.com/93945K115/	5	$7.66	$38.30	4 in assembly plus one spare
1/4 oversize washer	McMaster-Carr	https://www.mcmaster.com/90313A107/	1	$8.28	$8.28	1 pk 50; 12 in assembly
1/4-20 lg 1.75 hex head bolt	McMaster-Carr	https://www.mcmaster.com/91257A548/	1	$15.45	$15.45	1 pk 50; plate fixturing bolts; 4 in assembly
Sleeve bushing	McMaster-Carr	https://www.mcmaster.com/6389K113/	10	$0.80	$8.00	8 in assembly; 2 spare
3/8-16 lg 1 hex head	McMaster-Carr	https://www.mcmast	1	$11.40	$11.40	1 pk 25; strike plate bolts; 2 in

		er.com/92620A624/				assembly;

Hammer Subassembly						
Item	**Vendor**	**Link**	**Qty**	**Price (unit)**	**Price (total)**	**Comment**
					$785.01	
1.5" square tube stock, .12" wall. Low carbon steel. 6ft sections	mcmaster-carr	https://www.mcmaster.com/6527K374/	4	$65.18	$260.72	Hammer weldment stock
Rotary shaft stock	mcmaster-carr	https://www.mcmaster.com/1346K532/	1	58.44	58.44	Bearing shaft
1/2" aluminum stock	SPRL?					For adapter plate(4x 7"x4") and angle control (2x 10" diameter)
1/2" steel stock	SPRL?		20" x 12" plate (maybe smaller)			For weight plates (5x 5.5" diameter). Maybe a 5.5" rod parted into 1/2" thick sections would be better?
3" x 6" 4140 Alloy	Alro steel		1	48.42	48.42	Hammer tip stock

Steel Rod - stock for hammer tip						
1" nut, 1-12 UNF	mcmaster-carr	https://www.mcmaster.com/92673A331/	1	2.36	2.36	For weight plates
3/8" steel plate stock	mcmaster-carr	https://www.mcmaster.com/1388K204/	1	19.61	19.61	For hammer tip adapter
1" OD .12" wall thickness low carbon steel tube, 1ft	mcmaster-carr	https://www.mcmaster.com/7767T371-7767T372/	1	7.7	7.7	For weight plates
Flange mount ball bearing	McMaster-carr	https://www.mcmaster.com/6494K59/	2	59	118	
316 Stainless Steel Button Head Hex Drive Screw Super-Corrosion-Resistant, 3/8"-16 Thread Size, 1-1/2" Long	McMaster-carr	https://www.mcmaster.com/98164A306/	2		7.82	For hammer tip mounting

High-Strength Steel Nylon-Insert Locknut Grade 8, 1/2"-20 Thread Size	McMaster-carr	https://www.mcmaster.com/90630A160/	2	4.85	9.7	For bearing mounting
Zinc Yellow-Chromate Plated Hex Head Screw Grade 8 Steel, 1/2"-20 Thread Size, 2" Long, Partially Threaded	McMaster-carr	https://www.mcmaster.com/91257A748/	1	$16.61	$16.61	For bearing mounting
Zinc Yellow-Chromate Plated Hex Head Screw, Grade 8 Steel, 1/2"-13 Thread Size, 1-3/4" Long	McMaster-carr	https://www.mcmaster.com/92620A718/	1	$12.30	$12.30	For bearing mounting - shorter version
Medium-Strength Grade 5 Steel Hex	McMaster-carr	https://www.mcmaster.com/91247A634/	1	$13.43	$13.43	For shaft mounting

Head Screw Zinc-Plated, 3/8"-16 Thread Size, 2-1/2" Long, Partially Threaded						
3/8"-16 Locknuts	McMaster-carr	https://www.mcmaster.com/90630A121/	1	$4.50	$4.50	For shaft mounting
5/16" eyebolt, 2.25" shaft	McMaster-carr	https://www.mcmaster.com/3018T15/	1	$6.53	$6.53	For hoisting the hamer
Pulley for Wire Rope-for Lifting, Mounted, Single-Groove, for 3/8" Diameter Rope	McMaster-carr	https://www.mcmaster.com/3099T4/	1	$36.79	$36.79	For hoisting the hamer
Quick release pin with lanyard cotter pin	McMaster-carr	https://www.mcmaster.com/98412A505/	1	$12.92	$12.92	For dropping the hammer
3/8" rope, 25' long	McMaster-carr	https://www.mcmaster.com/3790T14/	1	$60.25	$60.25	For hoisting the hamer

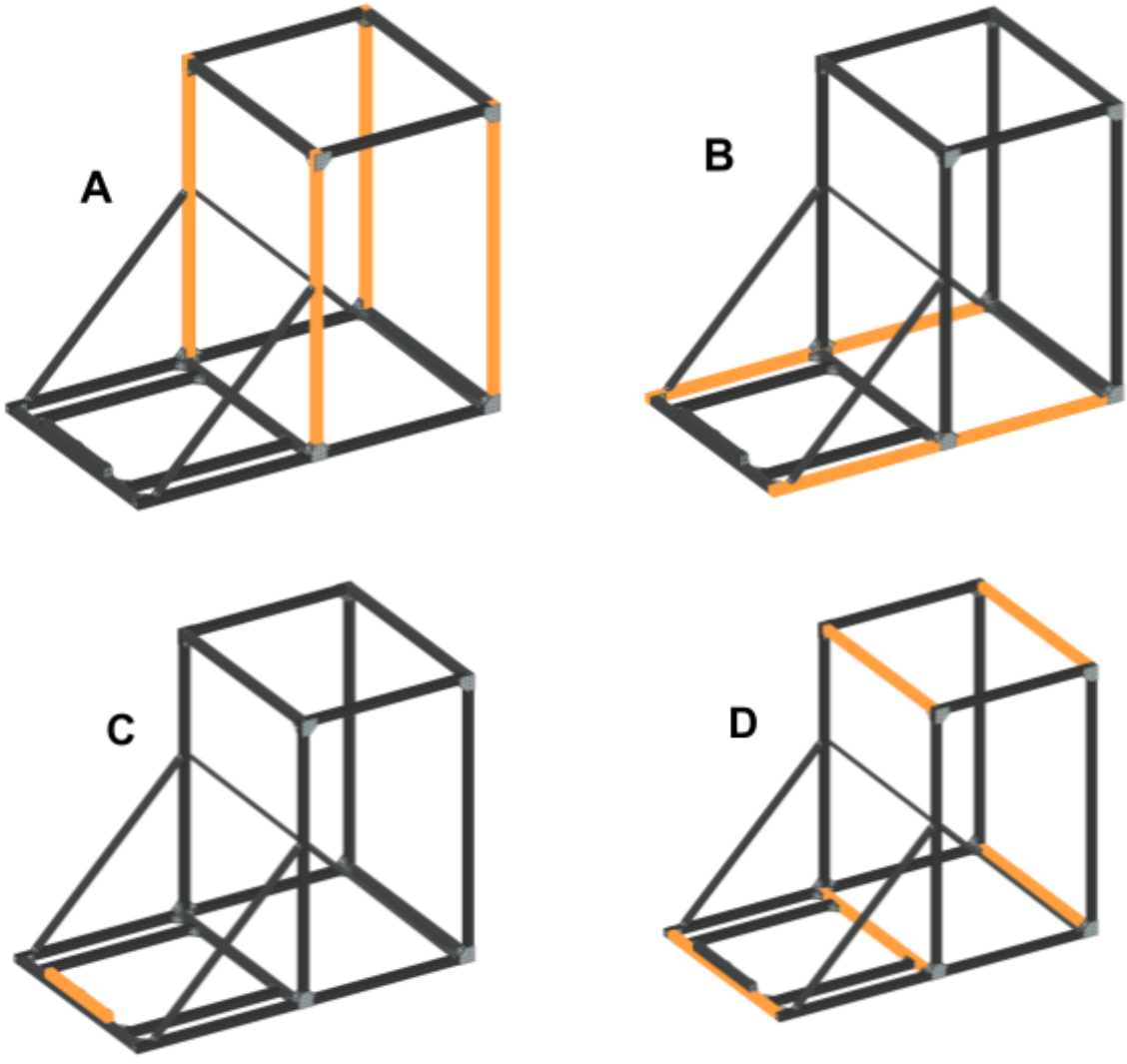
1/4-20 t-slot nut	McMaster-carr	https://www.mcmaster.com/3136N396/	8	$5.45	$43.60	8 pks 4; 16 for hammer, 4 for ringing plate, 4 for pulley, 2 for cleat, 6 extra
Cleat	McMaster-carr	https://www.mcmaster.com/33805T43/	1	$3.42	$3.42	to tie off rope
1/4-20 pulley bolts	McMaster-carr	https://www.mcmaster.com/92620A535/	1	$15.70	$15.70	1 pk 100; 4 for pulley
1/4-20 adapter plate bolts	McMaster-carr	https://www.mcmaster.com/92620A540/	1	$17.28	$17.28	1 pk 100; 8 for hammer
1/4-20 cleat bolts	McMaster-carr	https://www.mcmaster.com/92620A544/	1	$8.91	$8.91	1 pk 25; 2 for cleat

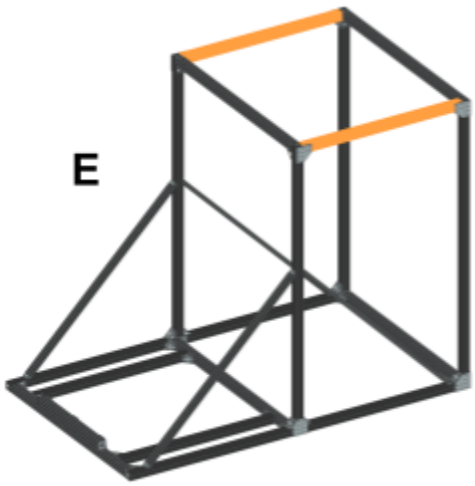
Frame Subassembly						
Item	**Vendor**	**Link**	**Qty**	**Price (unit)**	**Price (total)**	**Comment**
					$2,263.87	
2" **Quad** T-slot aluminum, PART A	SPRL		1	$0.00	0	Stand side poles (actual 71in or 5.91667ft) - **Use 6' 8" from SPRL**
2" **Quad** T-slot aluminum, PART B	SPRL		1	$0.00	0	Stand legs (actual 89.7988in or 7.483ft) - **Use 10' 4" from SPRL**
2" **Quad** T-slot aluminum, PART C	SPRL		1	$0.00	0	Backstop - **Use 26.75" from SPRL**

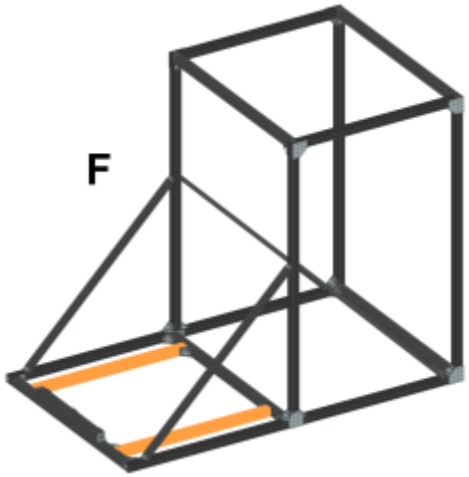
2" **Quad** T-slot aluminum, PART B	mcmaster-carr	https://www.mcmaster.com/47065T501/	1	$104.76	$104.76	Stand legs (actual 89.7988in or 7.483ft) - **Buy 8ft section**
2" **Quad** T-slot aluminum, PART A	mcmaster-carr	https://www.mcmaster.com/47065T501/	3	$78.57	$235.71	Stand side poles (actual 71in or 5.91667ft) - **Buy 6ft section**
2" **Quad** T-slot aluminum, PART D	mcmaster-carr	https://www.mcmaster.com/47065T501/	5	$69.13	$345.65	Stand bar (actual 50in or 4.16667ft) - **Buy 5ft section**
2" **Quad** T-slot aluminum, PART E	mcmaster-carr	https://www.mcmaster.com/47065T501/	2	$56.04	$112.08	Top parallel bars (actual 41.9238in or 3.49365ft) **- Buy 4 ft section**
2" **Quad** T-slot aluminum, PART F	mcmaster-carr	https://www.mcmaster.com/47065T501/	2	$56.04	$112.08	Ringing plate mounting (actual 38.25in or 3.1875ft) - **Buy 4 ft section**
2" **Double** T-slot aluminum, PART G	mcmaster-carr	https://www.mcmaster.com/47065T107/	4	$49.07	$196.28	Double Angled brace (actual 54 in or 4.5ft) - **Buy 5 ft Section**
Diagonal Brace ends	mcmaster-carr	https://www.mcmaster.com/47065T335/	8	$18.06	$144.48	For connecting double t slot to the stand legs and poles
Gusset Brackets	mcmaster-carr	https://www.mcmaster.com/47065T893/	26	$25.63	$666.38	For various T slot joints

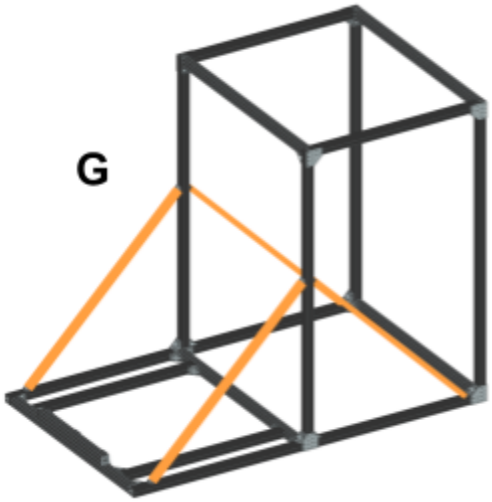
Corner Surface Bracket	mcmaster-carr	https://www.mcmaster.com/47065T274/	6	$30.60	$183.60	For joining legs to pole and pole to top parallel bar
Tee Surface Bracket	mcmaster-carr	https://www.mcmaster.com/47065T281/	5	$32.57	$162.85	For joining legs to pole and backstop to structure

Frame component reference

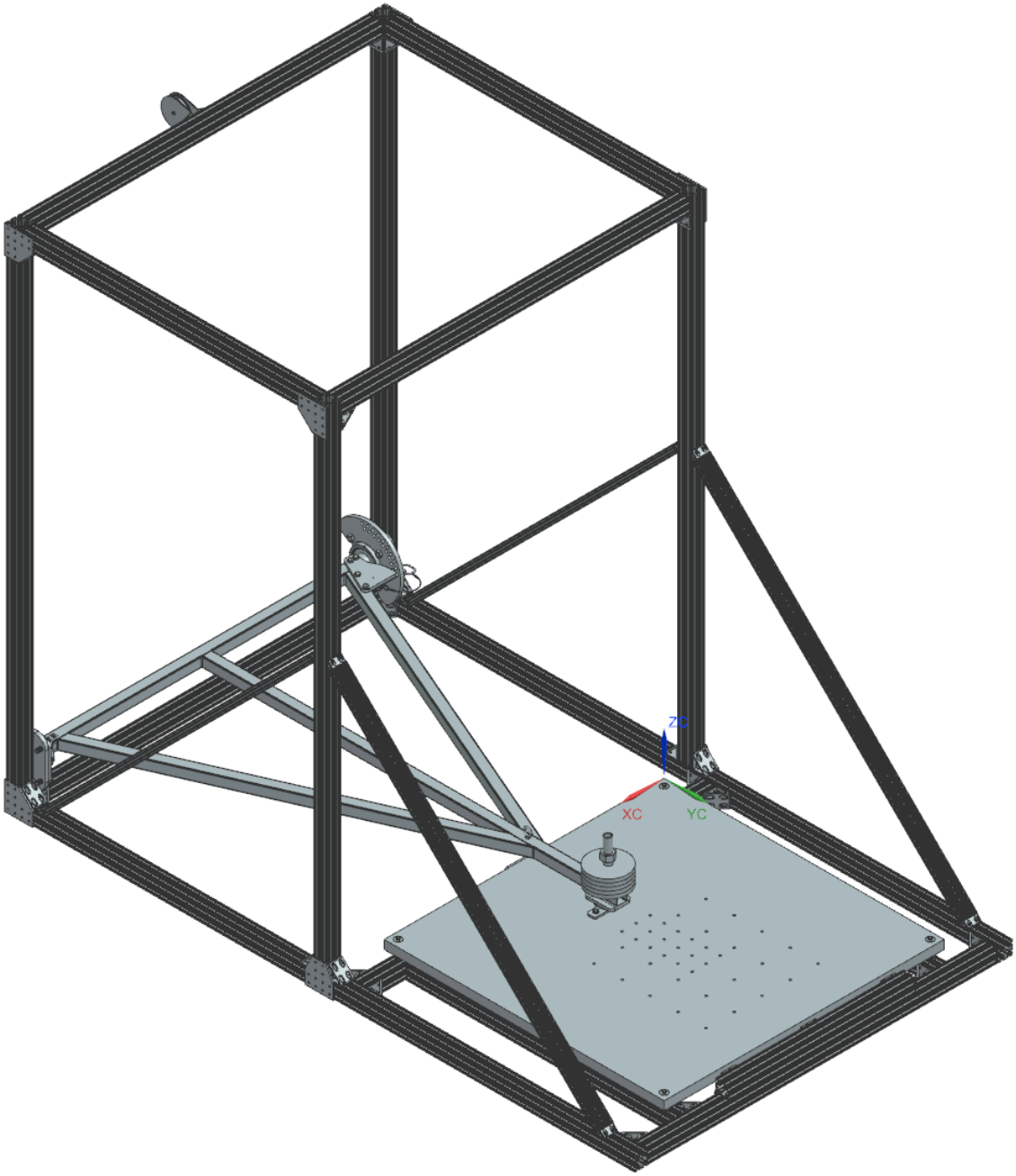


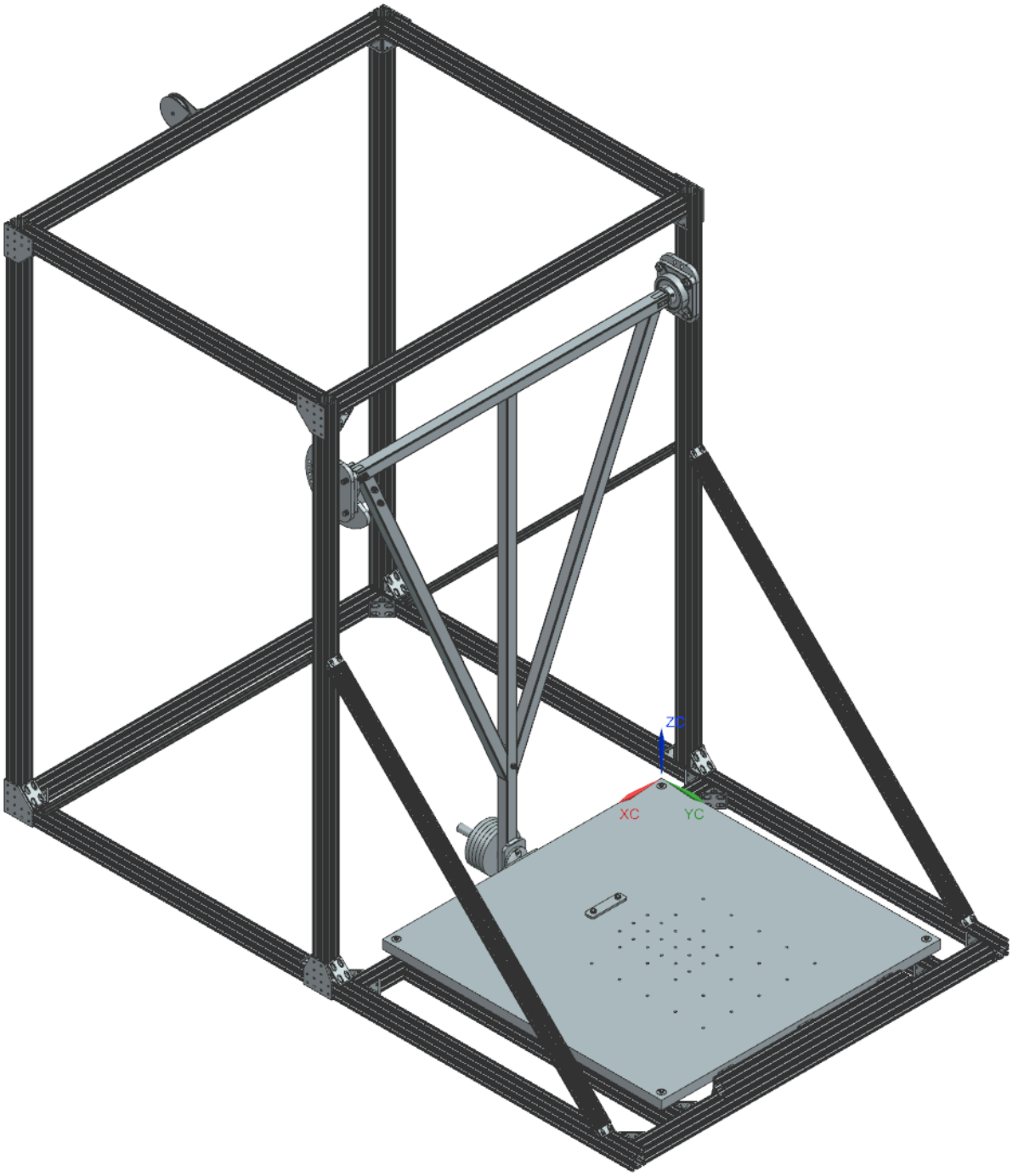

E

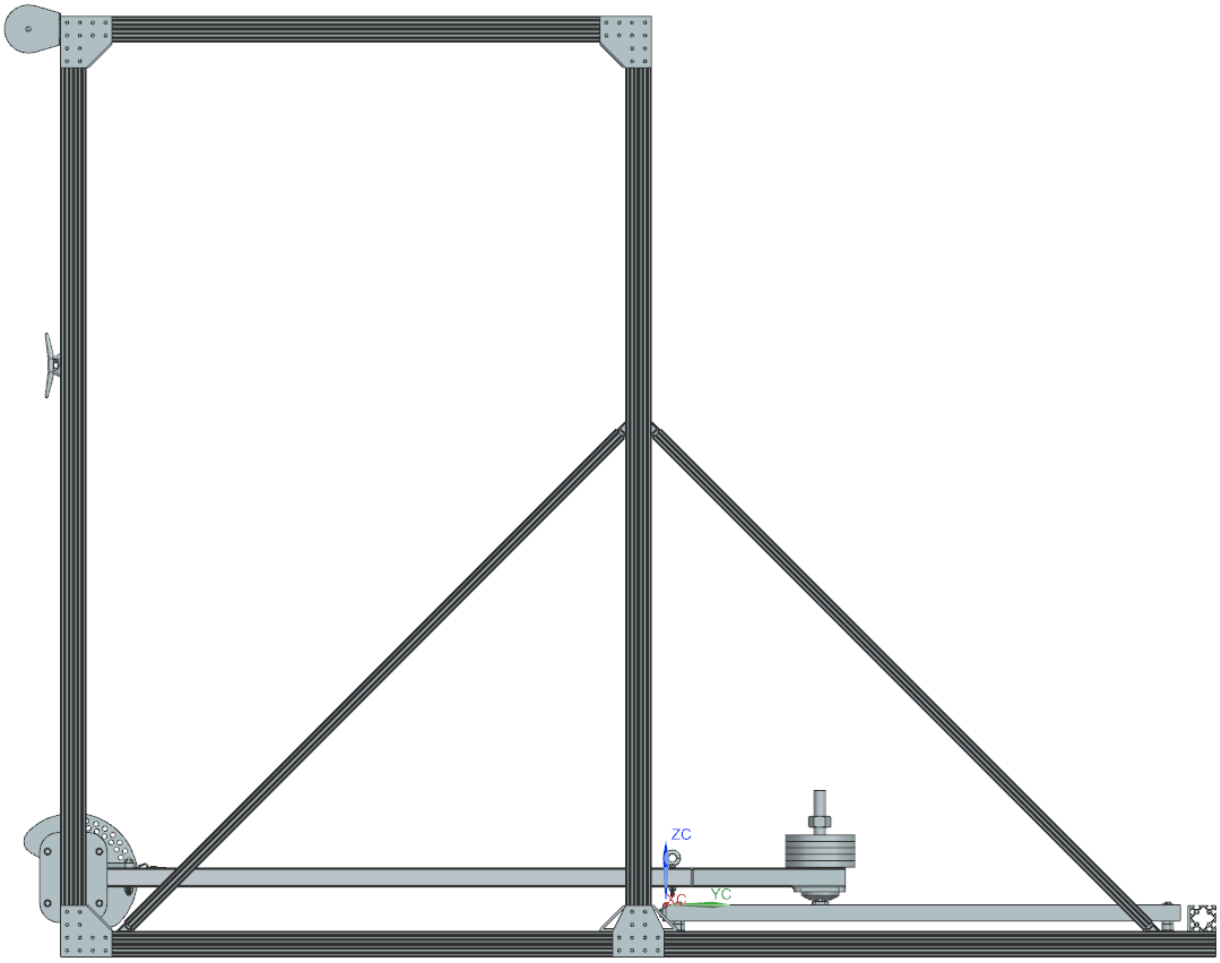

F

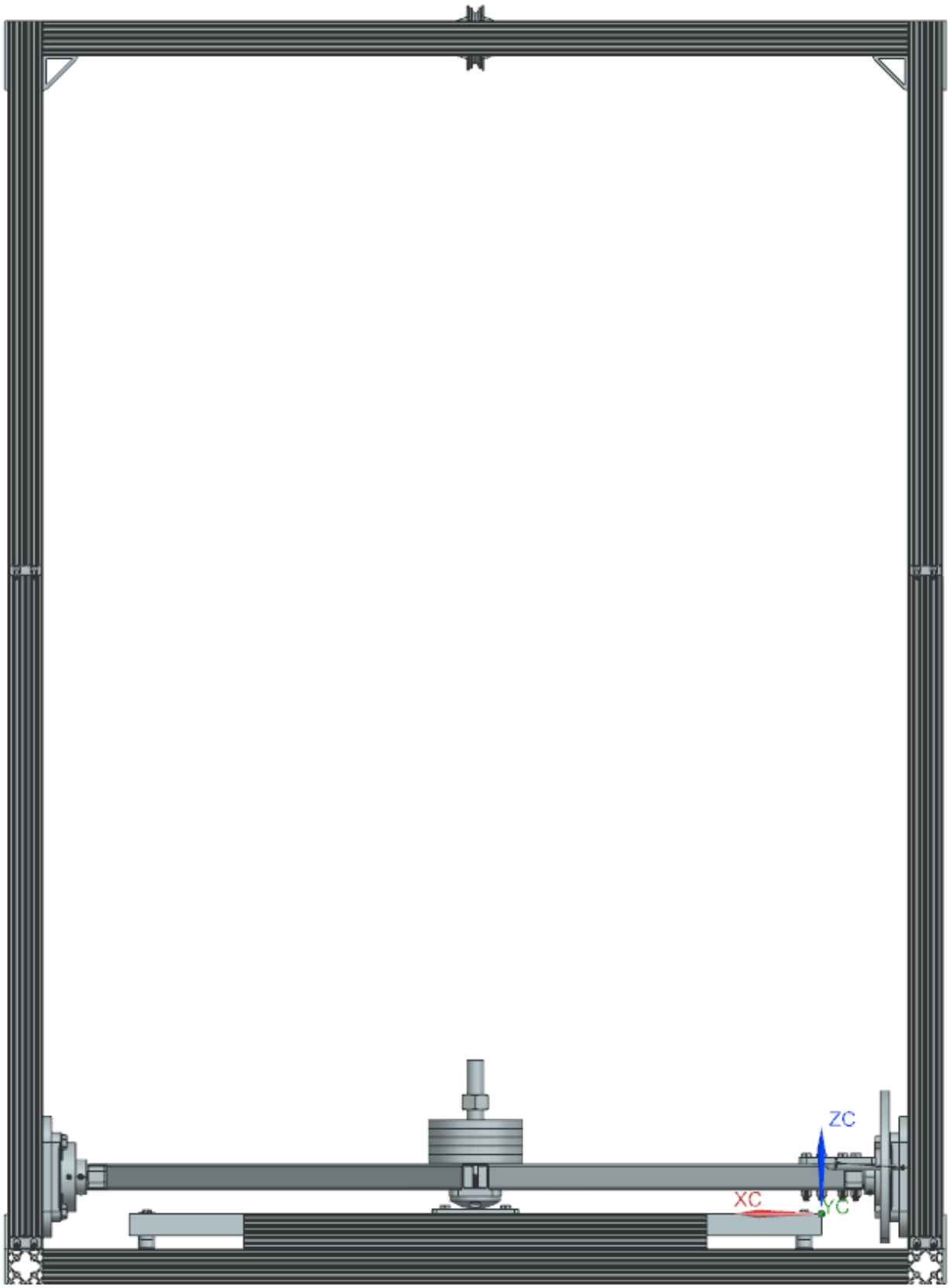

G

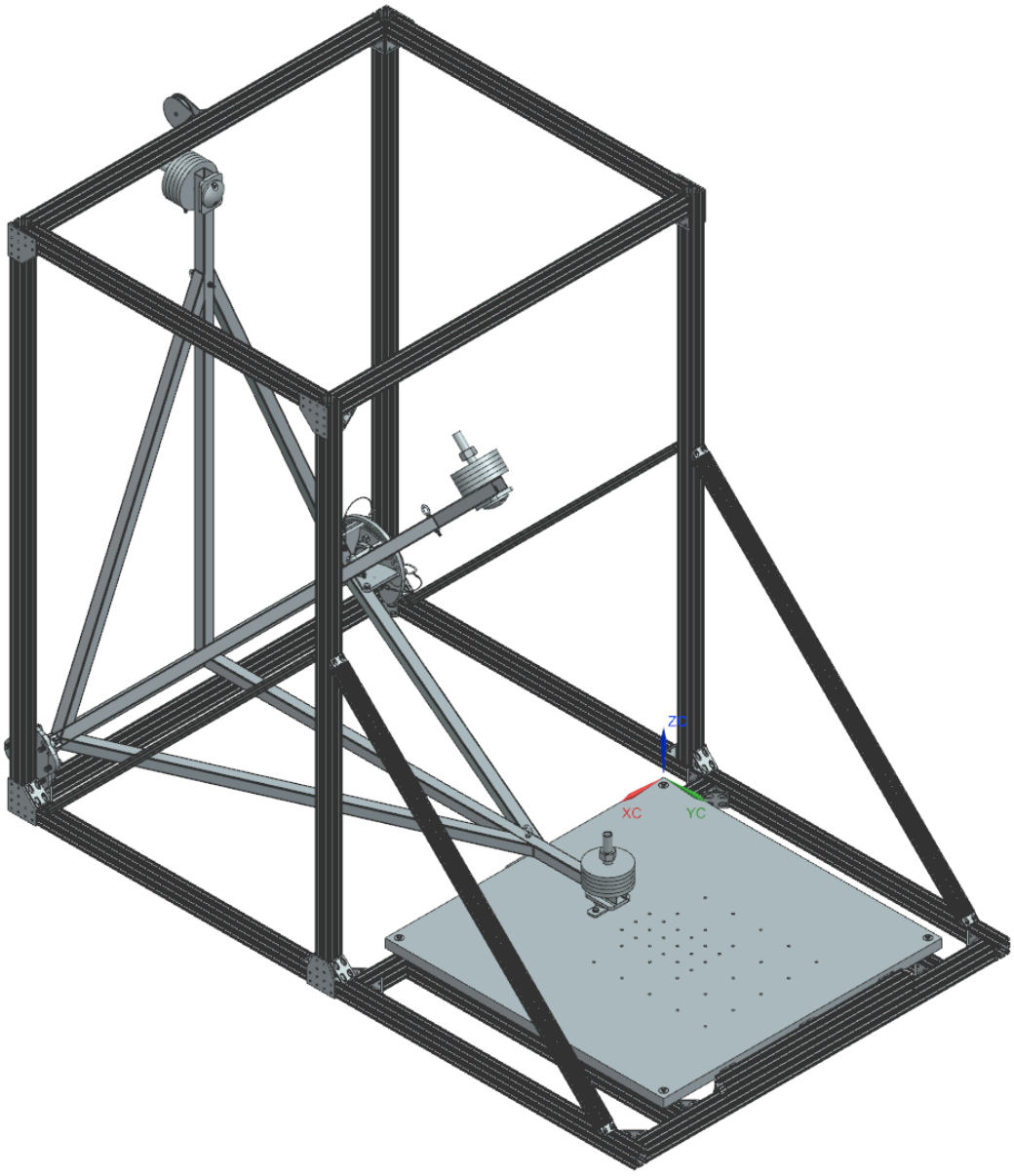
Appendix C: Supplementary CAD Views

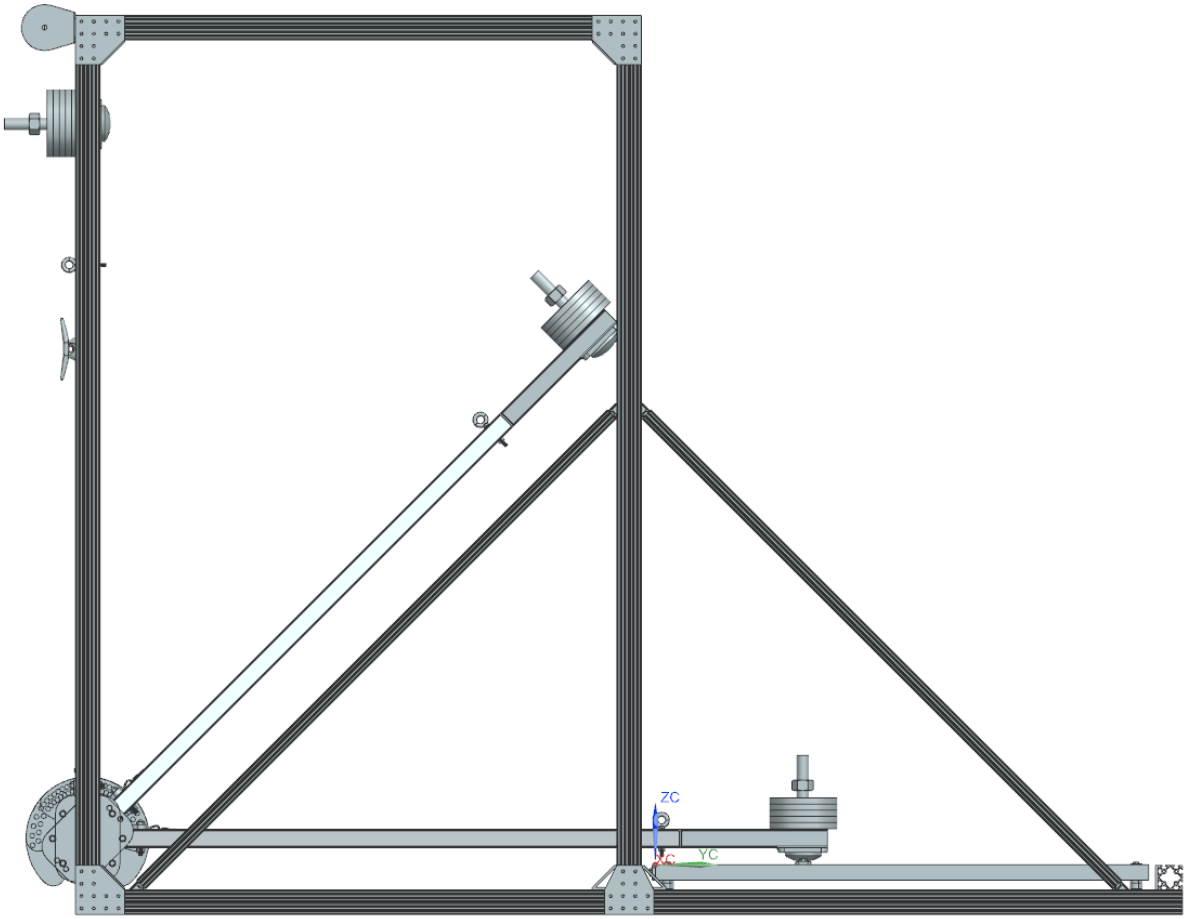


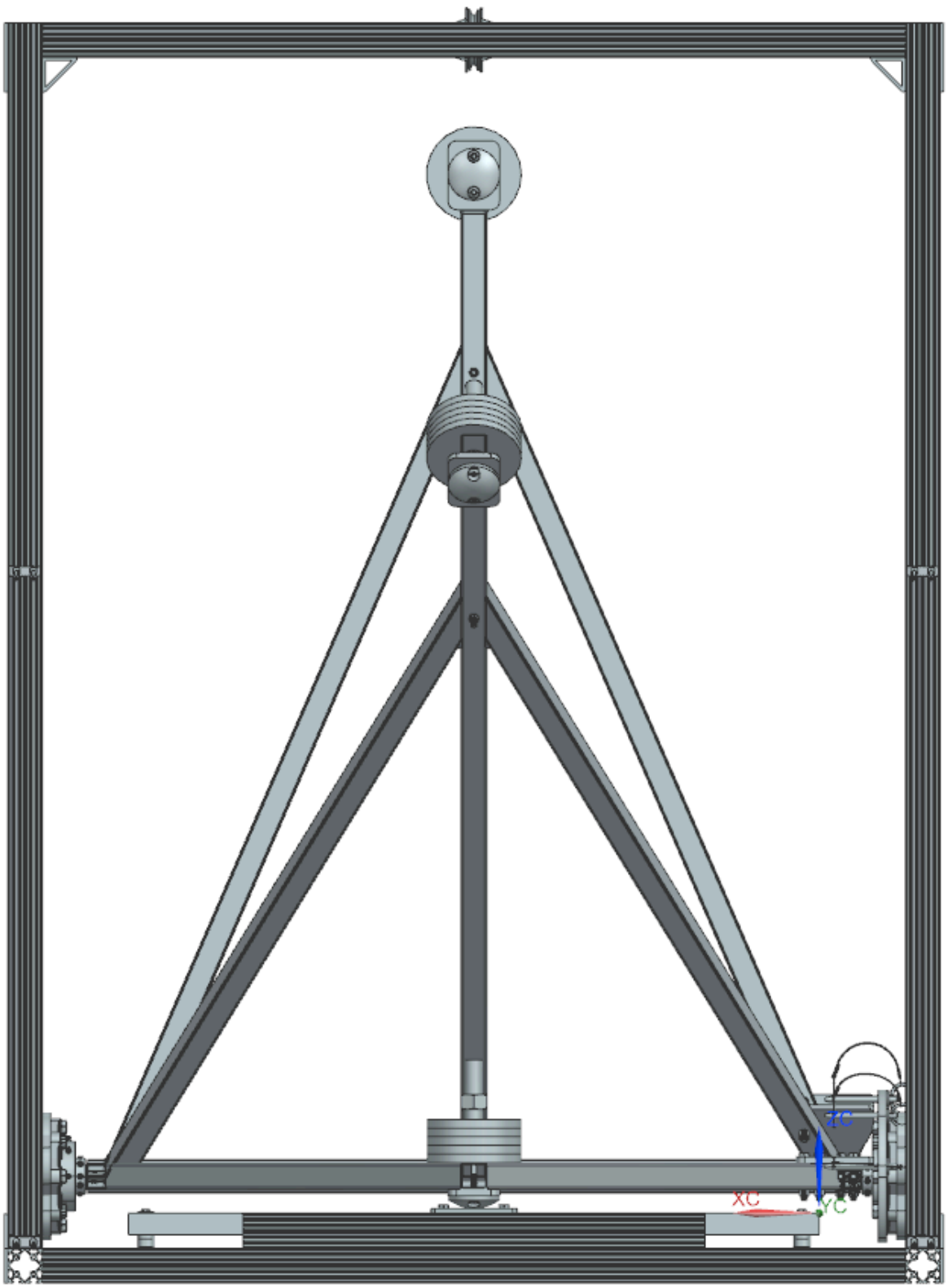

ZC
XC
YC

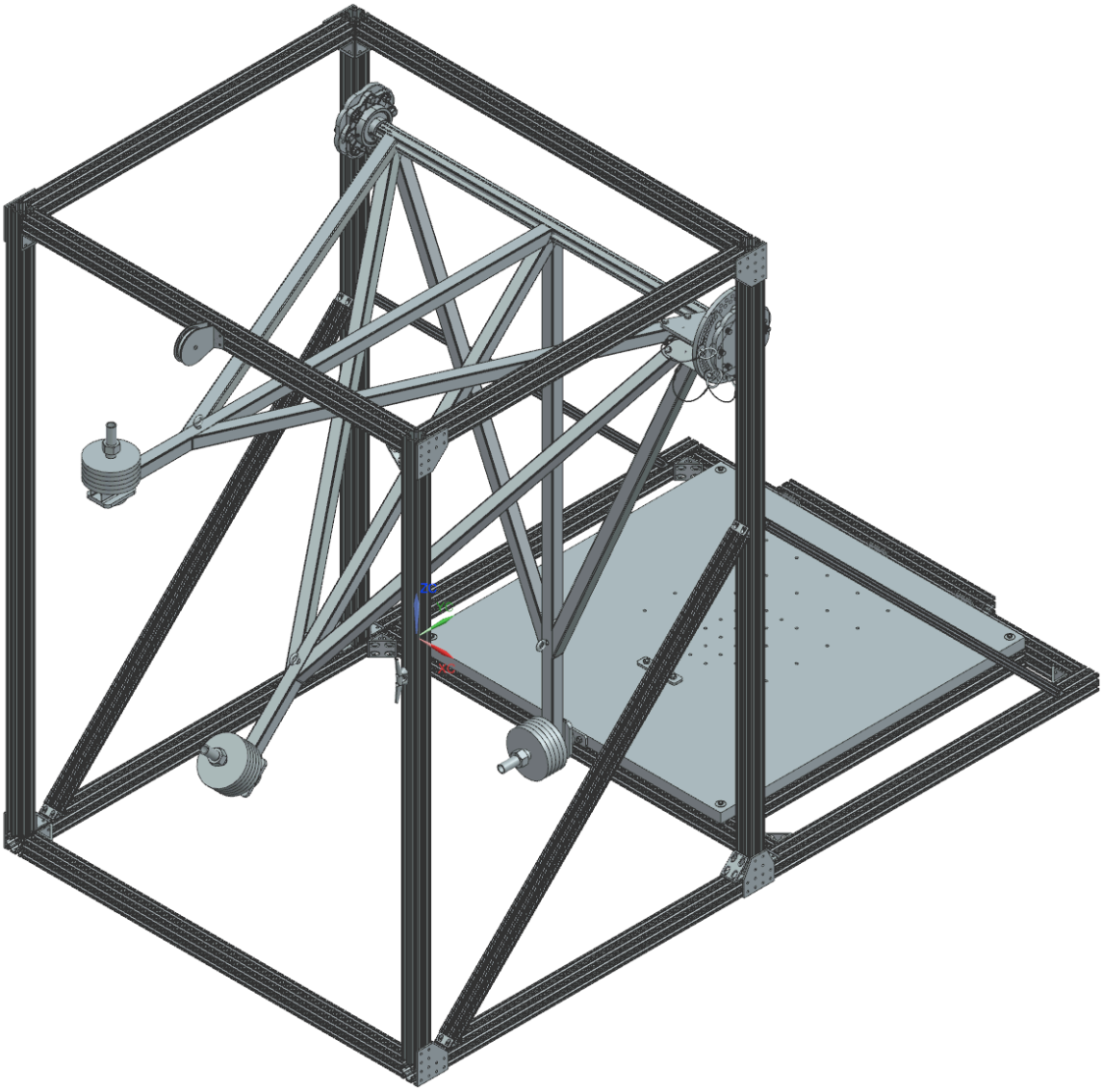

ZC
YC

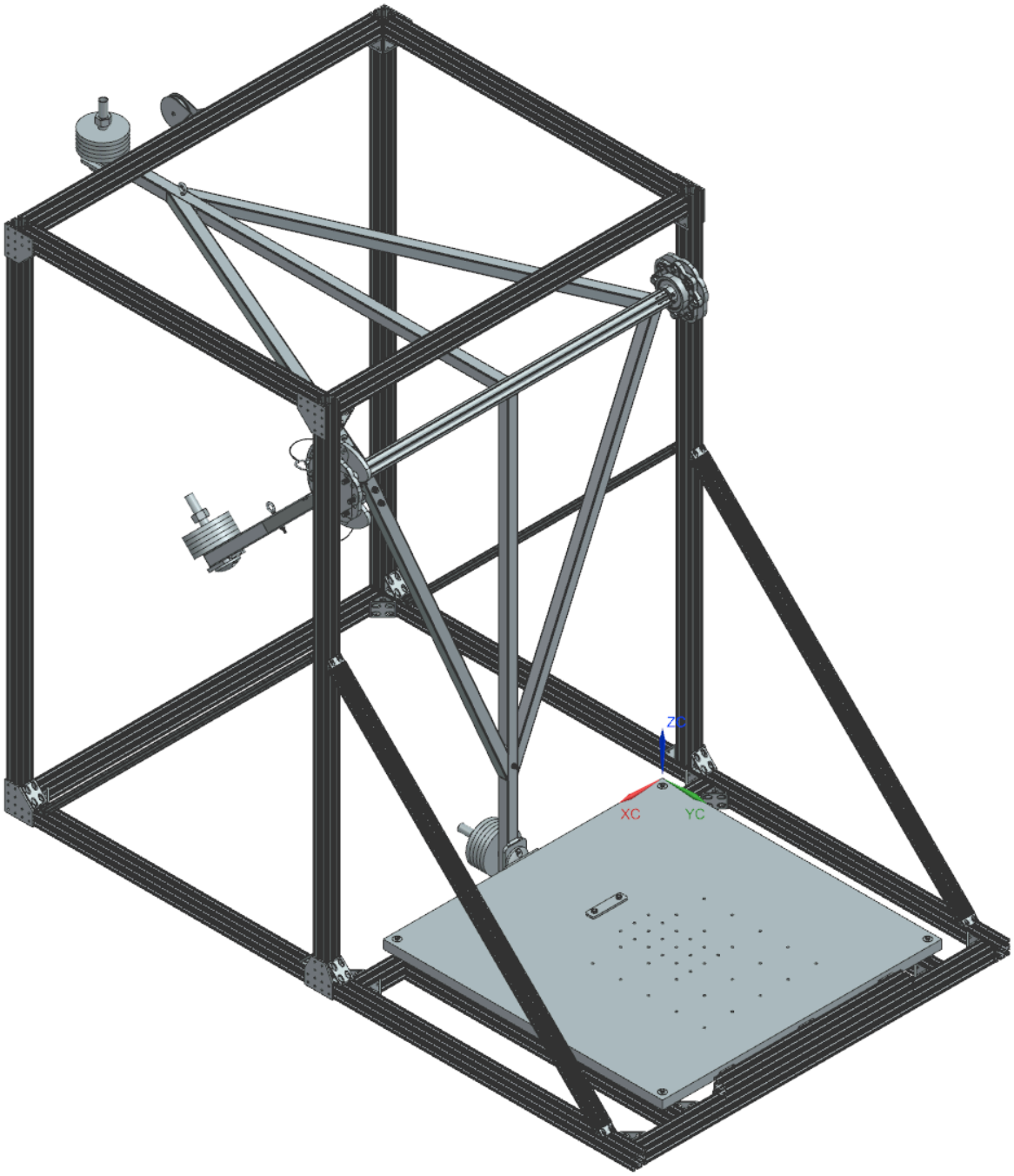

ZC
XC
YC

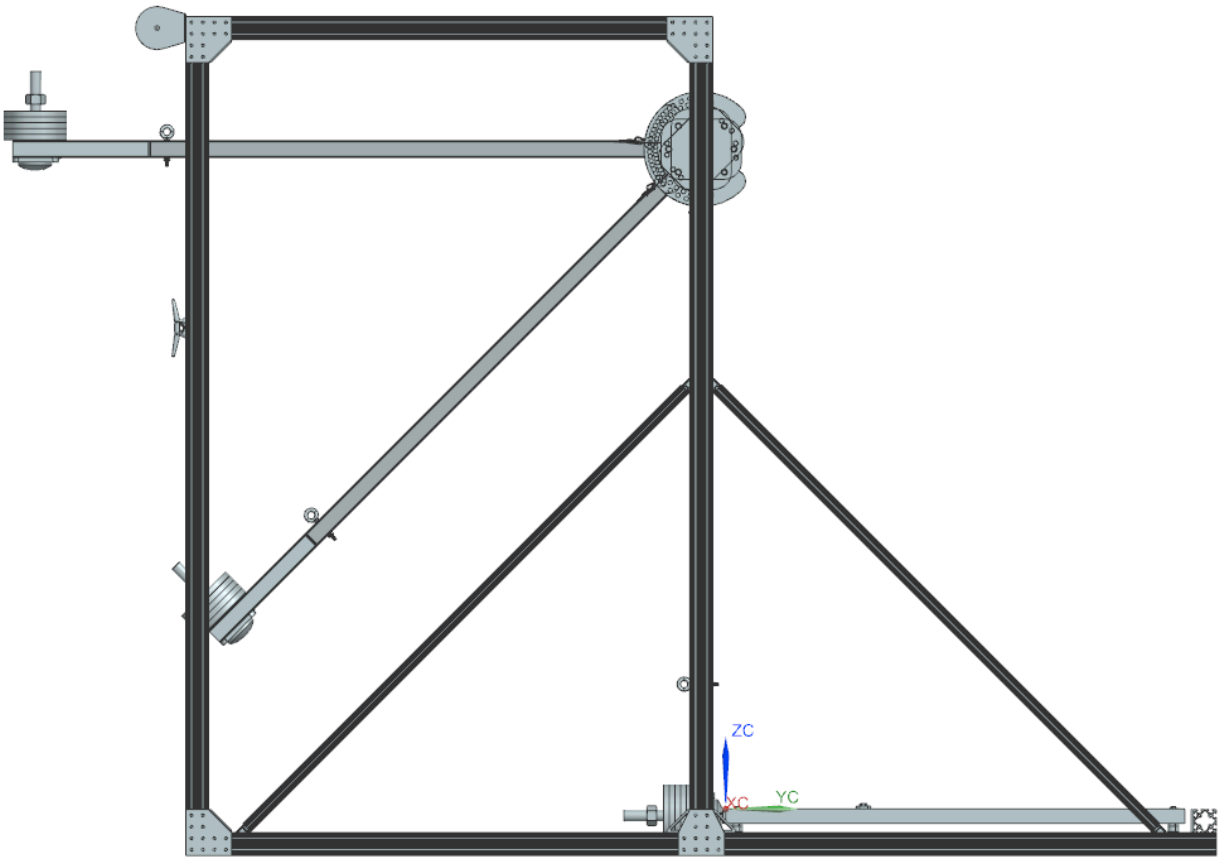

ZC
XC
YC

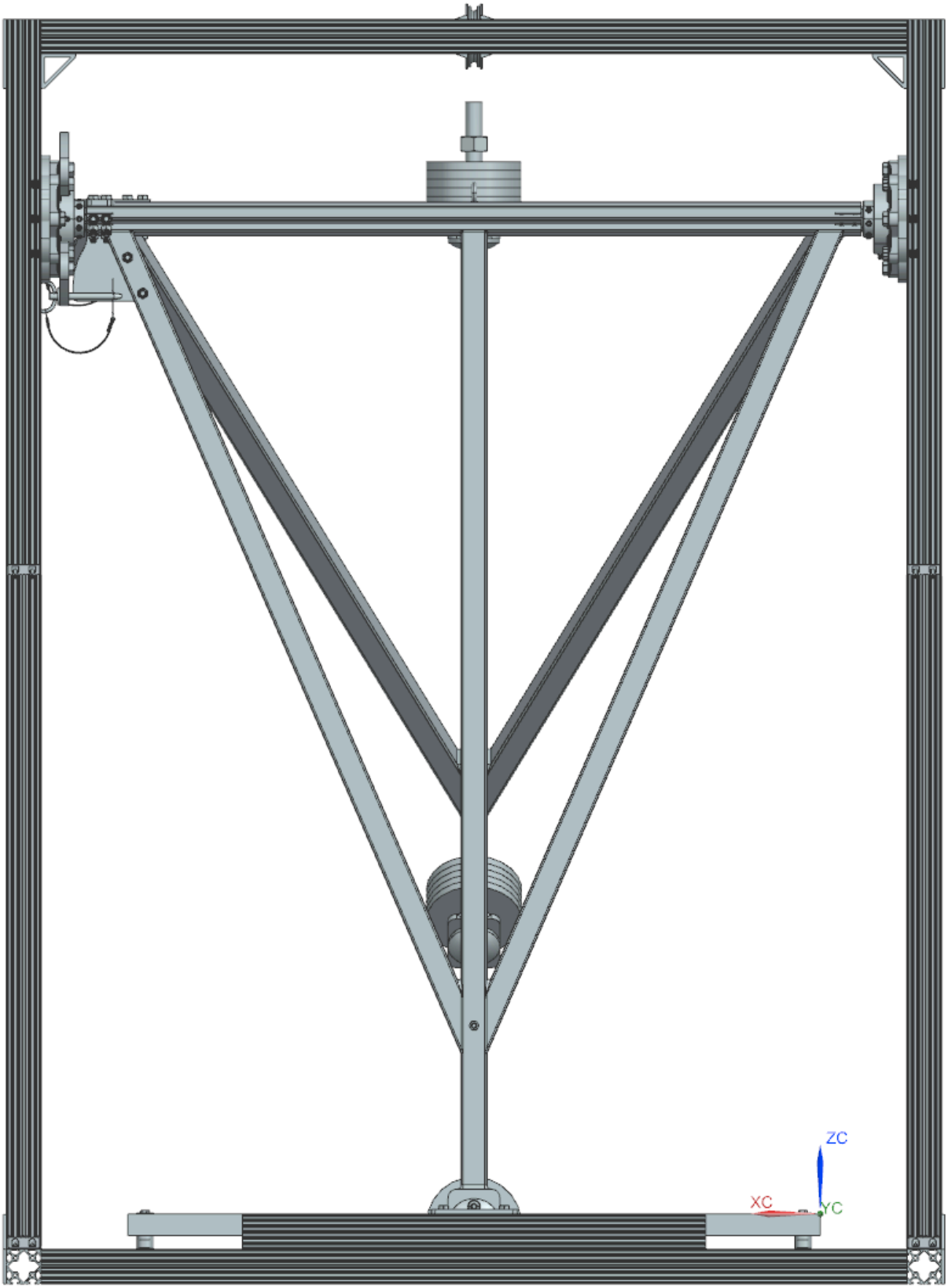

ZC
YC

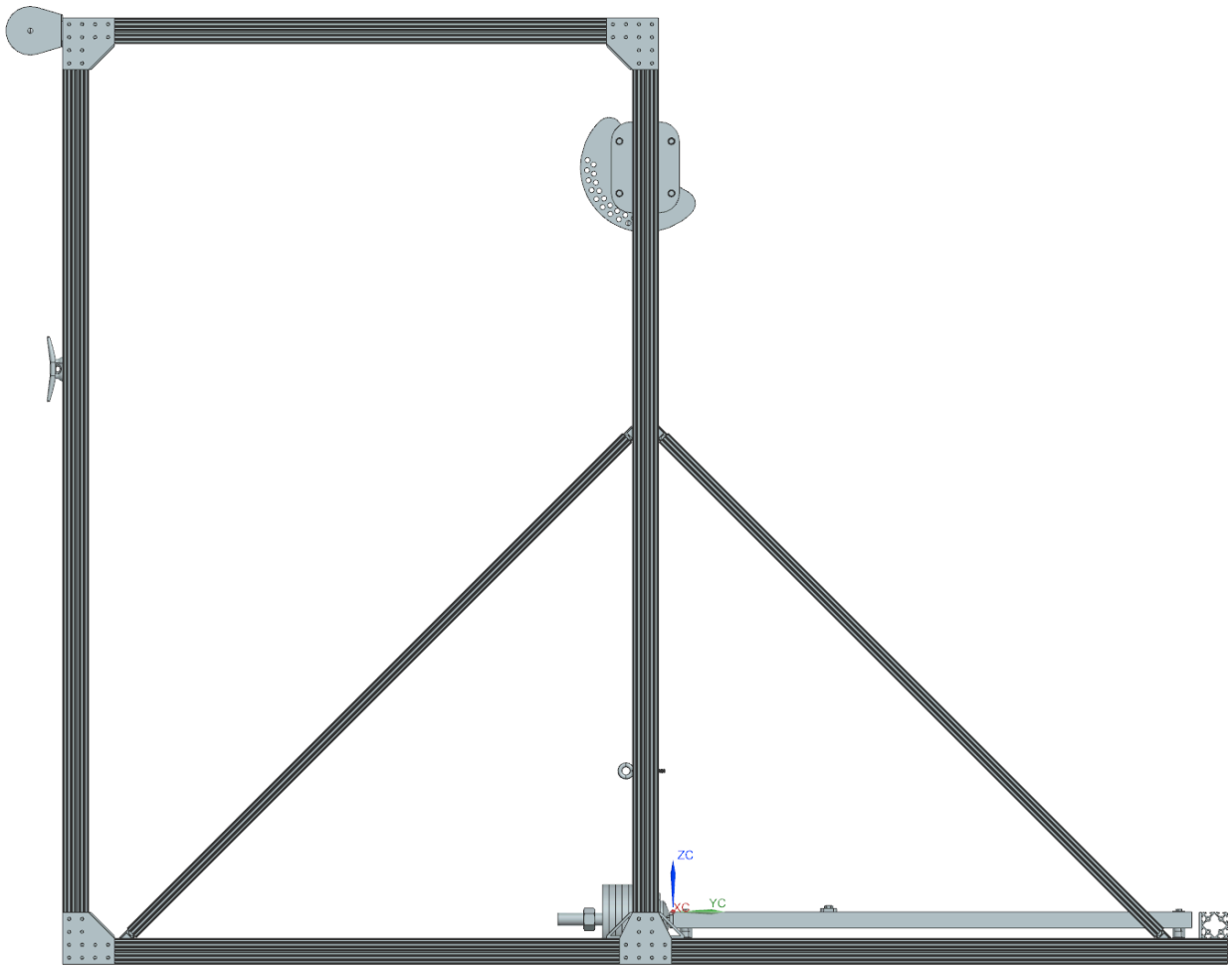

ZC
XC
YC

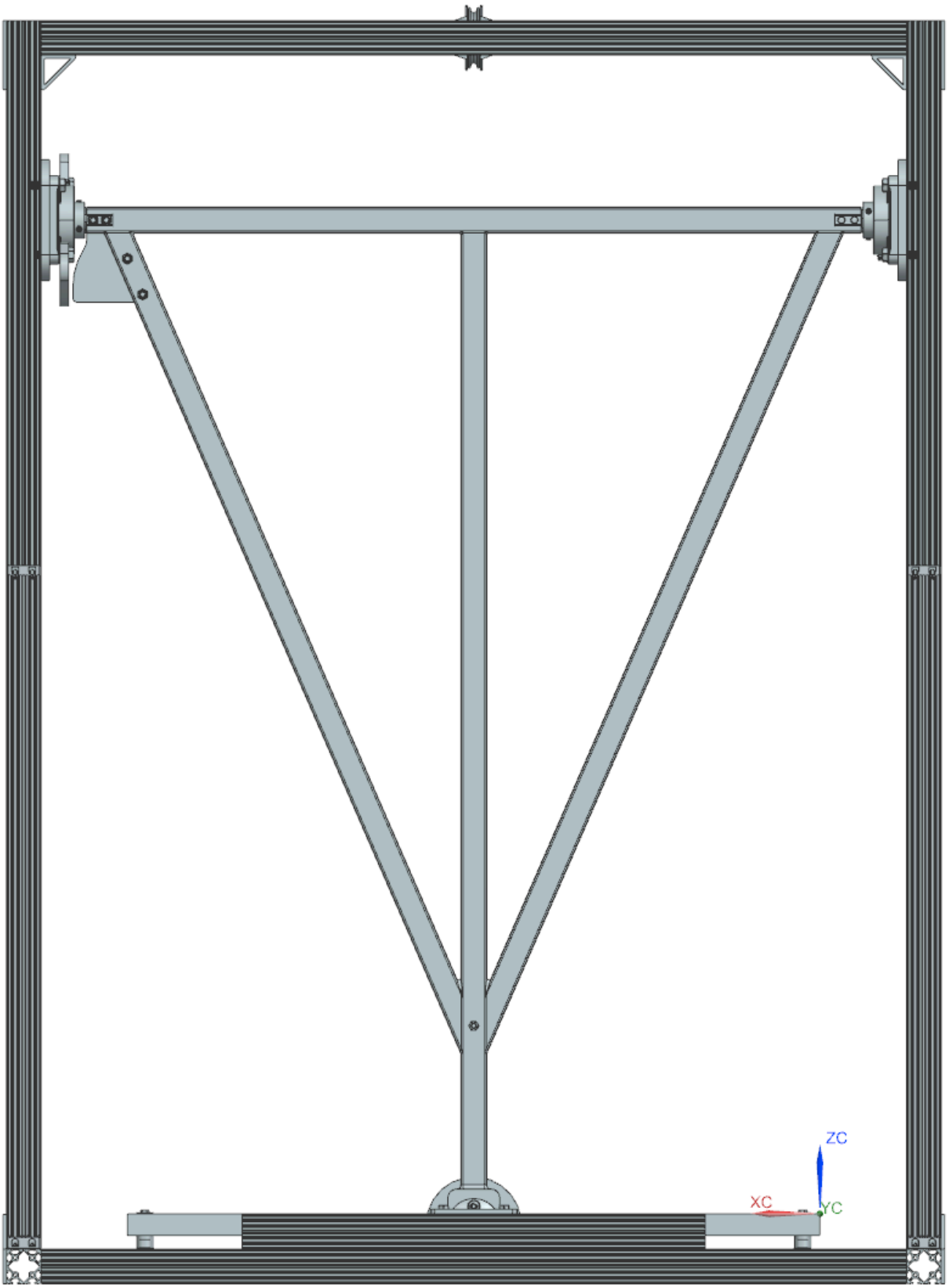


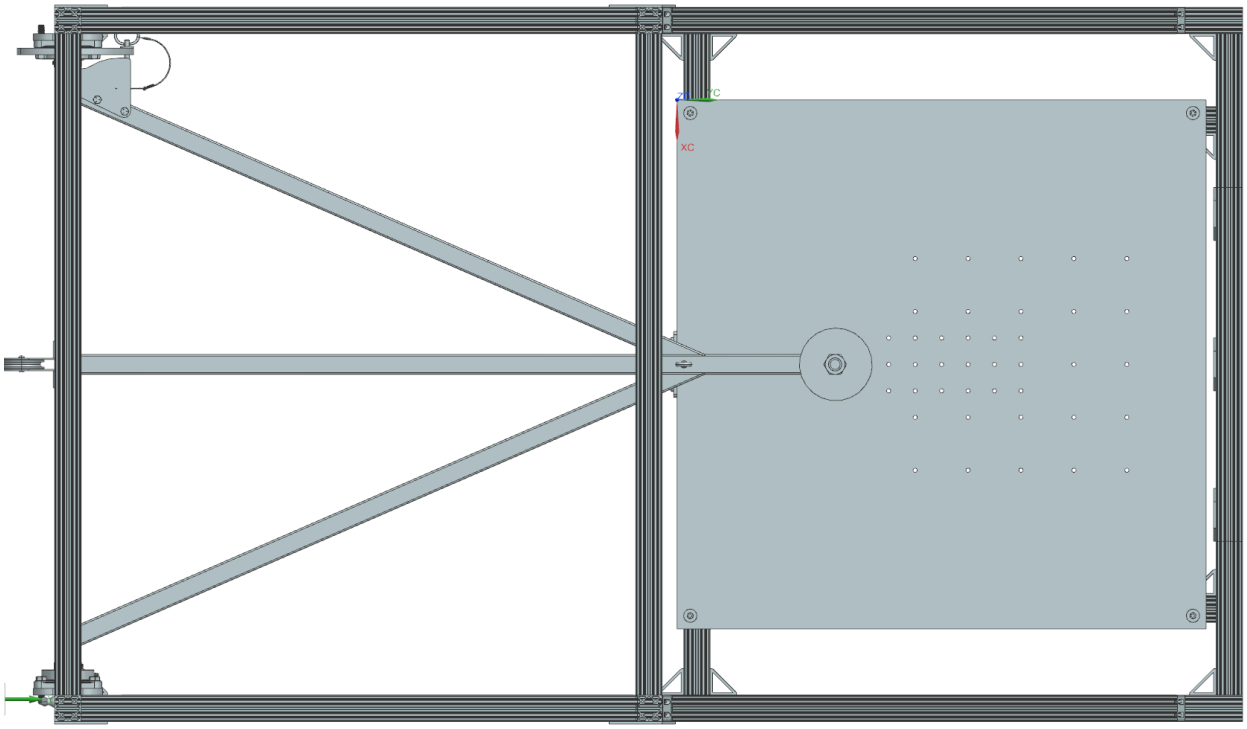

ZC
XC
YC


ZC
YC
XC

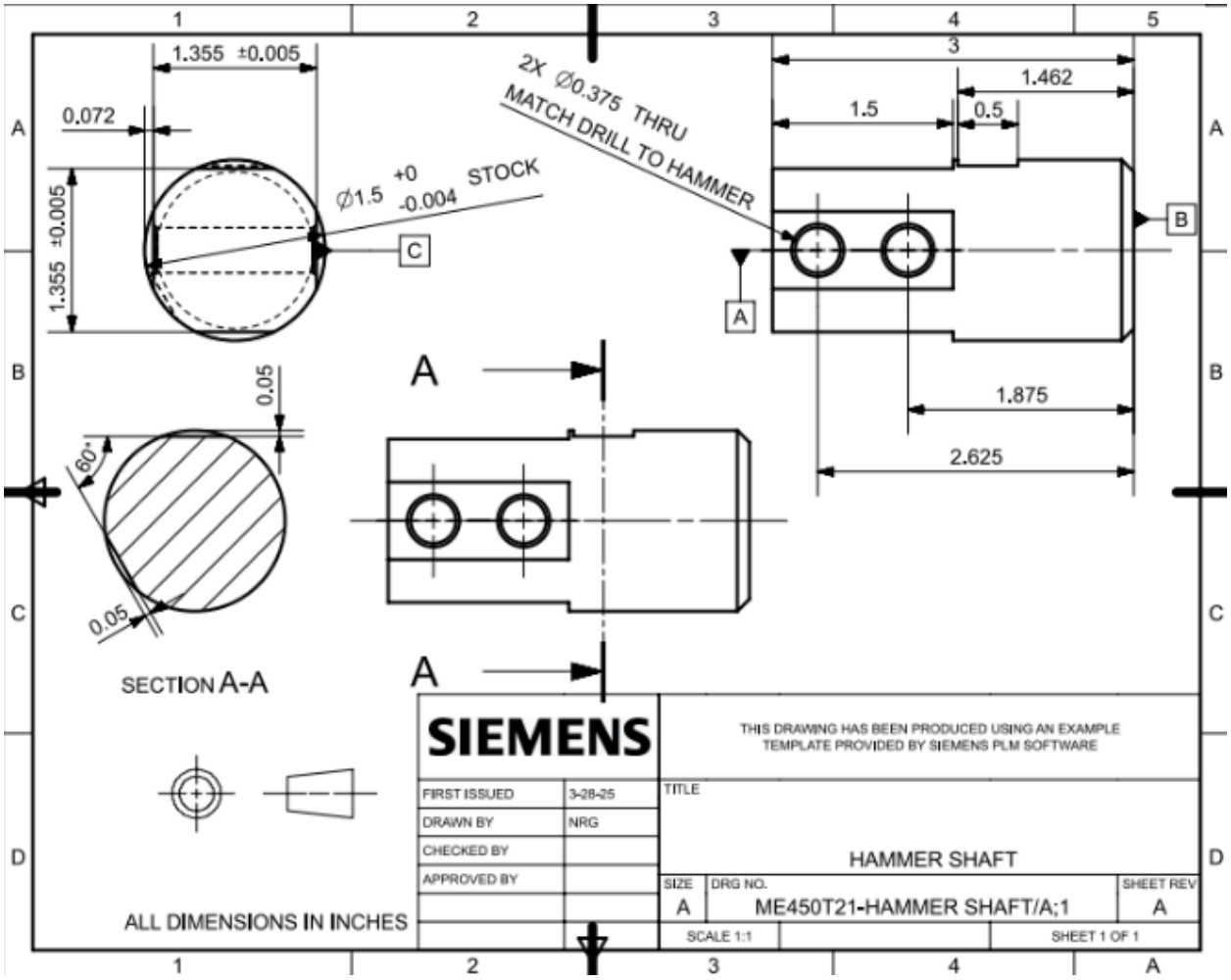

ZC
XC
YC

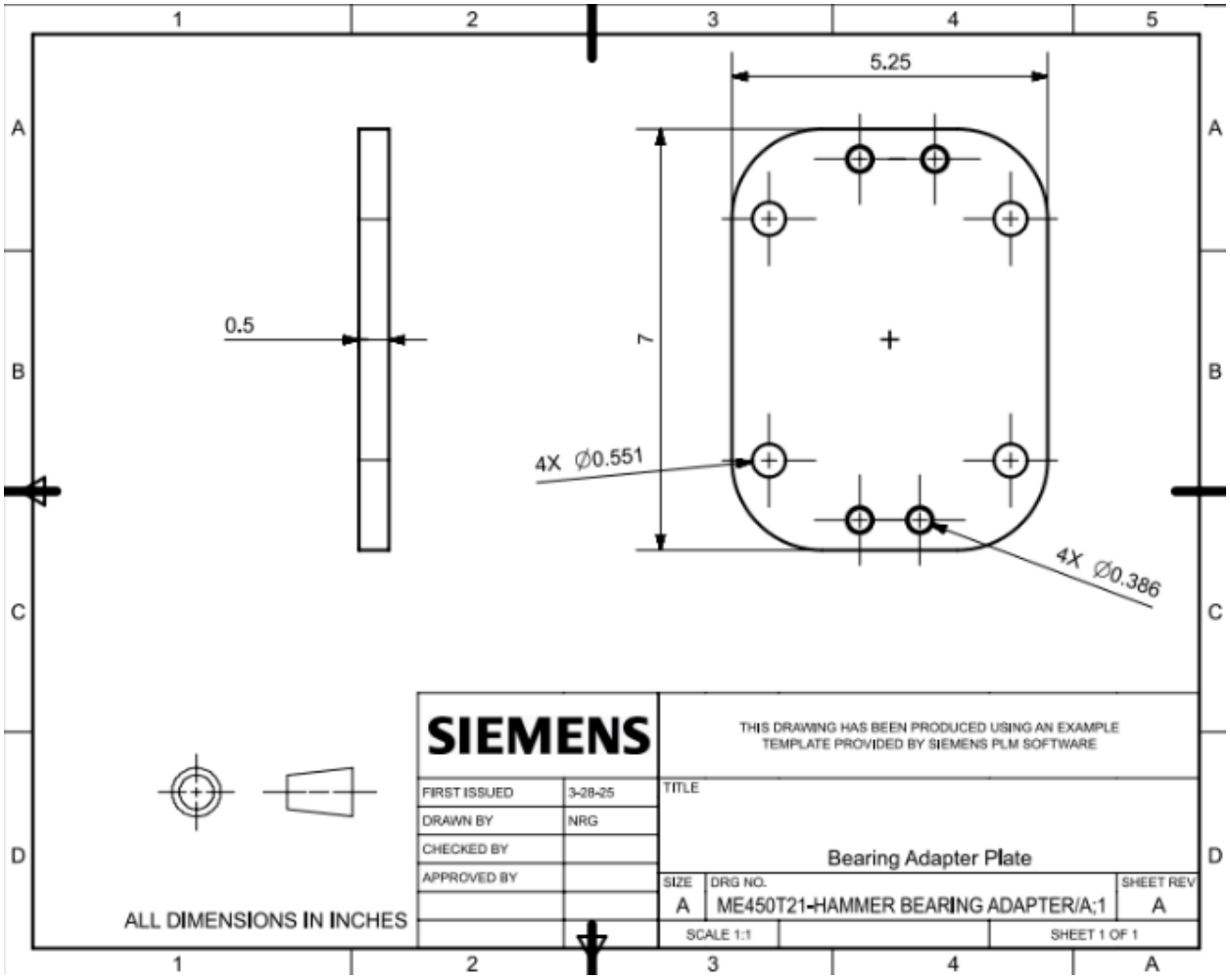

ZC
XC
YC

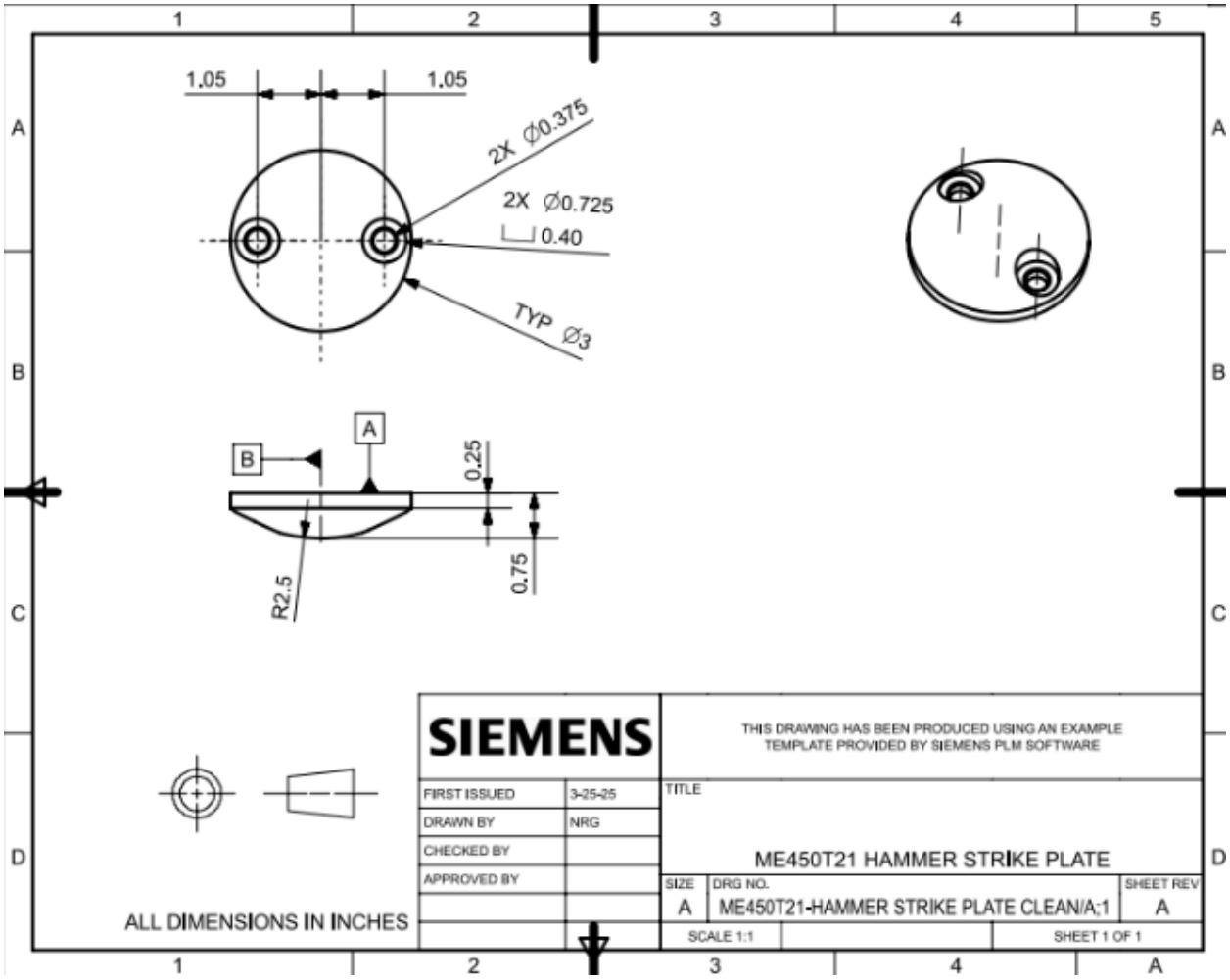

ZC
XC
YC

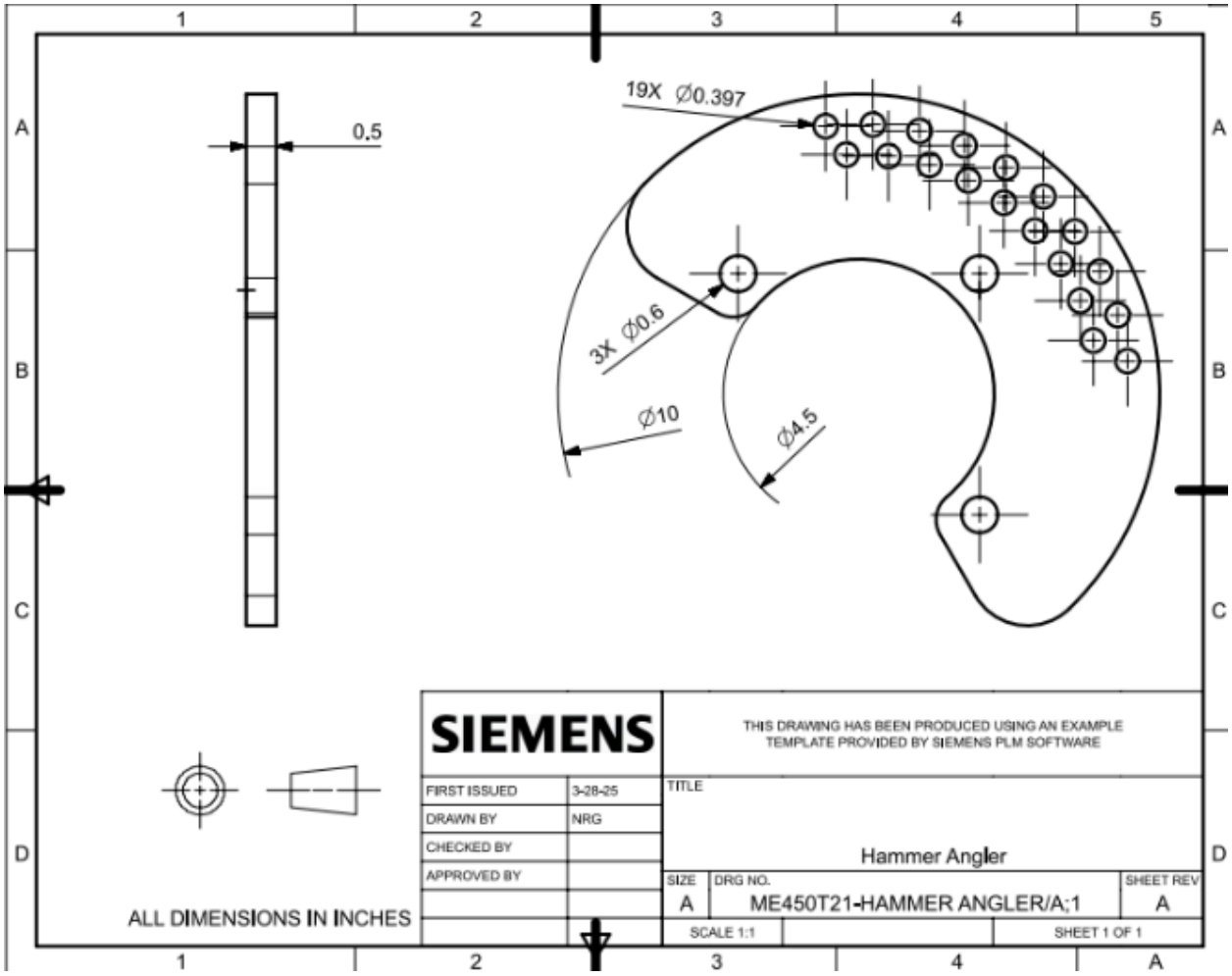

ZC
XC

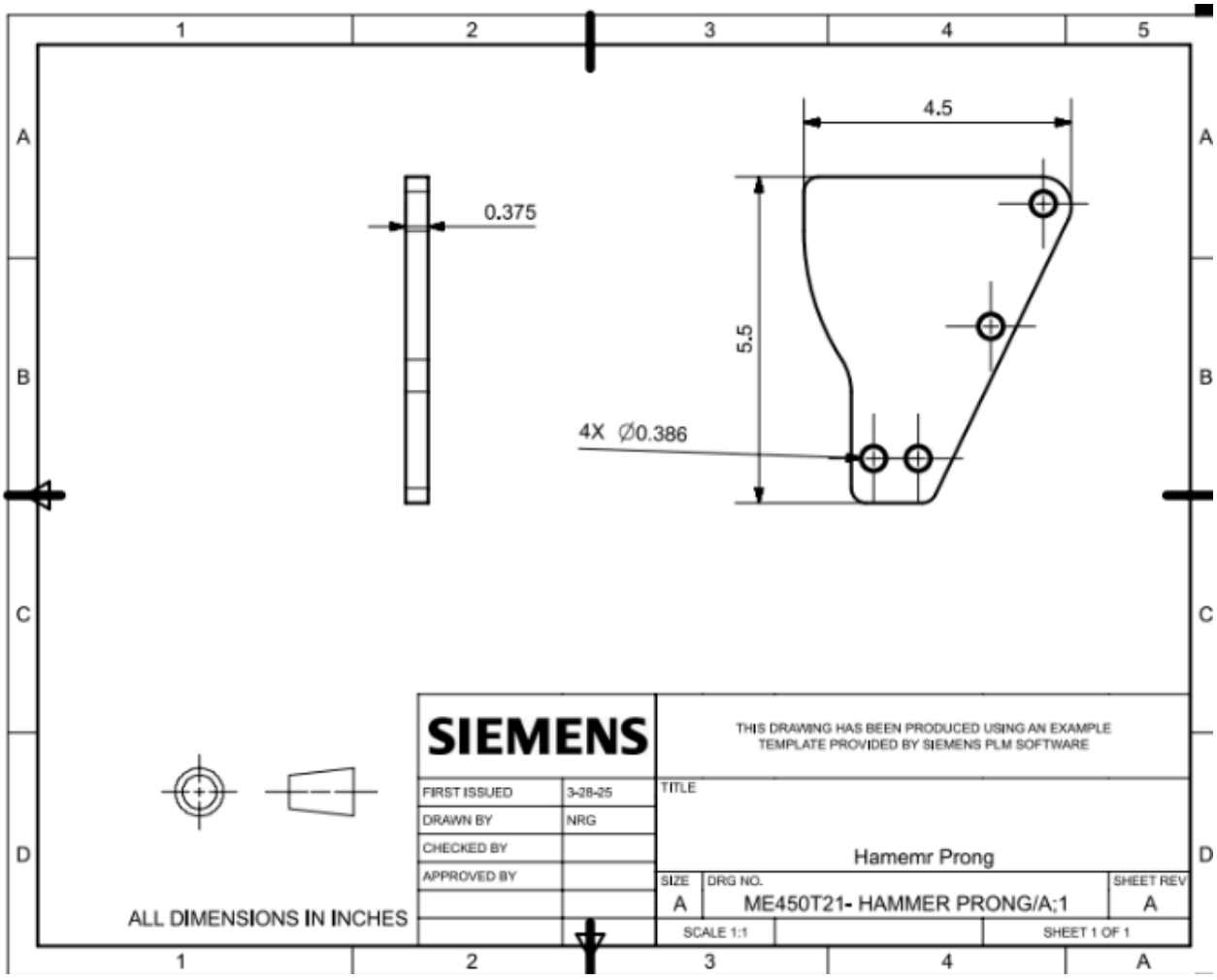
Appendix D: Engineering Drawings

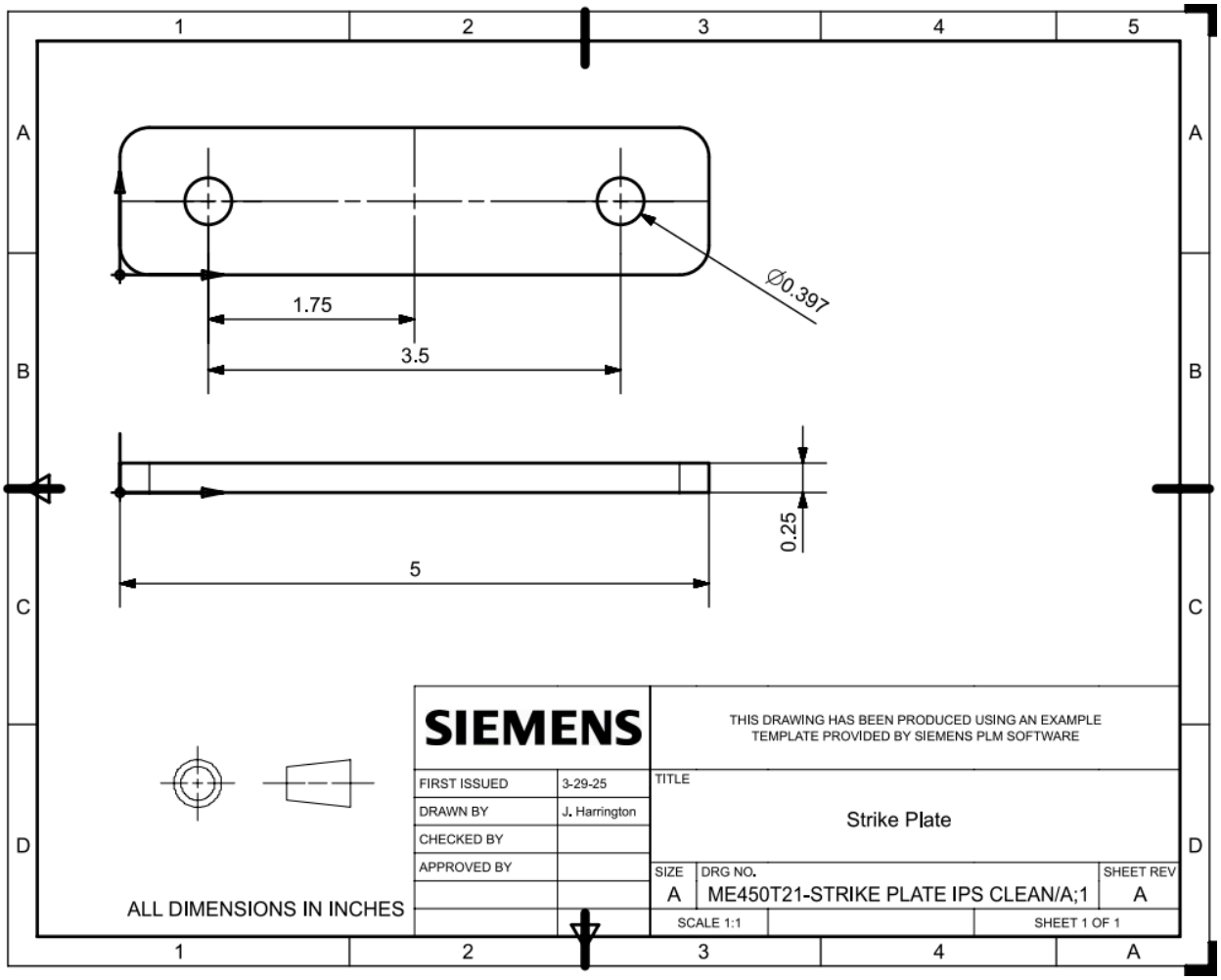


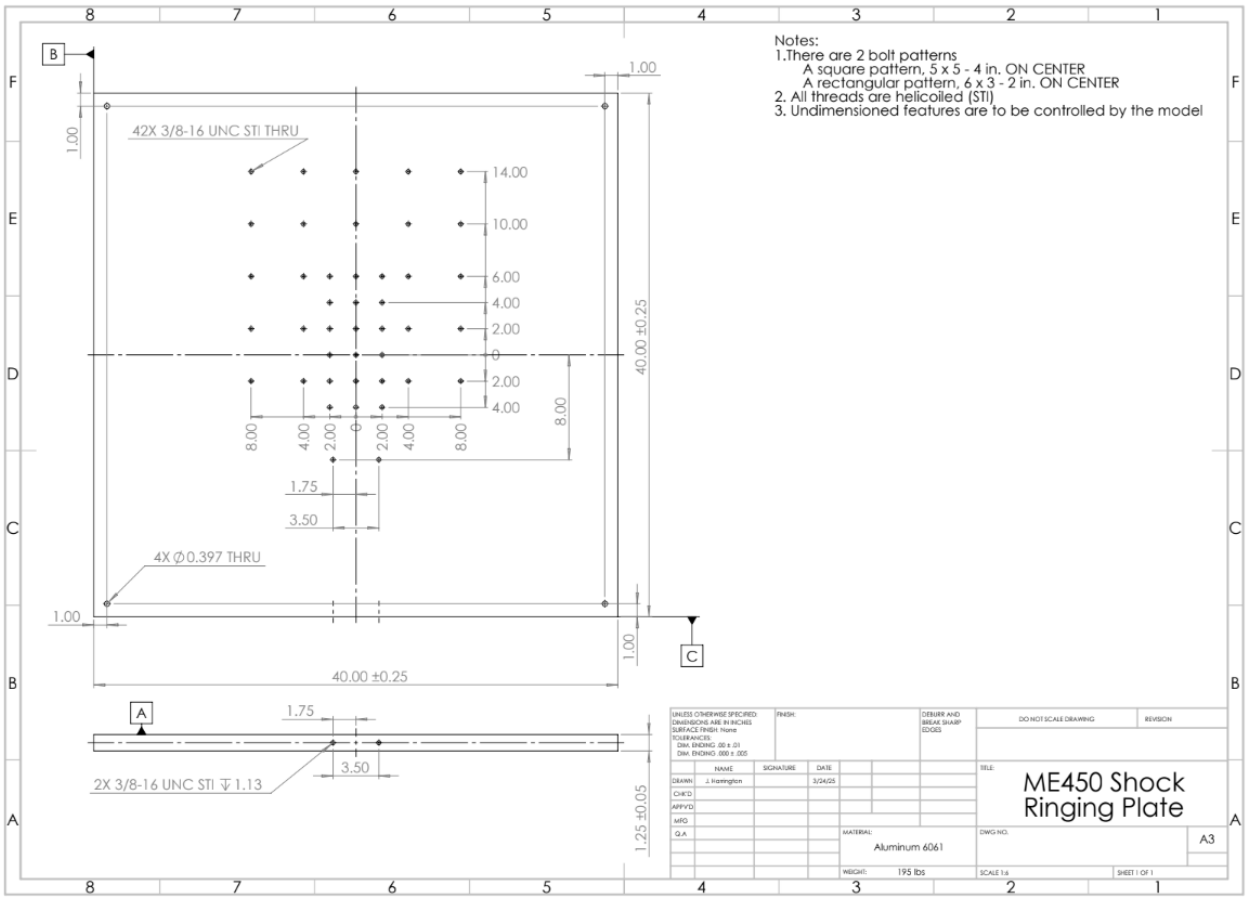

5.25
0.5
7
4X Ø0.551
4X Ø0.386
SIEMENS
THIS DRAWING HAS BEEN PRODUCED USING AN EXAMPLE TEMPLATE PROVIDED BY SIEMENS PLM SOFTWARE
FIRST ISSUED 3-28-25
DRAWN BY NRG
CHECKED BY
APPROVED BY
TITLE
Bearing Adapter Plate
SIZE A
DRG NO. ME450T21-HAMMER BEARING ADAPTER/A;1
SHEET REV A
SCALE 1:1
SHEET 1 OF 1
ALL DIMENSIONS IN INCHES


1.05
1.05
2X Ø0.375
2X Ø0.725
0.40
TYP Ø3
A
B
0.25
0.75
R2.5
SIEMENS
THIS DRAWING HAS BEEN PRODUCED USING AN EXAMPLE TEMPLATE PROVIDED BY SIEMENS PLM SOFTWARE
FIRST ISSUED 3-25-25
DRAWN BY NRG
CHECKED BY
APPROVED BY
TITLE
ME450T21 HAMMER STRIKE PLATE
SIZE A
DRG NO. ME450T21-HAMMER STRIKE PLATE CLEAN/A;1
SHEET REV A
SCALE 1:1
SHEET 1 OF 1
ALL DIMENSIONS IN INCHES


19X Ø0.397
0.5
3X Ø0.6
Ø10
Ø4.5
SIEMENS
THIS DRAWING HAS BEEN PRODUCED USING AN EXAMPLE TEMPLATE PROVIDED BY SIEMENS PLM SOFTWARE
FIRST ISSUED 3-28-25
DRAWN BY NRG
CHECKED BY
APPROVED BY
TITLE
Hammer Angler
SIZE A
DRG NO. ME450T21-HAMMER ANGLER/A;1
SHEET REV A
SCALE 1:1
SHEET 1 OF 1
ALL DIMENSIONS IN INCHES


4.5
0.375
5.5
4X Ø0.386
SIEMENS
THIS DRAWING HAS BEEN PRODUCED USING AN EXAMPLE TEMPLATE PROVIDED BY SIEMENS PLM SOFTWARE
FIRST ISSUED 3-28-25
DRAWN BY NRG
CHECKED BY
APPROVED BY
TITLE
Hamemr Prong
SIZE A
DRG NO. ME450T21- HAMMER PRONG/A;1
SHEET REV A
SCALE 1:1
SHEET 1 OF 1
ALL DIMENSIONS IN INCHES


1
2
3
4
5
A
B
C
D
Ø0.397
1.75
3.5
0.25
5
SIEMENS
THIS DRAWING HAS BEEN PRODUCED USING AN EXAMPLE TEMPLATE PROVIDED BY SIEMENS PLM SOFTWARE
FIRST ISSUED 3-29-25
DRAWN BY J. Harrington
CHECKED BY
APPROVED BY
TITLE
Strike Plate
SIZE A
DRG NO. ME450T21-STRIKE PLATE IPS CLEAN/A;1
SHEET REV A
SCALE 1:1
SHEET 1 OF 1
ALL DIMENSIONS IN INCHES


Notes:
1.There are 2 bolt patterns
A square pattern, 5 x 5 - 4 in. ON CENTER
A rectangular pattern, 6 x 3 - 2 in. ON CENTER
2. All threads are helicoiled (STI)
3. Undimensioned features are to be controlled by the model
42X 3/8-16 UNC STI THRU
4X Ø0.397 THRU
2X 3/8-16 UNC STI ↧1.13
40.00 ±0.25
1.25 ±0.05
ME450 Shock Ringing Plate
Aluminum 6061
195 lbs
A3

Appendix E: Impact Dynamics Model

```
% Predicting impact dynamics of a pendulum hammer striking a surface
% jsharr 3/11/2025
clc
clear
close all

%% Define input parameters
ms = 5; % [kg] mass of the impactor/hammer
Es = 68; % [GPa] Young's modulus of impactor/hammer material
vs = .32; % [ ] Poisson's ratio of impactor/hammer material
rs = 25; % [mm] radius of the impactor/hammer tip
Ep = 200; % [GPa] Young's modulus of strike plate
vp = .3; % [ ] Poisson's ratio of strike plate
% strike plate is assumed to have infinte radius (flat)
% mass of strike plate is assumed to be >> mass of hammer

L = 1.5; % [m] Hammer/pendulum arm length
theta = 88; % [deg] drop release angle (value should be between 0 and 90)

%% Use conservation of energy to obtain impact velocity
g = 9.81; % [m/s^2] constant acceleration due to gravity
h_OOP = L.*sind(theta); % [m] out of plane (OOP) configuration height of
the hammer head from the strike plate calculated from release angle
h_IP = L.*(1-cosd(theta)); % [m] in plane (IP) height of the hammer head
from the strike plate calculated from release angle
vi = (2.*g.*h_OOP).^0.5; % [m/s] impact velocity calculated from
conservation of energy assuming all gravitational potential engergy is
converted to kinetic energy

%% Calculate displacement, velocity, acceleration, and force response by
numerically solving equations of motion
req = rs/1000; % [m] assume rp >> rs
keq = ((3/4)*(((1-vs^2)/(Es*1e9))+((1-vp^2)/(Ep*1e9)))*(1/(req^0.5)))^-1;
% [N/m^3/2] equivalent stiffness from morias-vasques
alpha = 3/2; % [ ] non-linearity constant from morais-vasques

odefun = @(t, X) [X(2); -(keq/ms)*X(1)^alpha]; %rewrite second order ODE
into system of first order ODEs; equation of motion from morais-vasques
X0 = [0;vi]; %define intial conditions, assume initial position is always
zero (contanct point) and impact velocity from above
tspan = [0 5e-4]; %define time to plot over

[t, X] = ode45(odefun, tspan, X0); %solve system of nonlinear differential
equations
xt = X(:,1); %position
```

```
vt = X(:,2); %velocity
at = (-keq.*xt.^alpha)/ms;
ft = -at.*ms;

%% Plot results

figure();
subplot(2,2,1);
plot(t,xt);
xlabel('time [s]')
ylabel('displacement [m]')

subplot(2,2,2);
plot(t,vt);
xlabel('time [s]')
ylabel('velocity [m/s]')

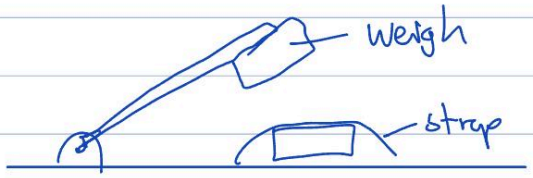
subplot(2,2,3);
plot(t,at);
xlabel('time [s]')
ylabel('acceleration [m/s]')

subplot(2,2,4);
plot(t,ft);
xlabel('time [s]')
ylabel('force [N]')
```

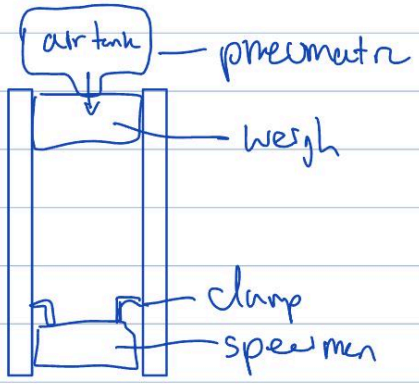
Appendix F: Concept Sketches and Ideas

subsystems			
Energy generation	gravity	pneumatic	Electromagnetic
Impact delivery	Hammer	rail guided	launcher
Specimen securing	mech clamps	straps	Bench supports

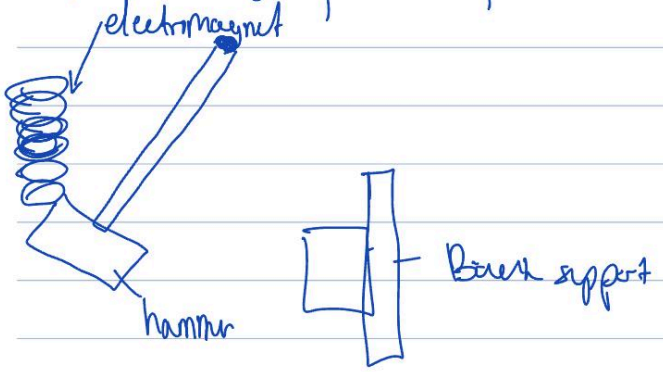
1) Drop, Hammer, strap



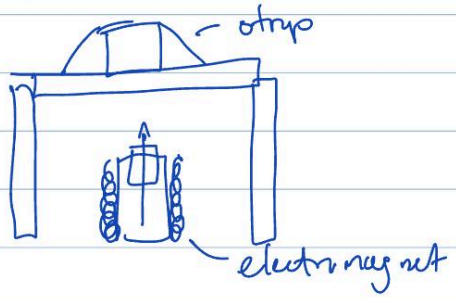
2) pneumatic, rail guided, clamp



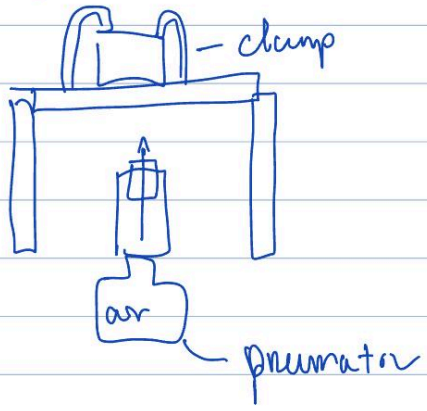
3) Electromagnet, hammer, Back support



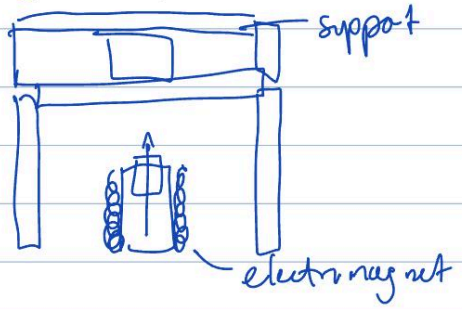
4) Electromagnetic, launcher, strips



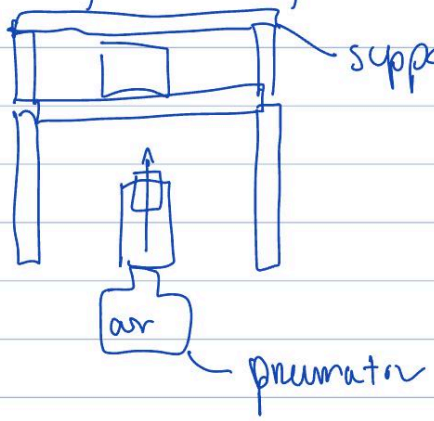
5) pneumatic, launcher, strips



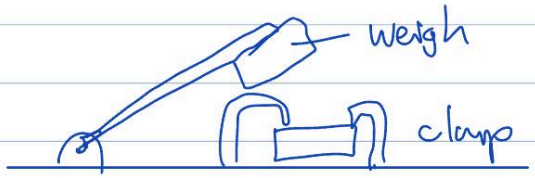
6) Electromagnetic, launcher, Backsupport



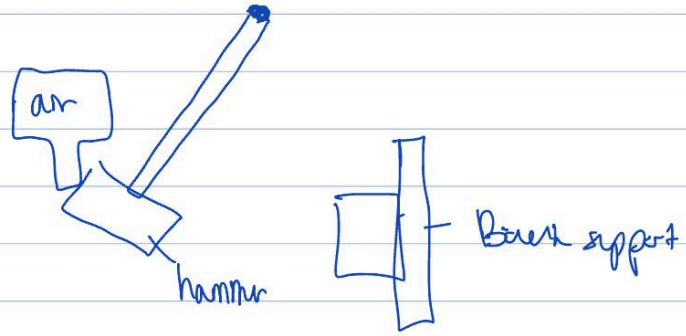
7) pneumatic, launcher, Backsupport



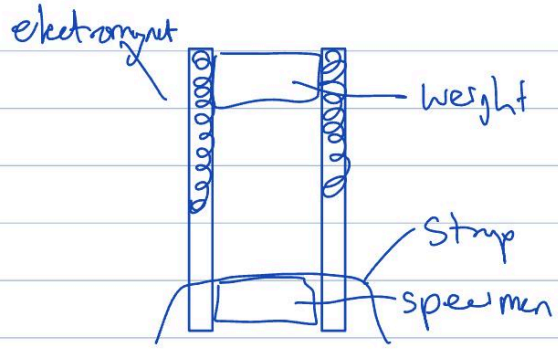
8) Drop, Hammer, strap



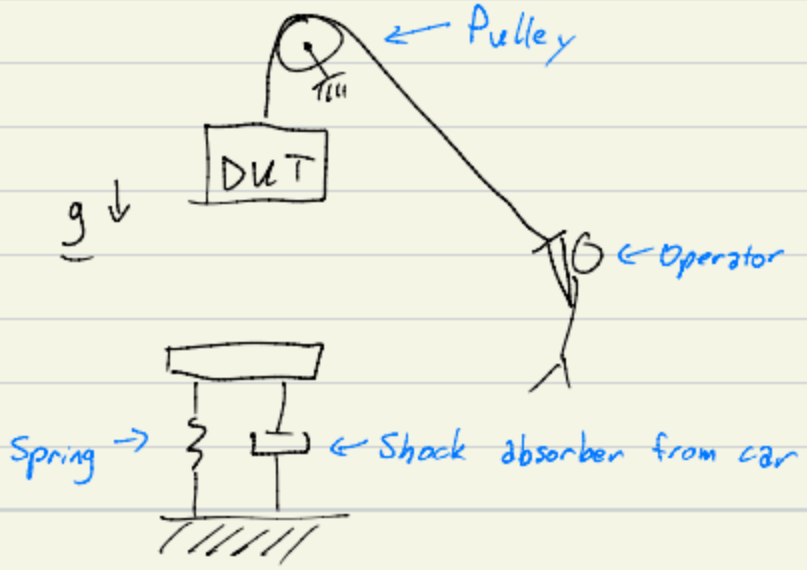
9) pneumatic, hammer, Back support



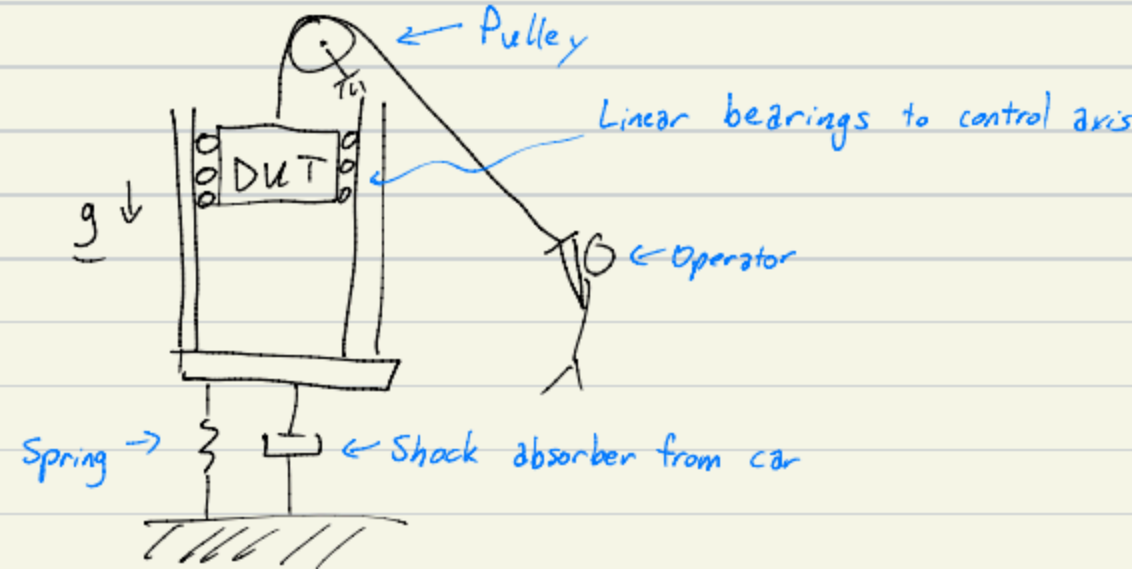
10) electromagnet, rail guided, strip



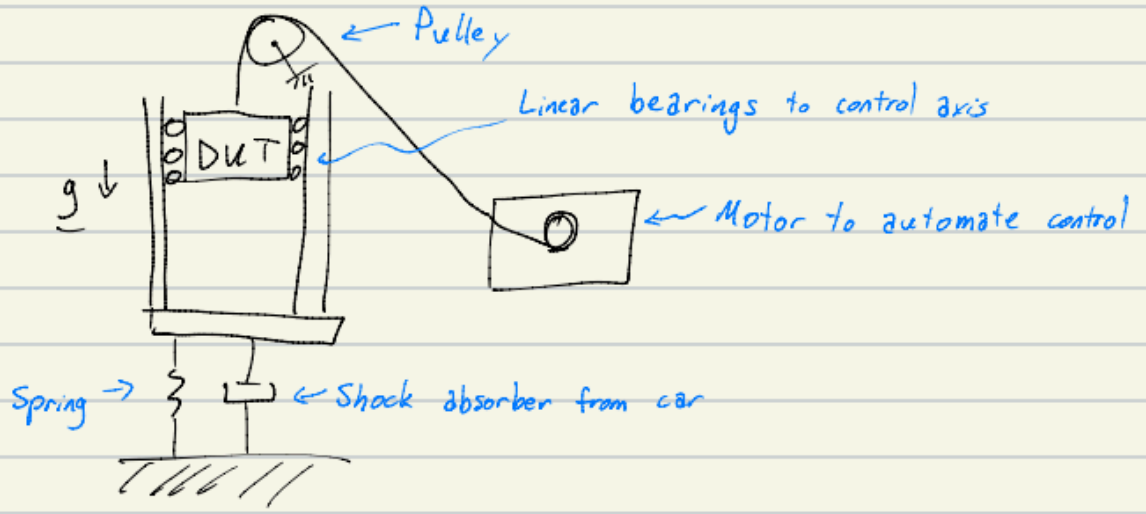
1)


Pulley
DUT
g
Operator
Spring
Shock absorber from car

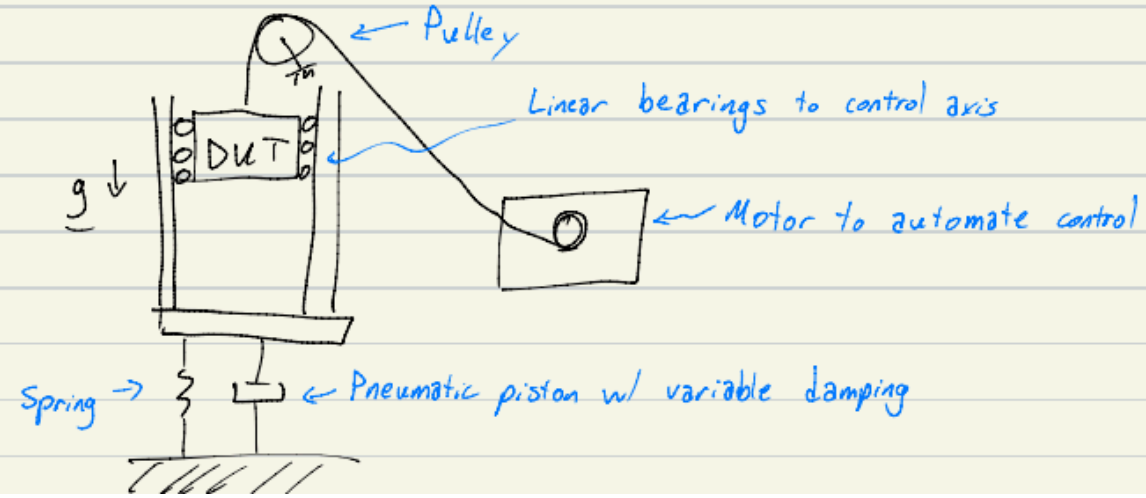
2)


Pulley
Linear bearings to control axis
DUT
g
Operator
Spring
Shock absorber from car

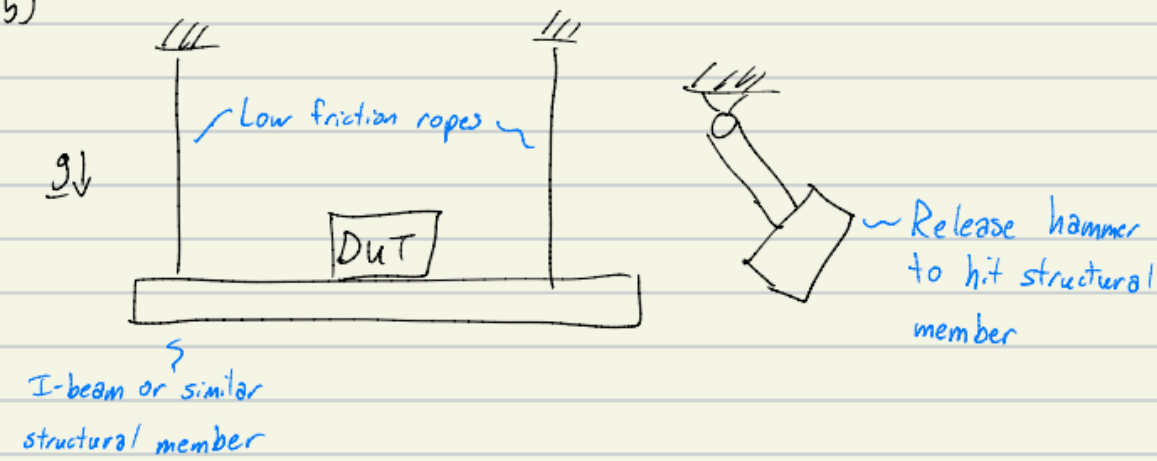
3)


Pulley
Linear bearings to control axis
DUT
g
Motor to automate control
Spring
Shock absorber from car

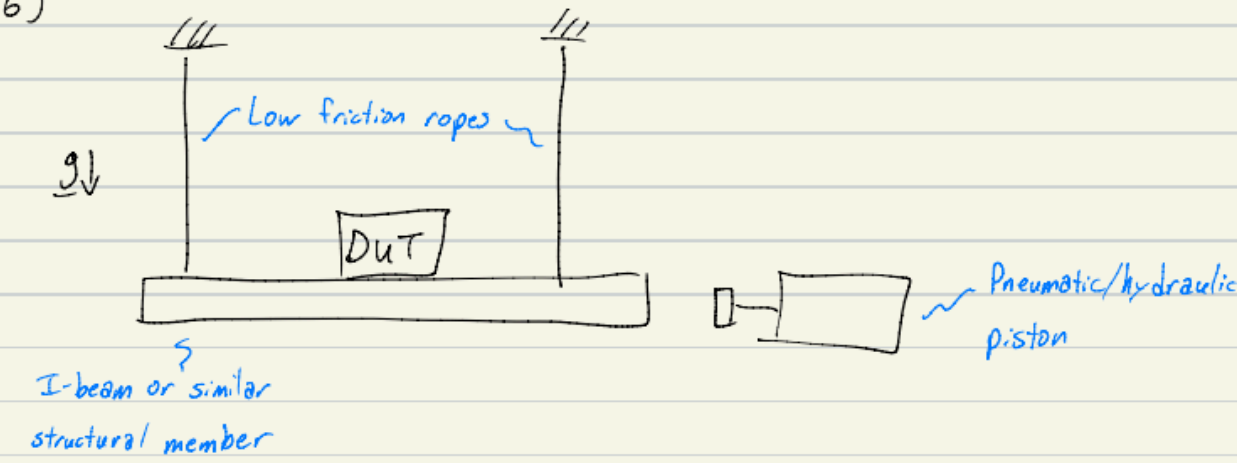
4)


Pulley
Linear bearings to control axis
DUT
g
Motor to automate control
Spring
Pneumatic piston w/ variable damping

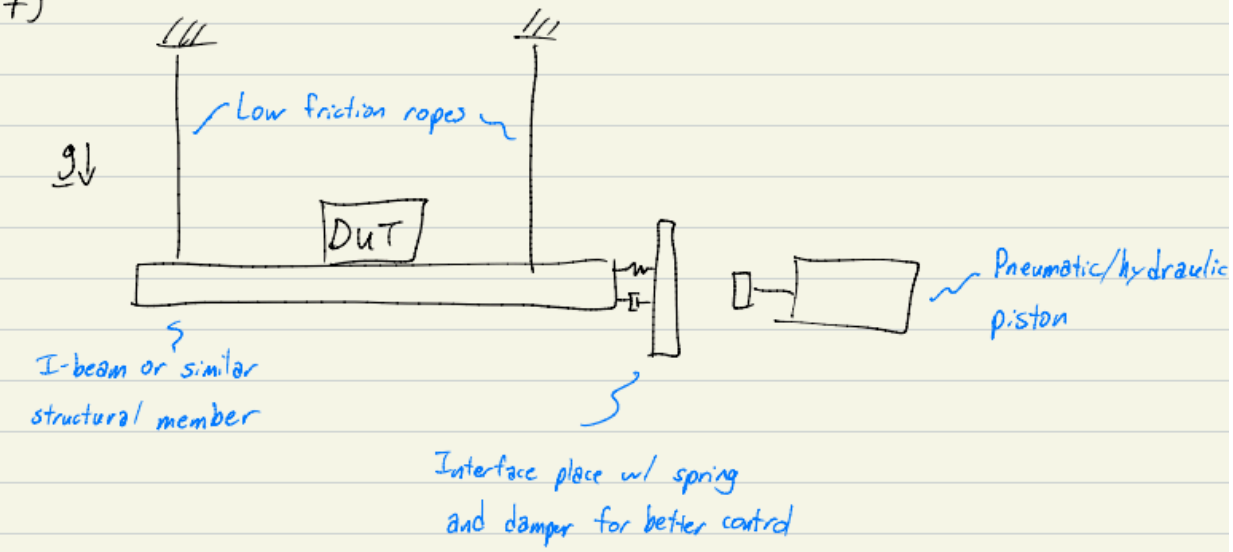
5)


Low friction ropes
g
DUT
Release hammer to hit structural member
I-beam or similar structural member

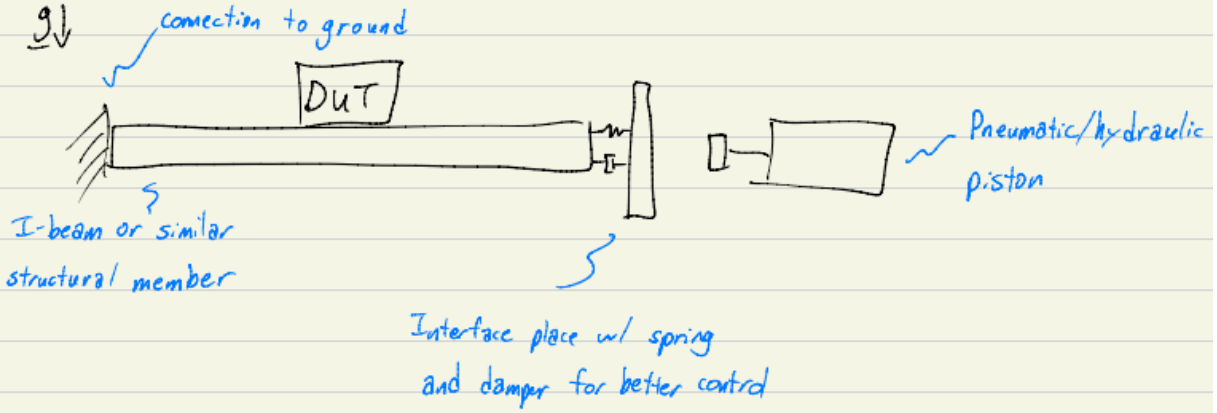
6)


Low friction ropes
g
DUT
Pneumatic/hydraulic piston
I-beam or similar structural member

7)


Low friction ropes
g
DUT
Pneumatic/hydraulic piston
I-beam or similar structural member
Interface place w/ spring and damper for better control

8)


g
connection to ground
DUT
Pneumatic/hydraulic piston
I-beam or similar structural member
Interface place w/ spring and damper for better control

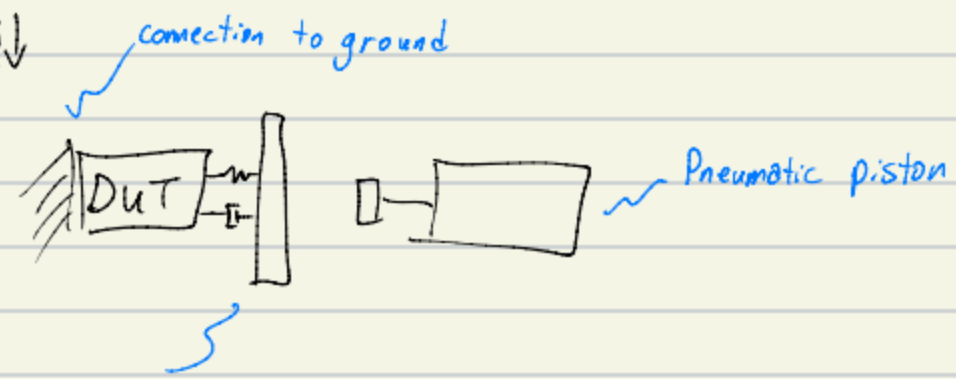
9)



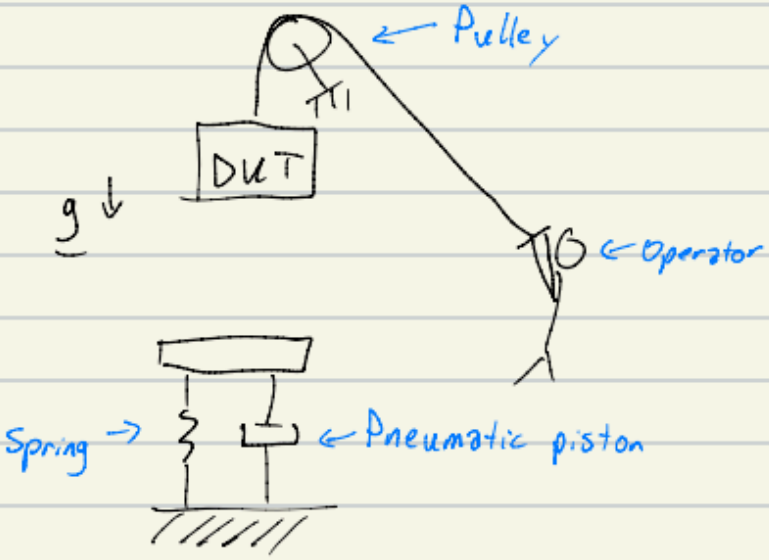
Rocket w/ similar dynamics to expected

10)

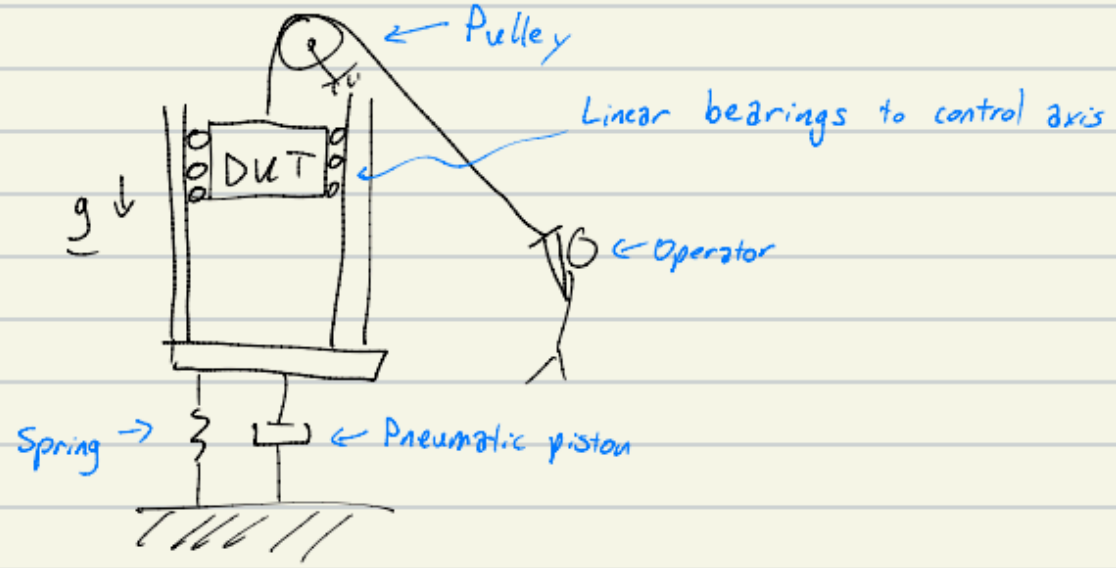
9↓



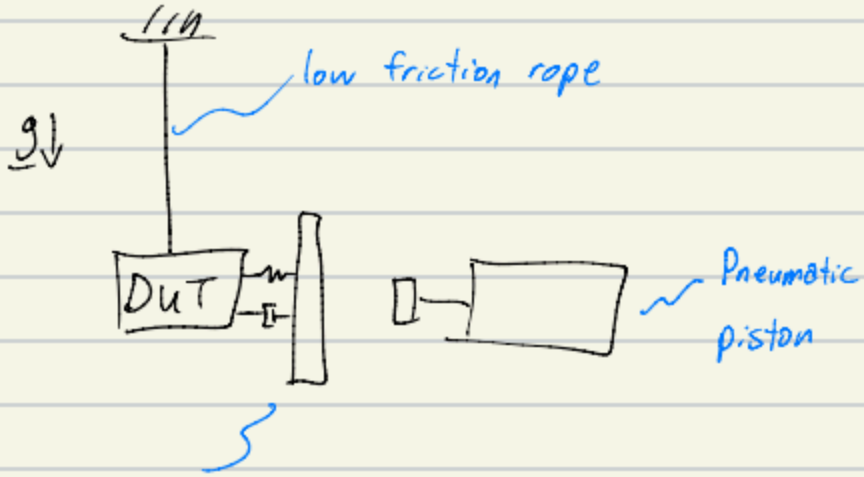
(1)


Pulley
DUT
g
Operator
Spring
Pneumatic piston

(2)

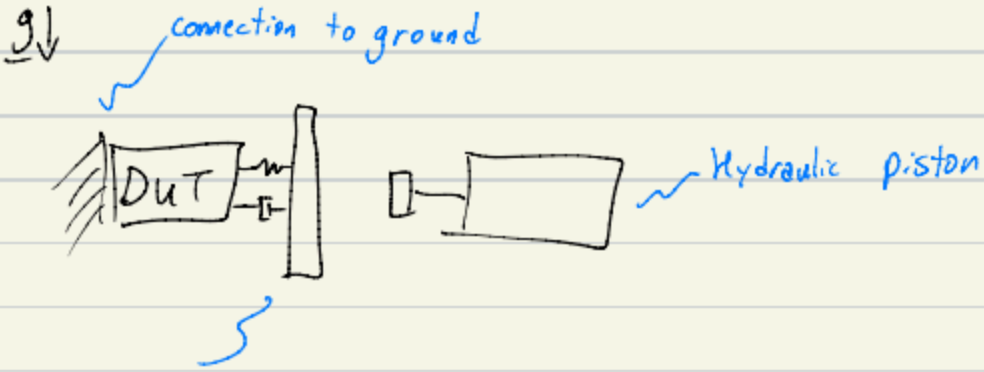

Pulley
Linear bearings to control axis
DUT
g
Operator
Spring
Pneumatic piston

(3)



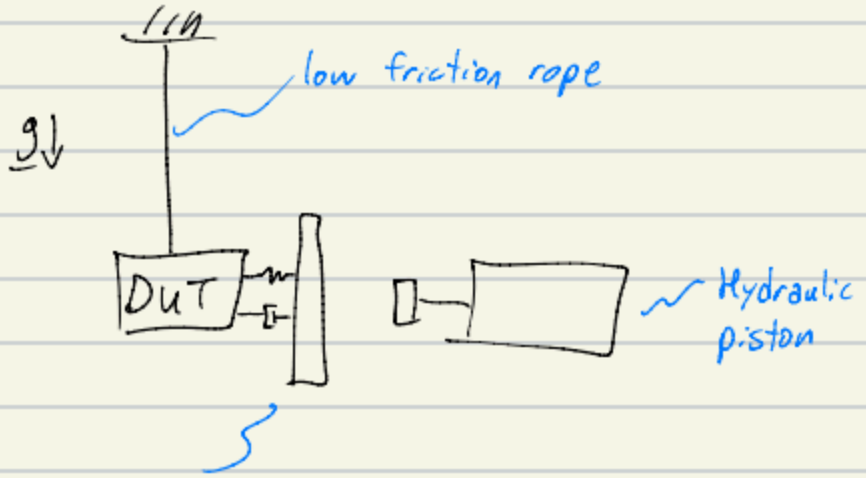
Interface place w/ spring and damper for better control

(4)

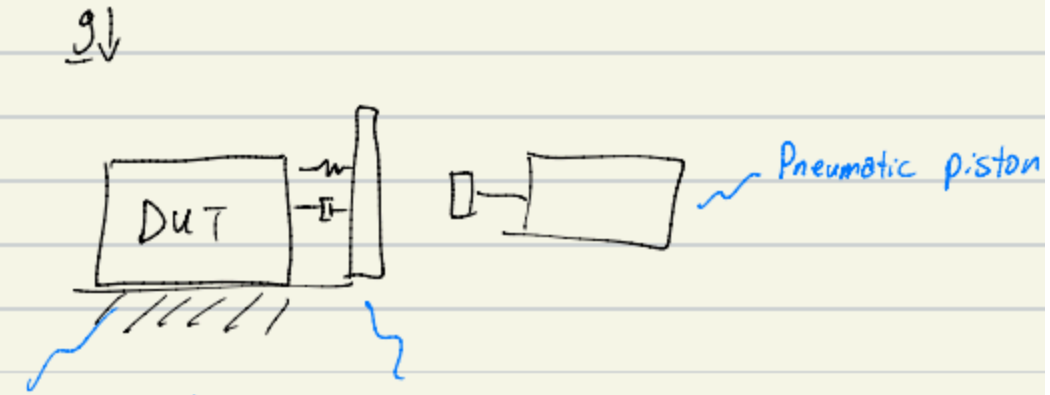


Interface place w/ spring and damper for better control

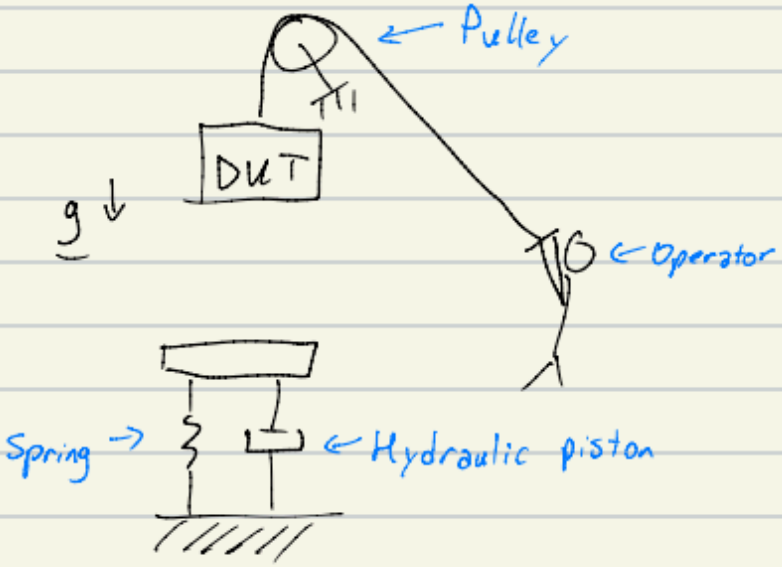
(5)


low friction rope
g
DUT
Hydraulic piston
Interface piece w/ spring and damper for better control

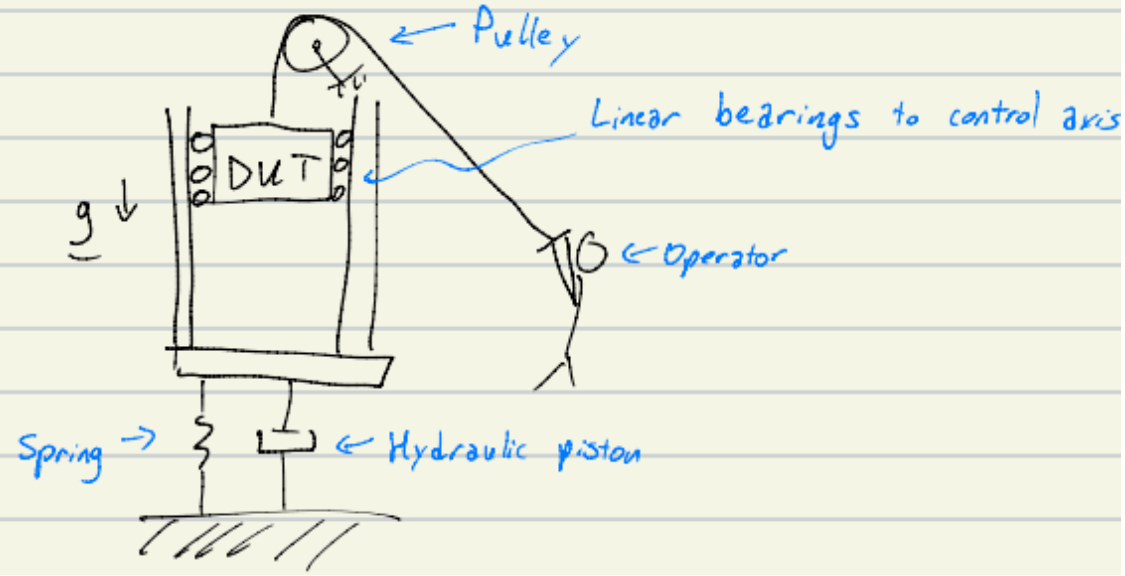
(6)


g
DUT
Pneumatic piston
frictional contact to ground
Interface piece w/ spring and damper for better control

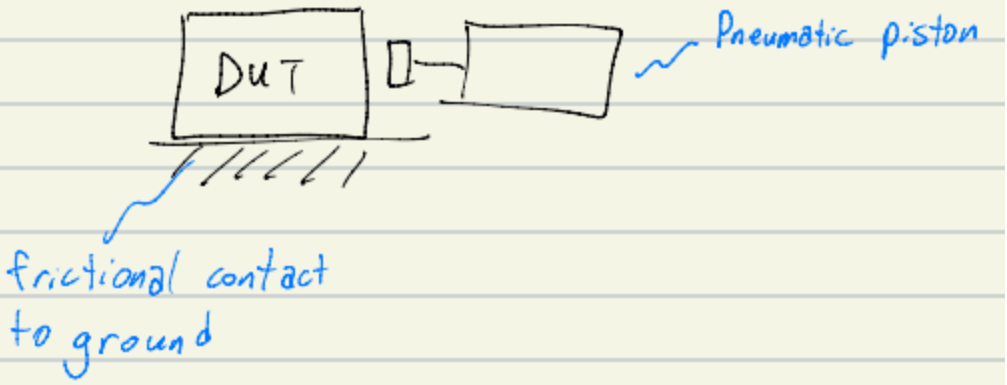
(17)


Pulley
DUT
g
Operator
Spring
Hydraulic piston

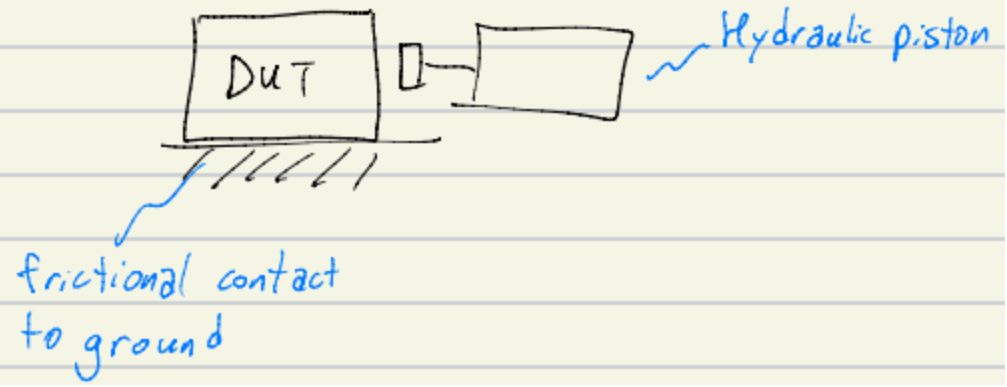
(18)


Pulley
Linear bearings to control axis
DUT
g
Operator
Spring
Hydraulic piston

19)

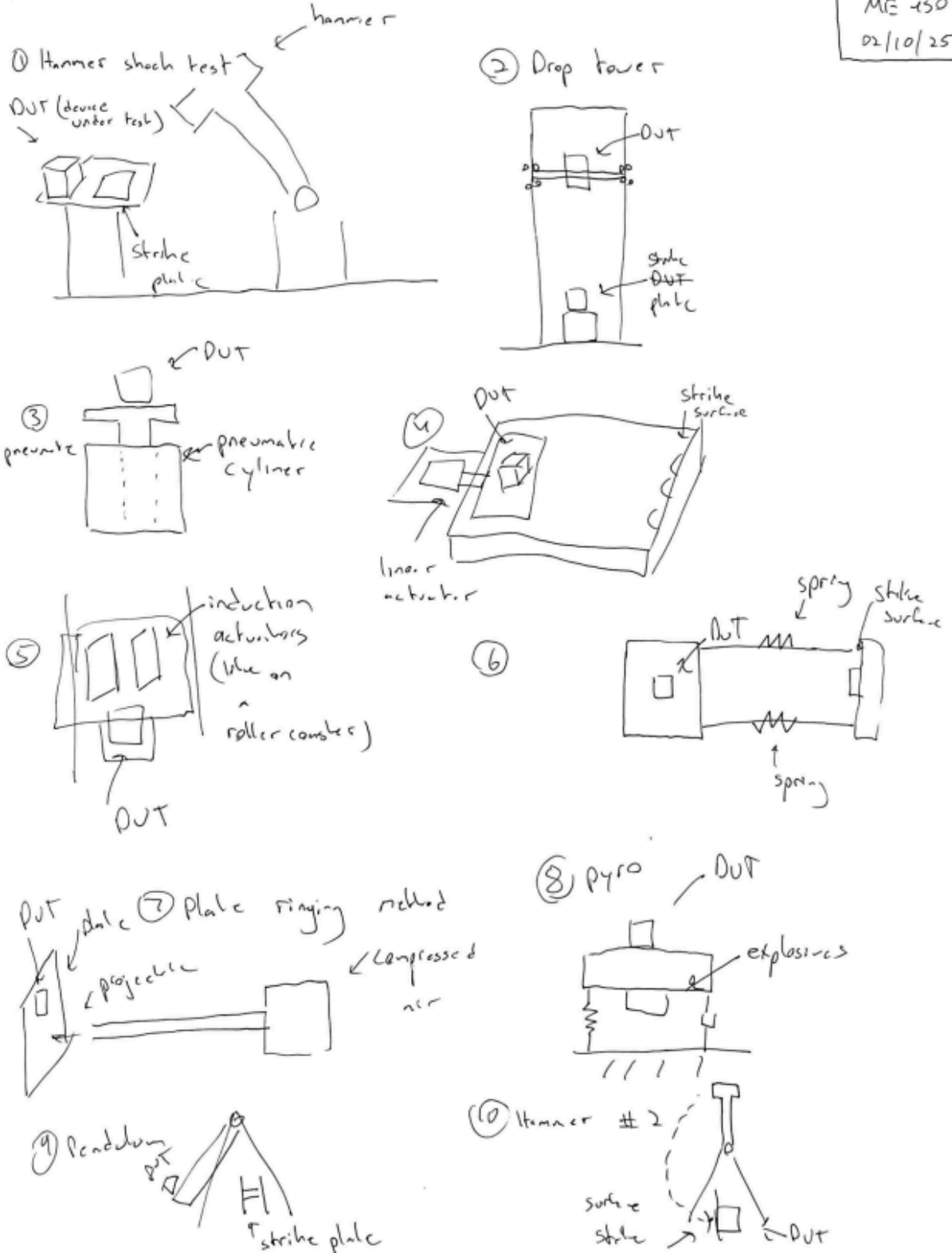

g
DUT
Pneumatic piston
frictional contact
to ground

20)


g
DUT
Hydraulic piston
frictional contact
to ground

Joseph Harrington
ME 450
02/10/25

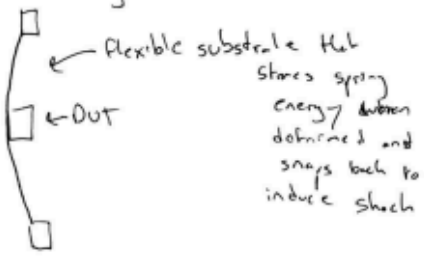
Part 1 #2



Part II #1

Joseph Harrington
ME 450
2/10/2025

(11) Use design heuristic 16. "Bend"



(12)



Design heuristic #65 - telescope

L
drop
tower
telescopes to increase
drop height and impact
velocity.

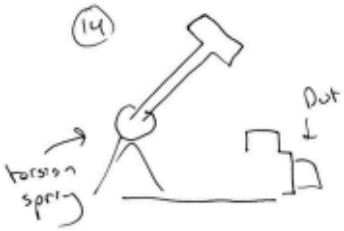
Functional decomposition

Design Problem: induce shocks up to 3000g <25 ms on payload
- to add energy to storage device
- to release energy in short time to induce shock
- to attenuate external shock
- to mount device

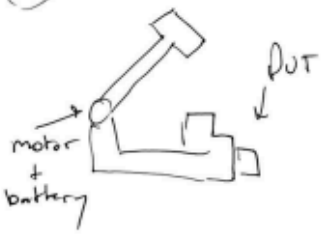
(13)



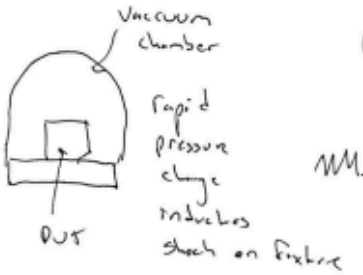
(14)



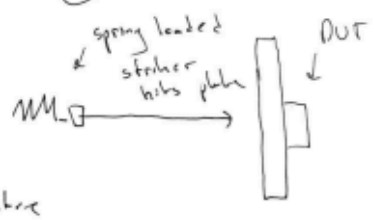
(15)



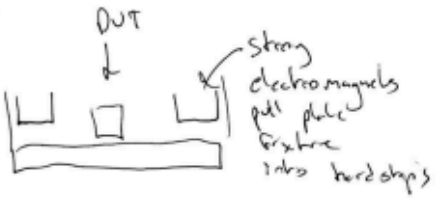
(16)



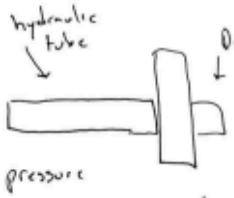
(17)



(18)



(19)



(20)

